

TECHNISCHE  
UNIVERSITÄT  
DRESDEN

---

# Hierarchy of Quantum Trajectories applied to Photosynthetic Complexes

Diplomarbeit  
zur Erlangung des wissenschaftlichen Grades  
Diplom-Physiker

vorgelegt von

Daniel Süß  
geboren am 18.10.1987 in Dresden

Institut für Theoretische Physik  
der Technischen Universitaet Dresden  
2013

Eingereicht am 23. Oktober 2013

1. Gutachter: Herr Prof. Dr. Walter Strunz
2. Gutachter: Herr PD Dr. Frank Großmann

## **Zusammenfassung**

Stochastische Schrödinger-Gleichungen haben sich als effiziente Werkzeuge zur Beschreibung der Dynamik Markov'scher offener Quantensysteme etabliert. Im Gegensatz zur numerischen Integration der Mastergleichung erlauben sie die parallele Propagation unabhängiger Realisierungen. Eine entsprechende Erweiterung auf nicht-Markov'sche Systeme ist Gegenstand der vorliegenden Diplomarbeit. Aufbauend auf der nicht-Markov'schen stochastischen Schrödinger-Gleichung, die im ersten Abschnitt der Arbeit wiederholt wird, beschäftigt sich der Hauptteil mit der Herleitung einer äquivalenten Hierarchie von stochastischen Differentialgleichungen. Die anschließende Anwendung auf Energietransfer in Lichtsammelkomplexen behandelt die Fragestellung, inwiefern quantenmechanische Effekte die Wirkungsweise von Pigment-Proteinen beeinflusst. Außerdem bietet die vorgestellte Methode eine effektive Möglichkeit zur Berechnung von Absorptionsspektren, die wichtige Informationen über den Aufbau von chemischen Komplexen liefern.

## **Abstract**

Stochastic Schrödinger equations have been established as an efficient tool to describe the dynamics of Markovian open quantum systems. Contrary to a numerical integration of the master equation, they admit parallel propagation of independent trajectories. An appropriate generalization to non-Markovian systems is the subject of the present diploma thesis. Based on the non-Markovian stochastic Schrödinger equation, which is recapitulated in the first section, an equivalent hierarchy of stochastic differential equations is derived. The following application to energy transfer in light-harvesting systems is concerned with the question, to what extent quantum mechanical effects influence the operation of pigment-proteins. Furthermore, the newly-devised method provides an effective approach to calculate absorption spectra, which contain crucial information on the structure of chemical complexes.



# Contents

<b>1. Introduction</b>	<b>1</b>
1.1. Open Quantum Systems . . . . .	1
1.2. Unravellings and Stochastic Schrödinger Equations . . . . .	3
1.3. Outline . . . . .	5
<b>2. Non-Markovian Quantum State Diffusion</b>	<b>7</b>
2.1. The Microscopic Model . . . . .	8
2.2. Linear NMSSE . . . . .	11
2.2.1. Convolutionless Formulation . . . . .	14
2.2.2. Markov Limit . . . . .	15
2.2.3. Equivalent Master Equation . . . . .	17
2.3. Nonlinear NMSSE . . . . .	19
2.4. Interpretation of the NMSSE . . . . .	23
2.5. Finite Temperature Theory . . . . .	27
2.6. Jaynes-Cummings Model . . . . .	30
2.6.1. O-Operator Method . . . . .	31
2.6.2. Noise-Expansion Method . . . . .	32
<b>3. Hierarchy of Stochastic Pure States</b>	<b>35</b>
3.1. Derivation of the Hierarchy . . . . .	36
3.1.1. Linear Hierarchy . . . . .	36
3.1.2. Nonlinear Hierarchy . . . . .	39
3.1.3. Multiple Bath-Modes . . . . .	41
3.2. Bath Correlation Function Expansion . . . . .	43
3.3. Spin-Boson Model . . . . .	46
3.3.1. Sample Size . . . . .	47
3.3.2. Truncation Order and Terminator . . . . .	51

<b>4. Molecular Aggregates and the NMSSE</b>	<b>53</b>
4.1. The Aggregate Hamiltonian . . . . .	53
4.2. Energy Transfer in Light-Harvesting Complexes . . . . .	58
4.3. Absorption Spectra of Molecular Aggregates . . . . .	66
4.3.1. NMSSE for Spectra . . . . .	66
4.3.2. Results . . . . .	68
<b>5. Conclusions and Outlook</b>	<b>73</b>
<b>A. Discrete Time Evolution of Time-Oscillators</b>	<b>77</b>
<b>B. Analytic Solution of the Jaynes-Cummings Model</b>	<b>79</b>
B.1. General Approach . . . . .	79
B.2. Exponential Bath Correlation Function . . . . .	81
<b>C. NMSSE-Hierarchy and Application</b>	<b>83</b>
C.1. The Memory-Integral Term . . . . .	83
C.2. Drude Spectral Densities . . . . .	84
C.3. Parameters for Calculations . . . . .	85

# 1. Introduction

The explanation of the discrete Hydrogen-spectrum in terms of Matrix-mechanics by Heisenberg and Wave-mechanics by Schrödinger is often perceived as the hour of birth for modern quantum theory. Since then, the desire to understand systems with an increasing number of degrees of freedom and ever-growing complexity has been a main driving force behind the development of new theoretical ideas. However, the overwhelming majority of quantum mechanical insights relies on more or less severe approximations, as even apparently simple models like the Helium atom have not been solved analytically. One simplification that underlies all physical investigation is the distinction between relevant and irrelevant degrees of freedom for a certain setting: Even the simple Hydrogen model consisting of an electron-proton pair and the mutual Coulomb attraction ignores the surrounding electrons and protons in the same container, to give an example. While under many circumstances the relevant degrees of freedom approximately behave like an isolated unit, there are examples where environmental effects significantly shape the dynamical behavior of the system under consideration—these are referred to as open quantum systems. Clearly, the cut distinguishing between relevant system and irrelevant environment is not uniquely defined, but generally, the requirement to account for a given experimental setting eliminates ambiguities to the greatest possible extent.

## 1.1. Open Quantum Systems

(2.6) The fundamental dynamical equation of non-relativistic quantum mechanics, namely the *Schrödinger equation*, is valid only for closed systems. Embedding the open system into a larger, approximately closed system allows for a systematic treatment of its dynamics based on first principles. Mathematically, the kinematic structure is given by the product  $\mathcal{H}_{\text{sys}} \otimes \mathcal{H}_{\text{env}}$  (or any Hilbert space isomorphic to it). Since the environment's purpose is merely to restore a unitary time evolution, all relevant

## 1. Introduction

---

information about the system is encoded in the *reduced state*  $\rho(t) = \text{Tr}_{\text{env}} \rho_{\text{tot}}(t)$  obtained by tracing over the environmental degrees of freedom. Formally, this amounts to assigning the expectation value

$$\langle A \rangle := \text{Tr}(\rho_{\text{tot}}(t) A \otimes I_{\text{env}}) = \text{Tr}_{\text{sys}}(\rho(t) A) \quad (1.1)$$

to each observable  $A$  on  $\mathcal{H}_{\text{sys}}$ . The second part, namely that  $\langle \cdot \rangle$  defines a genuine trace-class operator  $\rho_t$  on  $\mathcal{H}_{\text{sys}}$ , follows under some additional regularity assumptions [BR03]. But even if the total system-bath state is pure at any given time, the reduced state is not necessarily a pure-state projector. On the contrary, due to quantum entanglement caused by the interaction between the system and its environment, the reduced state must be described by a mixture.

Although the reduced state's time evolution is uniquely defined by the von Neumann equation for  $\rho_{\text{tot}}(t)$  and Eq. (1.1), a dynamical equation purely in terms of  $\rho(t)$  is more desirable for all practical purposes. In general, the derivation of a closed equation in  $\rho(t)$  from the unitary system-bath evolution relies on quite severe approximations. A typical example is the *Redfield*-equation [BP02], which is based on the following physical assumptions: First, one starts with an initial product state  $\rho_{\text{tot}}(0) = \rho(0) \otimes \rho_{\text{env}}$ . By the weak-coupling or *Born*-approximation, this product form with a fixed environmental state  $\rho_{\text{env}}$  is preserved for all times. Furthermore, we assume that the dynamics of the environment proceed on a much smaller timescale compared to the system and any “memory”-effects are negligible small—this is the *Markov*-approximation. However, because it is derived from a truncated perturbation expansion, the Redfield-master equation does not necessarily preserve all properties of a genuine density matrix.

A more robust approach based on similar physical assumptions, but more axiomatic in spirit has been elaborated among others by Kossakowski and Linblad [Kos72,Lin76]: It is formulated purely in terms of propagators  $\Lambda_t$  on the system's Hilbert space without making reference to a certain environment. The Born-Markov approximation is rephrased to the condition that the family of maps  $(\Lambda_t)_{t \geq 0}$  constitute a quantum dynamical semi-group [AL87], namely  $\Lambda_{s+t} = \Lambda_s \Lambda_t$ . Provided the  $\Lambda_t$  are completely-positive as well (and certain regularity assumptions are satisfied), the corresponding

time evolution equation for the reduced state necessarily takes the form of a *Lindblad master equation*

$$\partial_t \rho_t = -\frac{i}{\hbar} [H, \rho_t] + \frac{1}{2} \sum_n \left( [L_n \rho_t, L_n^\dagger] + [L_n, \rho_t L_n^\dagger] \right). \quad (1.2)$$

Here  $H = H^\dagger$  is a self-adjoint operator and  $L_n$  are Linbladians describing various irreversible channels [WM10].

However, for many open systems the Born-Markov approximation turns out to be too severe to account for a realistic environment: Non-Markovian effects arise for example in the radiative decay of an atom into a structured environment [BP02] or the tunneling of the trapped flux in a super-conducting qubit [CL83, LCD<sup>+</sup>87]. Also, recent experiments suggest that the high efficiency of exciton-transfer in light-harvesting systems is achieved by virtue of non-Markovian effects [ECR<sup>+</sup>07]. Unfortunately, no universally valid and tractable non-Markovian generalization of Lindblad's master equation (1.2) is known today. Although the projection formalism of Nakajima-Zwanzig provides a closed equation in the reduced state  $\rho_t$  by separating relevant and irrelevant degrees of freedom in the von Neumann equation [BP02], non-Markovian effects are included by means of a memory-integral such that the evolution of  $\rho(t)$  depends on all reduced states at times prior to  $t$ . This makes an analytical or numerical solution without further approximations very difficult.

## 1.2. Unravellings and Stochastic Schrödinger Equations

Of course, the previous discussion is not exclusive to quantum mechanics: To account for the influence of an environment on a classical system, its equations of motion are simply extended by fluctuation- and friction-forces giving rise to the *Langevin equation* [Gar85]. A different description is obtained by averaging trajectories corresponding to different noise-realizations. The time evolution of the resulting probability density on phase space is governed by the *Fokker-Planck equation*. For numerical purposes, Monte-Carlo simulations of individual stochastic trajectories are often preferred over the integration of the Fokker-Planck equation due to reduced computational demand and better parallel-computing performance.

## 1. Introduction

---

Similar Monte-Carlo techniques have been developed to deal with Markovian open quantum systems. So called “*unravellings*” of the Lindblad master equation (1.2) determine stochastic pure states  $|\psi_t\rangle$  in the system’s Hilbert space, such that averaging over the corresponding projectors yields the reduced density matrix

$$\rho_t = \mathbb{E} (|\psi_t\rangle\langle\psi_t|). \quad (1.3)$$

In accordance with the classical theory, the stochastic states  $|\psi_t\rangle$  are often referred to as *quantum trajectories* [Car93]. Their time evolution is described in terms of stochastic Schrödinger equations driven either by jump-processes [GZ04] or time-continuous, diffusive processes [Car93, Per98, BP02]. As an example for the latter we mention the *quantum state diffusion* (QSD) in its Itō- version for a single Linbladian  $L_1 = L$  [Per98]

$$d|\psi'_t\rangle = \left( -iH + \langle L^\dagger \rangle_t L - \frac{1}{2} L^\dagger L - \frac{1}{2} \langle L^\dagger \rangle_t \langle L \rangle_t \right) |\psi'_t\rangle dt + (L - \langle L \rangle_t) |\psi'_t\rangle d\xi_t^*. \quad (1.2)$$

Here,  $d\xi_t^*$  is a complex-valued standard Brownian motion and  $\langle \cdot \rangle_t$  denotes the quantum average with respect to  $|\psi'_t\rangle$ . By omitting from Eq. 1.2 all terms nonlinear in  $|\psi'_t\rangle$ , we obtain its equivalent linear form

$$d|\psi_t\rangle = \left( -iH - \frac{1}{2} L^\dagger L \right) |\psi_t\rangle dt + L|\psi_t\rangle d\xi_t^*. \quad (1.4)$$

Both solutions  $|\psi_t\rangle$  and  $|\psi'_t\rangle$  of the linear and nonlinear stochastic Schrödinger equation, respectively, recover the reduced density operator by averaging over all realizations of the noise  $\xi_t^*$  as stated in Eq. (1.3). However, as we discuss in Sect. 3.3, the nonlinear version is better suited for a Monte-Carlo evaluation, since it preserves the norm of the states  $|\psi'_t\rangle$ . Combined with the computational advantages of propagating pure-state trajectories, nonlinear unravellings provide a highly efficient numerical method for the solution of (1.2) [Car93, Per98]. Indeed, if  $N$  denotes the system’s Hilbert space dimension, integrating the Linblad master equation directly amounts to solving a system of  $N^2$  real-valued, linear, ordinary differential equations. Even though the QSD-approach requires the solution of a nonlinear,  $2N$ -dimensional system of real-valued ODEs for many noise-realizations, the ability to compute trajec-

tories independently is often crucial for the efficient utilization of high-performance computers.

The *non-Markovian stochastic Schrödinger equation* (NMSSE) constitutes a generalization of the stochastic Schrödinger equations (1.2) and (1.4) to the non-Markovian regime. It has been derived independently based on a microscopic model of the system and its harmonic environment without any approximations: One approach utilizes the full Schrödinger equation in a coherent state basis [Dió96], while the other emanates from the Feynman-Vernon influence functional [Str96]. Remarkably, the treatment of the NMSSE does not assume the existence of a master equation for the reduced density matrix at any point. Quite on the contrary, by virtue of its exact microscopic foundation, it is a suitable point of departure to derive an approximate master equation for the latter [YDGS00]. Furthermore, within the NMSSE-formalism all information on the environment is encoded in a single function, namely the bath correlation function. This unified approach to arbitrarily structured environments allows to study the influence and emergence of non-Markovian effects. Since large parts of this work are based on the NMSSE, we postpone the detailed account to Chap. 2.

### 1.3. Outline

The main goal of this work is to investigate the dynamics of large open quantum systems coupled to structured environments. As a primary example, we study the energy transfer in light-harvesting complexes, which provides insight to the question, to what extent quantum mechanical effects influence the operation of organic cells. Since common density-matrix formalisms are limited by their large computational demands, we devise a new method based on non-Markovian quantum trajectories. Unlike established approaches to the solution of the NMSSE [YDGS99, RSE11], it does not rely on the auxiliary assumption of the  $O$ -operator substitution presented in Sect. 2.2.1, but attacks the NMSSE directly. Inspired by the hierarchical equations of motion (HEOM) for density matrices [Tan06], we deal with memory effects by introducing auxiliary pure-state trajectories. The resulting hierarchy of stochastic Schrödinger equations combines the advantages of the HEOM-approach, namely a systematic way to incorporate memory effects, with the computational virtues of quantum trajectories.

## 1. Introduction

---

This work is organized as follows: In Chapter 2 we recapitulate the NMSSE-approach to non-Markovian open quantum systems based on the microscopic model presented in Sect. 2.1. The derivation of the linear NMSSE as well as its connection to the Markovian stochastic Schrödinger equations and the master equation formalism is presented in Sect. 2.2. Subsequently, the nonlinear version of the NMSSE is reviewed. Both versions of the NMSSE only deal with a zero-temperature initial state; the generalization to arbitrary temperature is carried out in Sect. 2.5. One result of this work, namely a pictorial interpretation of the NMSSE, which helps to visualize memory effects of the environment, is derived in Sect. 2.4. We conclude this chapter with an analytically solvable model and discuss some implications of the insights gained to the general case.

Chapter 3 constitutes a central part of this work. It contains the derivation of the NMSSE-hierarchy in its linear (Sect. 3.1.1) and its nonlinear version (Sect. 3.1.3). Since the simple form of the hierarchy crucially depends on an exponential bath correlation function (or sums thereof), Sect. 3.2 is concerned with an expansion providing the required form. Finally, we demonstrate the influence of sample- and hierarchy-size on the accuracy of the results utilizing the Spin-Boson model.

The application of the NMSSE to more complex systems, namely molecular aggregates, is the subject of Chapter 4. In Sect. 4.1 we show how a complex chemical compound is approximately described by the open system model used throughout this work. We illustrate the capabilities of the NMSSE-hierarchy studying exciton energy transfer in light-harvesting systems (Sect. 4.2) and absorption spectra of molecular aggregates (Sect. 4.3).

The final Chapter 5 contains a summary of this work as well as a short outlook. Throughout this work we employ units with  $\hbar = k_B = 1$ .

## 2. Non-Markovian Quantum State Diffusion

[MT99] The description of Markovian open quantum systems in terms of diffusive stochastic differential equations has a long tradition [Car93, Per98, GZ04]. Especially the related Monte-Carlo methods have become an efficient tool to calculate the time evolution of the system's reduced density operator. In the present work we are concerned with a generalization of the numerical methods to non-Markovian systems based on the non-Markovian stochastic Schrödinger equation (NMSSE). But the latter provides much more than just a favorable unravelling of the reduced density operator: Actually, it constitutes an equivalent representation of the Schrödinger equation of a full system-environment model without any approximation. The key to an efficient numerical technique is the Monte-Carlo evaluation of the partial trace over the environmental degrees of freedom to obtain the reduced density operator.

At the beginning, we introduce the standard open-system model, which constitutes the foundation for the rest of this work. Following the lines of Diósi, Strunz and Gisin [DS97, DGS98, SDG99], we derive the linear NMSSE and demonstrate its connection to the well-known Markovian stochastic Schrödinger equations as well as the usual approach to open quantum systems in terms of Master equations. The nonlinear version presented in Sect. 2.3 helps to improve the efficiency of the Monte-Carlo evaluation. Section 2.4 provides a new pictorial interpretation of the NMSSE that helps to understand the role of individual interaction-terms. Since the previous sections crucially rely on the vacuum initial conditions of the environment, we show in Sect. 2.5 how to modify our approach to incorporate an initial thermal state. This chapter is concluded by an analytic treatment of the Jaynes-Cummings model.

??

## 2.1. The Microscopic Model

It is the foremost goal of this work to obtain a dynamical description of an open-system's reduced state. Nevertheless, we introduce a full model of system and environment first, that is the non-relativistic standard model of an open quantum system coupled to a bosonic environment extensively studied for example in the book of Weiss [Wei99]. There are three reasons for such a microscopic approach: On one hand, this serves the purpose to better understand the physical origin of macroscopical properties used to characterize the environment later on. But more importantly, starting with a closed quantum system is the only strategy allowing us to derive the NMSSE from first principles, namely the Schrödinger equation. As a last argument we mention that the reduced dynamics are greatly influenced by the choice of initial conditions. Especially entanglement between the system and its environment may change the reduced dynamics dramatically [SB01]—in what follows we ignore this point and always work with separable initial conditions.

As a starting point, we consider an environment consisting of a finite number  $N$  of uncoupled harmonic oscillators<sup>1</sup>. A generalization to an infinite number can be carried out formally along the same lines, replacing sums by infinite series or even integrals; a different approach within our framework is presented later. The dynamics of both system and environment are then described by a unitary time evolution with Hamiltonian

$$H_{\text{tot}} = H \otimes I + I \otimes H_{\text{env}} + H_{\text{int}}, \quad (2.1)$$

where  $H$  and  $H_{\text{env}}$  are the free Hamiltonians of the system and the bath respectively and  $I$  denotes the identity on the appropriate Hilbert space. The latter is a sum over free harmonic oscillators  $H_{\text{env}} = \sum_{\lambda} \omega_{\lambda} a_{\lambda}^{\dagger} a_{\lambda}$  expressed in bosonic ladder operators  $a_{\lambda}$  and  $a_{\lambda}^{\dagger}$  of the  $\lambda^{\text{th}}$  mode with frequency  $\omega_{\lambda}$ . Treating a finite number of independent reservoirs poses no further difficulties and therefore is not elaborated in this section.

---

<sup>1</sup>We use “environment”, “reservoir” and “bath” interchangeably though the latter two suggest a large size compared to the system.

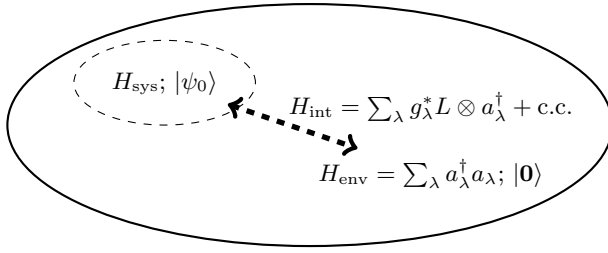


**Figure 2.1.:** Standard model of an open system immersed into a bosonic bath at zero temperature. The environmental oscillators with frequencies  $\omega_\lambda$  are described in terms of ladder operators  $a_\lambda$  and  $a_\lambda^\dagger$ . A coupling operator  $L$  mediates the influence of the environment.

For the interaction between environment and system we confine ourselves to the case of linear coupling

$$H_{\text{int}} = \sum_\lambda g_\lambda^* L \otimes a_\lambda^\dagger + g_\lambda L^\dagger \otimes a_\lambda. \quad (2.2)$$

Here  $L$  denotes the coupling operator in the system's Hilbert space and  $g_\lambda \in \mathbb{C}$  the coupling strength of the  $\lambda^{\text{th}}$  mode. In the field of condensed matter physics, typical models involve a coupling of an individual bath mode that scales inversely with the environment size [Wei99], hence, the linear coupling in (2.2) seems reasonable for macroscopic large reservoirs. Also, the interaction of an electron with the electromagnetic field is described by a Hamiltonian (2.2) up to very high precision—leaving aside some extreme conditions [WM08]. But our framework is not restricted to such weak-coupling regimes, therefore, in such cases the linearity is imposed as another assumption.

Beside the full Hamiltonian, another important influence on the system's time evolution is the initial state, specifically the initial entanglement between system and bath. Throughout this work we only consider product initial conditions, where the bath is in the vacuum state with respect to all  $a_\lambda$

$$|\Psi_0\rangle = |\psi_0\rangle \bigotimes_\lambda |0_\lambda\rangle. \quad (2.3)$$

Such a choice is not as restrictive as it seems on first glance: In Sect. 2.5 we show how a thermal bath state can be mapped to this case. However, it is far from clear if

the results of this work carry over to more general initial conditions, as the NMSSE and most strategies to solve it crucially depend on Eq. (2.3).

To absorb the free dynamics of the environment in time dependent creation and annihilation operators, we switch to the interaction picture with respect to  $H_{\text{env}}$ . Since the bath operators merely obtain an additional phase  $e^{\pm i\omega_\lambda t}$ , the transformed Hamiltonian from Eq. (2.1) reads<sup>2</sup>

$$H_{\text{tot}}(t) = H \otimes I + \sum_{\lambda} \left( g_{\lambda}^* e^{i\omega_{\lambda} t} L \otimes a_{\lambda}^{\dagger} + g_{\lambda} e^{-i\omega_{\lambda} t} L^{\dagger} \otimes a_{\lambda} \right). \quad (2.4)$$

Our choice of separable initial conditions with a vacuum bath state ensures that the reduced density operator remains unaffected under the change of time evolution picture.

It is instructive to rewrite the last equation using the operator valued “force”

$$B(t) = \sum_{\lambda} g_{\lambda} a_{\lambda} e^{-i\omega_{\lambda} t}. \quad (2.5)$$

The total Hamiltonian then reads  $H_{\text{tot}}(t) = H \otimes I + L \otimes B(t)^{\dagger} + L^{\dagger} \otimes B(t)$ . From this equation it can already be seen that the complete action of the environment on the system is encoded in the operator  $B(t)$ . An important—and within our model the only—characteristic of the environment is the *two-time correlation function*  $\alpha(t-s) = \langle (B(t) + B(t)^{\dagger})(B(s) + B(s)^{\dagger}) \rangle_{\rho}$ , where  $\langle \cdot \rangle_{\rho}$  denotes the expectation value with respect to an arbitrary initial bath density matrix  $\rho$ . For a thermal state at temperature  $T$ , the correlation function can be calculated analytically [FHS10]

$$\alpha_T(t-s) = \sum_{\lambda} |g_{\lambda}|^2 \left( \coth \left( \frac{\omega_{\lambda}}{2T} \right) \cos \omega_{\lambda}(t-s) - i \sin \omega_{\lambda}(t-s) \right). \quad (2.6)$$

Introducing the *spectral density*  $J(\omega) = \sum_{\lambda} |g_{\lambda}|^2 \delta(\omega - \omega_{\lambda})$  and taking the limit  $T \rightarrow 0$ , Eq. (2.6) is written more concisely as

$$\alpha_0(t-s) = \langle B(t)B(s)^{\dagger} \rangle_0 = \int_0^{\infty} J(\omega) e^{-i\omega(t-s)} d\omega, \quad (2.7)$$

---

<sup>2</sup>We refrain from introducing another label to distinguish between time evolution pictures; in what follows we always work in the interaction picture unless stated otherwise.

provided all oscillator-frequencies  $\omega_\lambda$  are positive. In other words, the zero temperature correlation function is simply the (one-sided) Fourier transform of the spectral density. Since a genuine physical spectral density is real, we require admissible correlation functions to be hermitian  $\alpha(-t) = \alpha(t)^*$ .

Typical correlation functions of macroscopic systems decay exponentially on a timescale  $\tau_c$  called correlation time. The Markov limit  $\tau_c \rightarrow 0$  amounts to a completely memoryless time evolution and leads to the celebrated quantum dynamical semi-groups. On the other hand, a finite environment yields a purely oscillatory correlation function with  $\tau_c \rightarrow \infty$ .

## 2.2. Linear NMSSE

The linear non-Markovian stochastic Schrödinger equation (NMSSE) derived in this section is an equivalent reformulation of the interaction-picture Schrödinger equation

$$\partial_t |\Psi_t\rangle = -iH_{\text{tot}}(t)|\Psi_t\rangle, \quad |\Psi_0\rangle = |\psi_0\rangle \otimes |0\rangle, \quad (2.8)$$

corresponding to the model of the last section. As we elaborate in this section, expressing the bath degrees of freedom in the Bargmann Hilbert space of anti-holomorphic functions [Bar61] provides a representation well suited to a stochastic interpretation. To this end, we introduce the unnormalized coherent state  $|z_\lambda\rangle = \exp(z_\lambda a_\lambda^\dagger)|0_\lambda\rangle$  for each mode with resolution of the identity for the environment

$$I = \int \frac{e^{-|z|^2}}{\pi^N} |z\rangle \langle z| d^{2N}z. \quad (2.9)$$

Here, we employ the shorthand notation  $|z\rangle = \bigotimes_\lambda |z_\lambda\rangle$  and the “volume” integration measure for  $N$  complex numbers  $d^{2N}z = \prod_\lambda d\Re z_\lambda d\Im z_\lambda$ . Throughout this work the finite bath is often replaced by a continuum of oscillators, therefore, we simply write  $\mu(dz) = \pi^{-N} \exp(-|z|^2) d^{2N}z$  and drop the explicit reference to  $N$  to keep notation identical.

Equation (2.9) allows us to expand the full state in a time-independent environment basis

$$|\Psi_t\rangle = \int |\psi_t(z^*)\rangle \otimes |z\rangle \mu(dz).$$

For the following derivation it is crucial to notice that the Bargmann transform  $\mathbf{z} \mapsto \psi_t(\mathbf{z}^*)$  is an anti-holomorphic function with values in the system's Hilbert space  $\mathcal{H}_{\text{sys}}$ . Naturally, it is equivalent to any other representation of the full state  $|\Psi_t\rangle$ . As the coherent states are not orthogonal, but rather satisfy  $\langle \mathbf{w} | \mathbf{z} \rangle = \exp(\sum_\lambda w_\lambda^* z_\lambda)$ , the reduced density operator, obtained by tracing over the bath degrees of freedom reads

$$\rho(t) = \text{Tr}_{\text{env}} |\Psi_t\rangle\langle\Psi_t| = \int |\psi_t(\mathbf{z}^*)\rangle\langle\psi_t(\mathbf{z}^*)| \mu(d\mathbf{z}). \quad (2.10)$$

After having established the kinematic structure, the next step is to rewrite the dynamical equation: The representation of the ladder operators follows from the usual rules  $\langle \mathbf{z} | a_\lambda^\dagger = z_\lambda^* \langle \mathbf{z} |$  and  $\langle \mathbf{z} | a_\lambda = \partial_{z_\lambda^*} \langle \mathbf{z} |$ . These expressions applied to Eq. (2.8) yield the system-bath Schrödinger equation in the transformed space

$$\partial_t \psi_t(\mathbf{z}^*) = -iH\psi_t(\mathbf{z}^*) - iL \sum_\lambda g_\lambda^* e^{-i\omega_\lambda t} z_\lambda^* \psi_t(\mathbf{z}^*) - iL^\dagger \sum_\lambda g_\lambda e^{i\omega_\lambda t} \frac{\partial \psi_t}{\partial z_\lambda}(\mathbf{z}^*). \quad (2.11)$$

Introducing an effective bath operator analogous to Eq. (2.5)

$$Z_t^*(\mathbf{z}^*) = -i \sum_\lambda g_\lambda^* e^{-i\omega_\lambda t} z_\lambda^* \quad (2.12)$$

allows us to combine the effect of the first bath-interaction term into a single multiplication operator—or process for reasons explained in the next paragraph. A similar conversion works for the second term as well with the help of the functional chain rule  $\frac{\partial}{\partial z_\lambda^*} = \int \frac{\partial Z_s^*}{\partial z_\lambda^*} \frac{\delta}{\delta Z_s^*} ds$ . Combined, our new equation of motion, the *non-Markovian stochastic Schrödinger equation*, reads [DGS98]

$$\partial_t \psi_t = -iH\psi_t + LZ_t^*\psi_t - L^\dagger \int_0^t \alpha(t-s) \frac{\delta \psi_t}{\delta Z_s^*} ds. \quad (2.13)$$

As we show in Sect. 2.4, the integral boundaries arise by virtue of the initial conditions (2.3), but the basic idea is simple: By definition of our processes (2.12) an initial state  $|\psi_0\rangle \otimes |0\rangle$  translates to an initial  $\psi_0$  that is completely independent of the noise. Then, causality implies that  $\psi_t$  can only depend on  $Z_s^*$  for  $0 \leq s \leq t$ .

Up to this point we have merely rewritten the original Schrödinger equation (2.8) to an equivalent form: The original system-bath product Hilbert space  $\mathcal{H}_{\text{sys}} \otimes \mathcal{H}_{\text{env}}$

is simply replaced by a Hilbert space of  $\mathcal{H}_{\text{sys}}$ -valued functions holomorphic in  $\mathbf{z}^*$ . A different attitude is quite fruitful, especially with a numerical solution of the NMSSE in mind: Equation (2.10) can be rewritten as  $\rho_t = \mathbb{E}(|\psi_t\rangle\langle\psi_t|)$ , where  $\mathbb{E}$  denotes the average over  $\mu(dz) = \pi^{-N}\exp(-|\mathbf{z}|^2)d^{2N}z$ . Put differently, the reduced density matrix  $\rho_t$  arises from averaging over stochastic pure state projectors  $|\psi_t(\mathbf{z}^*)\rangle\langle\psi_t(\mathbf{z}^*)|$  with Gaussian weight  $\mu(dz)$ . Hence, we regard Eq. (2.13) as a stochastic differential equation for individual realizations  $\psi_t(\mathbf{z}^*)$ . We refer to the latter either as system state relative to  $|\mathbf{z}\rangle$  or, in the spirit of the stochastic Schrödinger equations emerging from continuous measurement theory [Car93], as *quantum trajectory*.

In this approach, the influence of the bath is implemented as a classical stochastic process  $Z_t^*$  defined by the concrete version (2.12) and the underlying probability measure  $\mu$ . It is a complex Gaussian process, uniquely characterized by its expectation value and covariances

$$\mathbb{E} Z_t = 0, \quad \mathbb{E} Z_t Z_s = 0, \quad \text{and} \quad \mathbb{E} Z_t Z_s^* = \alpha(t-s), \quad (2.14)$$

where  $\alpha(t-s)$  is the zero-temperature correlation function (2.7) for  $J(\omega) = \sum_\lambda |g_\lambda|^2 \delta(\omega - \omega_\lambda)$ . By virtue of the initial conditions,  $\psi_t$  depends on  $\mathbf{z}^*$  only through the noise process, thus, we can drop the coherent state labels and simply write  $\psi_t(Z^*)$  denoting the trajectory corresponding to the realization  $Z_t^*(\mathbf{z}^*)$ . To go one step further, we regard Eq. (2.14) as the defining properties of  $Z_t^*$  without any reference to the microscopic model. It is this alternative point of view that makes the NMSSE-approach so powerful. The entire influence of the environment is encoded in a complex function  $\alpha(t)$ , which acts both as correlation function for the driving noise  $Z_t^*$  and weight-function under the memory integral. A generalization to an arbitrary number of bath-oscillators is now straightforward: Simply replacing  $\alpha(t)$  by any admissible bath correlation function allows a unified treatment of arbitrary bosonic environments.

Except in the limit  $\alpha(t) \sim \delta(t)$ , elaborated in Sect. 2.2.2, the noise process  $Z_t^*$  is correlated for different times. This non-Markovian behavior, which makes a complete understanding of the dynamics highly desirable for application but also considerably harder, shows up in the equation of motion (2.13) as well. The memory integral contains the functional derivative over the whole timespan and therefore takes the complete history of  $\psi_t(Z^*)$  into account. In its own right the derivative is just as problematic: Since its computation requires not only the single realization  $Z_t^*$ , but in some

sense all adjacent ones as well, it seems questionable to regard the NMSSE (2.13) as a genuine stochastic differential equation [GW02]. Even from the purely pragmatic point of view, both kinds of non-local behavior complicate a direct numerical simulation of the NMSSE—or even make it completely impracticable. Nevertheless, there are two quite distinct solutions to this problem as shown in Sect. 2.2.1 and Chap. 3.

### 2.2.1. Convolutionless Formulation

As a cure for the non-locality issues, Diósi, Gisin, and Strunz [DGS98] proposed the powerful *O-Operator substitution*: It is based on the additional assumption, that one may replace the functional derivative by a system operator  $O(t, s, Z^*)$ , which only depends on the realization of  $Z^*$  itself

$$\frac{\delta\psi_t(Z^*)}{\delta Z_s^*} = O(t, s, Z^*)\psi_t(Z^*). \quad (2.15)$$

Besides getting rid of the derivative, this substitution enables us to rewrite the NMSSE (2.13) in its convolutionless form

$$\partial_t\psi_t(Z^*) = -iH\psi_t(Z^*) + LZ_t^*\psi_t(Z^*) - L^\dagger\bar{O}(t, Z^*)\psi_t(Z^*) \quad (2.16)$$

with the time-local operator

$$\bar{O}(t, Z^*) := \int_0^t \alpha(t-s)O(t-s, Z^*) ds. \quad (2.17)$$

Conclusively, Eq. (2.16) turns into a genuine stochastic differential equation for the trajectory  $\psi_t(Z^*)$ , but in the much smaller Hilbert space of the system. This makes it exceptionally well suited for dealing with infinite sized environments numerically, provided the  $\bar{O}$ -operator is known. Depending on how accurate we can determine  $O(t, s, Z^*)$ , the convolutionless NMSSE (2.16) is just as accurate as the original microscopic equation of motion (2.8).

In general this is done as described below [DGS98]: From the consistency condition

$$\partial_t \frac{\delta\psi_t(Z^*)}{\delta Z_s^*} = \frac{\delta}{\delta Z_s^*} \partial_t\psi_t(Z^*) \quad (2.18)$$

supplied with initial value

$$O(s, s, Z^*) = L \quad (2.19)$$

we derive an equation of motion for  $O(t, s, Z^*)$ . It still contains the functional derivative, but is converted to a system of coupled, deterministic equations using a power series ansatz

$$O(t, s, Z^*) = \sum_{n=0}^{\infty} \int_0^t \dots \int_0^t O_n(t, s, \nu_1, \dots, \nu_n) d\nu_1 \dots d\nu_n. \quad (2.20)$$

For a few simple systems—for example the Jaynes-Cummings model presented in Sect. 2.6 or its higher dimensional generalizations [JZYY12]—an exact analytic expression for  $O(t, s, Z^*)$  is known. Nevertheless, most treatments rely on approximation schemes, for example a perturbation expansion for small coupling parameters or almost-Markovian environments [YDGS99]. Also, for an exponential bath correlation function  $\alpha(t) = g e^{-\gamma|t| - i\Omega t}$  (or sums thereof), one can solve the equations of motion for

$$\bar{O}_n(t) := \int_0^t \dots \int_0^t \alpha(t-s)\alpha(t-\nu_1)\dots\alpha(t-\nu_n) O_n(t, s, \nu_1, \dots, d\nu_n) d\nu_1 \dots \nu_n ds$$

numerically. This yields a coupled set of equations similar to the hierarchy derived in Sect. 3.1. Setting all  $\bar{O}_n(t) = 0$  for  $n > 0$  is referred to as zero order functional expansion or ZOFE [RRSE11, RSE11].

### 2.2.2. Markov Limit

Markovian dynamics constitute an important limit in the description of open quantum systems. In this section we show how a bath correlation function with vanishing correlation time, namely  $\alpha(t) = \gamma\delta(t)$ , transforms the NMSSE into the linear, diffusive stochastic Schrödinger equation (1.4), thus establishing the link to the well-known Markovian theory.

The vacuum initial conditions  $\frac{\delta\psi_0}{\delta Z_s^*} = 0$  with  $s \in \mathbb{R}$  imply for an arbitrary bath correlation function

$$\frac{\delta\psi_t}{\delta Z_t^*} = \frac{1}{2} L\psi_t \quad (t > 0) \quad (2.21)$$

as we show now directly from the equations of motion<sup>3</sup>.

It is clear from its derivation that the NMSSE describes a unitary time evolution. Therefore, it can be solved formally using the Dyson series

$$\psi_t(Z^*) = \sum_{n=0}^{\infty} (-i)^n \int_0^t dt_1 \int_0^{t_1} dt_2 \dots \int_0^{t_{n-1}} dt_n H_{\text{tot}}(t_1) \dots H_{\text{tot}}(t_n) \psi_0, \quad (2.22)$$

where  $H_{\text{tot}}(t)$  is the reformulation of (2.4) given by

$$-iH_{\text{tot}}(t) = -iH + LZ_t^* - L^\dagger \int_{-\infty}^{\infty} ds \alpha(t-s) \frac{\delta}{\delta Z_s^*}. \quad (2.23)$$

Throughout this work we often use the shorthand notation  $\mathcal{D}_t = \int ds \alpha(t-s) \frac{\delta}{\delta Z_s^*}$  for the last term. Recall that the bounded integral domain in the NMSSE arises by virtue of the initial conditions—no such restriction applies to  $\mathcal{D}_t$ .

In order to calculate (2.21), note that the functional derivative  $\frac{\delta}{\delta Z_s^*}$  of  $H_{\text{tot}}(t)$  gives a single contribution  $i\delta(t-s)L$  due to  $\frac{\delta Z_s^*}{\delta Z_t^*} = \delta(t-s)$ . This allows us to calculate  $\frac{\delta \psi_t}{\delta Z_t^*}$  order by order in Eq. (2.22): With vanishing derivative of  $\psi_0$  as imposed by the initial conditions, we obtain for the first order

$$\frac{\delta}{\delta Z_t^*} \int_0^t dt_1 (-i)H_{\text{tot}}(t_1)\psi_0 = \int_0^t dt_1 \delta(t-t_1)L\psi_0 = \frac{1}{2} L\psi_0$$

and similarly for the second order

$$\begin{aligned} & \frac{\delta}{\delta Z_t^*} \int_0^t dt_1 \int_0^{t_1} dt_2 (-i)^2 H_{\text{tot}}(t_1) H_{\text{tot}}(t_2) \psi_0 \\ &= \int_0^t dt_1 \int_0^{t_1} dt_2 (-i) \left( \delta(t-t_1)LH_{\text{tot}}(t_2) + \delta(t-t_2)H_{\text{tot}}(t_1)L \right) \psi_0 \\ &= \frac{1}{2} L \int_0^t dt_2 (-i)H_{\text{tot}}(t_2)\psi_0 \end{aligned}$$

---

<sup>3</sup> Equation (2.21) deviates from the acquainted result (2.19) by a factor  $\frac{1}{2}$ , as the latter is derived without any reference to the functional derivative and therefore does not account for the singular behavior at  $s=t$ . Instead, the  $O$ -operator is already introduced in the microscopic model using the Heisenberg time evolution picture for the annihilation operator  $a_\lambda$  [Str01]. Therefore, the substitution Eq. (2.15) does not hold for  $s=t$ . However, this is insignificant for the integrated operator (2.17) as a single point has vanishing weight under the integral.

To justify the second identity, notice that  $\delta(t - t_2)$  contributes only if  $t_1 \geq t$ , since otherwise the singular point  $t$  of the  $\delta$ -function lies outside the integration domain. However, this condition is only satisfied with vanishing weight under the  $t_1$  integral, as the latter is confined to  $[0, t]$ . The same scheme carries over to all higher orders in Eq. (2.22), leading to Eq. (2.21).

Now, let us return to the Markov limit of our NMSSE. By virtue of the singular correlation function  $\alpha(t) = \gamma\delta(t)$ , the memory integral reduces to a time-local form

$$\mathcal{D}_t = \int \delta(t - s) \frac{\delta}{\delta Z_s^*} ds = \gamma \frac{\delta}{\delta Z_t^*}$$

as it is expected from a memoryless environment. Combined with Eq. (2.21), this leads to a simple stochastic differential equation

$$\partial_t \psi_t(Z^*) = -iH\psi_t(Z^*) + LZ_t^* \psi_t(Z^*) - \frac{\gamma}{2} L^\dagger L \psi_t(Z^*), \quad (2.24)$$

driven by a complex White Noise  $Z_t$  with  $\mathbb{E}Z_t Z_s^* = \gamma\delta(t - s)$ . In a formally exact fashion, the equation above should be written as

$$d\psi_t = (-iH\psi_t - \frac{\gamma}{2} L^\dagger L \psi_t) dt + \sqrt{\gamma} L \psi_t d\xi_t^* \quad (2.25)$$

with the increments of a standard complex Brownian motion  $d\xi_t^*$ . It is well known that, seen as an ordinary differential equation, Eq. (2.25) is problematic since  $\xi_t$  is not differentiable with respect to time. To define the solution  $\psi_t$  uniquely we need to specify an appropriate interpretation of the stochastic differential equation. Since we treat the original NMSSE—at least for a finite environment—in Euler-calculus, its Markovian limit should be interpreted in Stratonovich’s sense [Ber03]. However, in our case the Itô- and Stratonovich form agree since  $\mathbb{E}\xi_t \xi_s = 0$  [Gar85].

### 2.2.3. Equivalent Master Equation

Although this work is entirely dedicated to the NMSSE, for the sake of completeness we provide the connection to the customary master equations in this section. The latter are formulated in terms of reduced density operators, which we recover from the trajectories by averaging over the pure states projectors  $P_t = |\psi_t(Z^*)\rangle\langle\psi_t(Z^*)|$ .

Therefore, if the average over  $\dot{P}_t$  can be expressed purely in  $\rho_t = \mathbb{E}(P_t)$ , it yields a master equation for  $\rho_t$ . For certain systems this can be done analytically utilizing the  $O$ -operator introduced in Sect. 2.2.1. As a simple example, we focus on models with a  $Z^*$  independent  $\bar{O}$ -operator, though the general case is treated along the same lines [YDGS99, YDGS00]. We start from the pure-state projectors' equations of motion

$$\partial_t P_t = -i[H, P_t] + Z_t^* L P_t - L^\dagger \bar{O}(t) P_t + Z_t P_t L^\dagger - P_t \bar{O}(t)^\dagger L. \quad (2.26)$$

After averaging over the bath degrees of freedom, these yield a closed evolution equation for  $\rho_t$  only if we can restate the terms containing  $Z_t$  and  $Z_t^*$  in a noise-independent manner. This can be done with the help of Novikov's formula [Nov65]

$$\mathbb{E}(Z_t P_t) = \mathbb{E} \left( \int ds \alpha(t-s) \frac{\delta}{\delta Z_s^*} P_t \right), \quad (2.27)$$

which amounts to a partial integration under the Gaussian integrals (2.10).

The right hand side of Novikov's formula is simplified further using the  $O$ -operator substitution once again. Since  $|\psi_t(Z^*)\rangle$  is analytical in  $Z_s^*$ , and accordingly  $\langle\psi_t(Z^*)|$  analytical in  $Z_s$ , the derivative is further simplified to

$$\frac{\delta}{\delta Z_s^*} \left( |\psi_t(Z^*)\rangle\langle\psi_t(Z^*)| \right) = \left( \frac{\delta}{\delta Z_s^*} |\psi_t(Z^*)\rangle \right) \langle\psi_t(z)| = O(t, s) |\psi_t(Z^*)\rangle\langle\psi_t(Z^*)|.$$

Averaging over the pure state projectors' equations of motion (2.26) finally gives the master equation for the reduced density matrix  $\rho_t$

$$\partial_t \rho_t = -i[H, \rho_t] + [L, \rho_t \bar{O}(t)^\dagger] + [\bar{O}(t) \rho_t, L^\dagger]. \quad (2.28)$$

This expression closely resembles the well-known Lindblad master equation (1.2) for Markovian open quantum systems, but involves time-dependent Lindbladians. As elaborated in Sect. 2.2.2, the  $\bar{O}$ -operator reduces to  $\bar{O}(t) = \frac{\gamma}{2}L$  for a Markovian environment—thus the master equation (2.28) derived from the NMSSE reproduces the correct Linblad master equation (1.2).

## 2.3. Nonlinear NMSSE

From a fundamental point of view, the linear non-Markovian stochastic Schrödinger equation (2.13) is fascinating in its own right. It provides a unified description of arbitrary structured environments and admits a figurative interpretation presented in Sect. 2.4. But, there is a major drawback when it comes to practical application in terms of Monte-Carlo simulations. Recall that the reduced density matrix  $\rho_t$  is obtained by averaging over individual pure state projectors  $|\psi_t(Z^*)\rangle\langle\psi_t(Z^*)|$ . The quality of such a scheme is drastically reduced if there are few highly peaked contributions [DS11]. The NMSSE displays exactly such a behavior: Due to ever growing entanglement with the environment, the norm of most trajectories goes to zero as  $t \rightarrow \infty$ . In order to recover a unitary time evolution for system and bath, that is  $\mathbb{E}(\langle\psi_t|\psi_t\rangle) = \langle\Psi_t|\Psi_t\rangle = 1$ , in a Monte-Carlo simulation, the average has to be taken over many trajectories in order to catch the few with significant contribution. This requires an insurmountable sample size for certain parameter regimes as we show for the exemplary Spin-Boson model in Sect. 3.3.1.

Of course, we have just described the problem of importance sampling in statistics; for its solution let us return to the microscopic model from Sect. 2.1. The key observation is that the average yielding the reduced density operator (2.10) is not unique: A change in the integration measure  $\mu(dz)$  can be compensated using a Girsanov transformation on the quantum trajectories  $\psi_t(Z^*)$ . We use this fact to rewrite the density operator as an average over normalized states

$$\rho_t = \int \frac{d^{2N}z}{\pi^N} e^{-|z|^2} \langle\psi_t(z^*)|\psi_t(z^*)\rangle \frac{|\psi_t(z^*)\rangle\langle\psi_t(z^*)|}{\langle\psi_t(z^*)|\psi_t(z^*)\rangle} \quad (2.29)$$

$$= \int d^{2N}z Q_t(z, z^*) \frac{|\psi_t(z^*)\rangle\langle\psi_t(z^*)|}{\langle\psi_t(z^*)|\psi_t(z^*)\rangle}, \quad (2.30)$$

now with a time dependent density function under the integral

$$Q_t(z, z^*) = \frac{e^{-|z|^2}}{\pi^N} \langle\psi_t(z^*)|\psi_t(z^*)\rangle = \frac{e^{-|z|^2}}{\pi^N} \langle z | \text{Tr}_{\text{sys}}(|\Psi_t\rangle\langle\Psi_t|) | z \rangle. \quad (2.31)$$

Remarkably the latter coincides with the Husimi- or Q-function<sup>4</sup> of the environmental oscillators [Sch11]. Being non-negative and normalized to unity  $\int Q(\mathbf{z}, \mathbf{z}^*) d\mathbf{z} = 1$  makes the Husimi-function a genuine (quasi-)probability distribution on phase space. In this representation,  $|z\rangle$  resembles a wave packet localized around  $z = (q + i p)/\sqrt{2}$ , thus, there is a well defined correspondence between coherent state labels  $z$  and the canonical variables  $(q, p)$ . With Eq. (2.29), we conclude that the norm of a trajectory  $\psi_t(\mathbf{z}^*)$  determines the probability to find the environment in a quantum state localized in the vicinity of a point  $(\mathbf{q}, \mathbf{p})$  in phase space. So, instead of using a fixed environmental basis  $|\mathbf{z}\rangle$  to expand the full state  $|\Psi_t\rangle$  we can incorporate the dynamics of the environment in a comoving coherent state basis.

Making use of the microscopic Hamiltonian (2.11) and the analyticity of  $\psi_t(\mathbf{z}^*)$  in  $\mathbf{z}^*$ , that is  $\partial_{z_\lambda} |\psi_t(\mathbf{z}^*)\rangle = 0$ , we obtain an equation of motion, which closely resembles a Liouville equation

$$\partial_t Q_t(\mathbf{z}, \mathbf{z}^*) = - \sum_{\lambda} \partial_{z_\lambda^*} (ig_\lambda e^{-i\omega_\lambda t} \langle L^\dagger \rangle_t Q_t(\mathbf{z}, \mathbf{z}^*)) - \text{c.c.} \quad (2.32)$$

Clearly, it contains the full influence of the system on the environment due to the quantum average

$$\langle L^\dagger \rangle_t = \frac{\langle \psi_t(\mathbf{z}^*) | L^\dagger | \psi_t(\mathbf{z}^*) \rangle}{\langle \psi_t(\mathbf{z}^*) | \psi_t(\mathbf{z}^*) \rangle}.$$

Just like its counterpart from classical mechanics, Eq. (2.32) is solved using the method of characteristics. The corresponding drift velocities are given by

$$\dot{z}_\lambda^*(t) = ig_\lambda e^{-i\omega_\lambda t} \langle L^\dagger \rangle_t. \quad (2.33)$$

We denote the corresponding flow<sup>5</sup> by  $\phi_t^*$ , or, using the more common notation,  $z_\lambda^*(t) = \phi_{\lambda,t}^*(z_\lambda^*)$  with initial conditions  $z_\lambda^*(0) = \phi_{\lambda,0}^*(z_\lambda^*) = z_\lambda^*$ . Equation (2.33) admits the following interpretation: If we start with a total state  $|\psi_t(\mathbf{z}^*)\rangle \otimes |\mathbf{z}\rangle$  of system and environment at time  $t$ , then the most relevant contribution to the full state at  $t + \Delta t$  corresponds to the coherent state  $|\mathbf{z} + \dot{\mathbf{z}}(t)\Delta t\rangle$ . For this reason, we

---

<sup>4</sup>We point out that the Husimi function is usually defined in terms of normalized coherent states, hence, there is an additional factor  $\exp(-|z_\lambda|^2)$  for each oscillator in our notation.

<sup>5</sup>In the following, we do not indicate the flow's non-holomorphic dependence on  $\mathbf{z}^*$ , caused by the expectation value of  $L^\dagger$  in Eq. (2.33), explicitly, because we consider  $\phi_t^*$  as a function of the initial coherent state label  $\mathbf{z}^*$  and the corresponding trajectory  $\psi_t(\mathbf{z}^*)$ .

should expand  $|\Psi_t\rangle$  with respect to  $|\mathbf{z}(t)\rangle$  instead of a fixed basis in order to capture the dominant proportion and avoid propagating states irrelevant for the final average.

It is the method of characteristics' essential point that the flow  $\phi_t$  yields a solution of Eq. (2.32) by

$$Q_t(\mathbf{z}, \mathbf{z}^*) = \int d^{2N} z_0 Q_0(\mathbf{z}_0, \mathbf{z}_0^*) \delta(\mathbf{z} - \phi_t(\mathbf{z}_0)), \quad (2.34)$$

where  $\delta(\mathbf{z} - \mathbf{z}') = \prod_{\lambda} \delta(\Re(z_{\lambda} - z'_{\lambda})) \delta(\Im(z_{\lambda} - z'_{\lambda}))$ . Our initial product state  $|\Psi_0\rangle = |\psi_0\rangle \otimes |\mathbf{0}\rangle$  combined with Eq. (2.31) yields the Husimi-function at  $t = 0$  exactly as the original Gaussian weight  $Q_0(\mathbf{z}, \mathbf{z}^*) = \pi^{-N} e^{-|\mathbf{z}|^2}$  for the time-independent coherent state basis. Therefore, Eq. (2.34) finally reduces Eq. (2.29) to the sought-after average over normalized trajectories, but now with a time-independent probability measure

$$\rho_t = \int \frac{d^{2N} z}{\pi^N} e^{-|\mathbf{z}|^2} \frac{|\psi_t(\phi_t^*(\mathbf{z}^*))\rangle \langle \psi_t(\phi_t^*(\mathbf{z}^*))|}{\langle \psi_t(\phi_t^*(\mathbf{z}^*)) | \psi_t(\phi_t^*(\mathbf{z}^*)) \rangle} = \mathbb{E} \left( \frac{|\tilde{\psi}_t\rangle \langle \tilde{\psi}_t|}{\langle \tilde{\psi}_t | \tilde{\psi}_t \rangle} \right). \quad (2.35)$$

Here, we have introduced relative states  $\tilde{\psi}_t(\mathbf{z}^*) = \psi_t(\phi_t(\mathbf{z}^*))$  corresponding to the comoving coherent basis<sup>6</sup>.

Of course, a practical application of Eq. (2.35) in a Monte-Carlo calculation crucially depends upon whether a closed equation of motion for  $\tilde{\psi}_t$  exists. Remarkably, the latter satisfy a nonlinear version of our convolutionless NMSSE (2.16) [DGS98] as we show now starting from

$$\partial_t(\psi_t \circ \phi_t^*) = \partial_t \psi_t \circ \phi_t^* + \sum_{\lambda} (\partial_{z_{\lambda}^*} \psi_t \circ \phi_t^*) \cdot (\partial_t \phi_{t,\lambda}^*). \quad (2.36)$$

The flow  $\phi_t^*$  in the first term amounts to evaluating the original equation of motion at the comoving coherent state  $\mathbf{z}(t)$ . Using its integral form

$$\phi_{t,\lambda}^*(z_{\lambda}^*) = z_{\lambda}^* + ig_{\lambda} \int_0^t \exp(-i\omega_{\lambda}s) \langle L^{\dagger} \rangle_s ds \quad (2.37)$$

---

<sup>6</sup>It is more common in the literature to introduce normalized trajectories  $\psi'_t = \tilde{\psi}_t / |\tilde{\psi}_t|$  directly without any reference to  $\tilde{\psi}_t$ . In this work however, the interim state  $\tilde{\psi}_t$  plays a particularly important role for the hierarchical equations of motion and is therefore designated explicitly.

plugged into the microscopic version of the process (2.12) yields a shifted driving process

$$\tilde{Z}_t^*(\mathbf{z}^*) := Z_t^*(\phi_t^*(\mathbf{z}^*)) = Z_t^*(\mathbf{z}^*) + \int_0^t \alpha(t-s)^* \langle L^\dagger \rangle_s ds. \quad (2.38)$$

Since the  $O$ -operator substitution ensures that the equation of motion for  $\psi_t(Z^*)$  is local with respect to  $Z^*$ , the first summand on the left hand side of Eq. (2.36) is obtained replacing  $Z_t^*$  by  $\tilde{Z}_t^*$  in the convolutionless NMSSE.

For the second summand, which accounts for the intrinsic time dependence of the shifted coherent states, we utilize the functional chain rule once again

$$\begin{aligned} \sum_{\lambda} \frac{\partial \phi_{t,\lambda}^*}{\partial t}(z_{\lambda}^*) \cdot \frac{\partial \psi_t}{\partial z_{\lambda}^*}(\phi_t^*(\mathbf{z}^*)) &= i \sum_{\lambda} g_{\lambda} e^{-i\omega_{\lambda} t} \langle L^\dagger \rangle_t \frac{\partial \psi_t}{\partial z_{\lambda}^*}(\phi_t^*(\mathbf{z}^*)) \\ &= \langle L^\dagger \rangle_t \int_0^t \alpha(t-s) \frac{\delta \psi_t}{\delta Z_s^*}(\phi_t^*(\mathbf{z}^*)) ds \\ &= \langle L^\dagger \rangle_t \bar{O}(t, \tilde{Z}^*) \tilde{\psi}_t(\tilde{Z}^*), \end{aligned}$$

where the last line reflects the definition of the  $\bar{O}$ -operator in Eqs. (2.15) and (2.17). Both terms of (2.36) combined yield the desired equation for  $\tilde{\psi}_t$

$$\partial_t \tilde{\psi}_t(\tilde{Z}^*) = -iH \tilde{\psi}_t(\tilde{Z}^*) + L \tilde{Z}_t^* \tilde{\psi}_t(\tilde{Z}^*) - (L^\dagger - \langle L^\dagger \rangle_t) \bar{O}(t, \tilde{Z}^*) \tilde{\psi}_t(\tilde{Z}^*). \quad (2.39)$$

Although  $\tilde{\psi}_t$  allows taking the average over normalized states, its equation of motion (2.39) does not preserve normalization over time. This can be achieved by adding further nonlinear terms: Considering trajectories  $|\psi'_t(\tilde{Z}^*)\rangle = |\tilde{\psi}_t(\tilde{Z}^*)\rangle / |\tilde{\psi}_t(\tilde{Z}^*)|$  it is straightforward to derive the corresponding equation of motion [DGS98] (dropping the arguments of  $\psi'_t(\tilde{Z}^*)$ )

$$\begin{aligned} \partial_t \psi'_t &= -iH \psi'_t + (L - \langle L \rangle_t) \tilde{Z}_t^* \psi'_t \\ &\quad - \left( (L^\dagger - \langle L^\dagger \rangle_t) \bar{O}(t, \tilde{Z}^*) - \left\langle (L^\dagger - \langle L^\dagger \rangle_t) \bar{O}(t, \tilde{Z}^*) \right\rangle_t \right) \psi'_t, \end{aligned} \quad (2.40)$$

where the quantum average  $\langle \cdot \rangle_t$  is taken with respect to  $\psi'_t$ . Once again, the Markov-limit amounts to  $\bar{O}(t, \tilde{Z}^*) = \frac{1}{2}L$  and replacing the noise process  $Z_t^*$  by a complex White Noise. Thus, we obtain the well-known nonlinear unravelling of a Lindblad master equation 1.2.

As mentioned in the motivation, the nonlinear equations should be given precedence over the linear version when it comes to Monte-Carlo simulation. Although it requires propagating a new time-nonlocal, scalar quantity, namely  $\langle L^\dagger \rangle_s$  for  $0 \leq s \leq t$  in the shifted noise  $\tilde{Z}_t^*$ , the improved convergence with respect to the number of realizations compensates by far the additional computational demands.

## 2.4. Interpretation of the NMSSE

In contrast to classical mechanics, assigning a reduced pure state to an open quantum system fails in general. Due to entanglement with the environment built up by interaction, the reduced state is described consistently only by a mixture. However, quantum trajectories obtained as solutions of a linear or nonlinear Markovian stochastic Schrödinger equation are more than simply a convenient tool for calculations. They arise as trajectories of post-measurement pure states conditioned on a time-continuous measurement outcome, because the interaction with a measurement apparatus destroys system-environment entanglement [Car93, BG09].

The question, whether the NMSSE investigated in this work admits a similar interpretation, has been answered negative for a large class of models only recently: Krönke and Strunz [KS12] derived a consistency condition necessary for a measurement interpretation of the linear, convolutionless NMSSE with an  $O$ -operator that depends at most linearly on the noise process. This condition is violated by all exemplary systems under consideration, except in the Markov limit  $\alpha(t) \sim \delta(t)$ .

We now present a different, less practical and more figurative interpretation of the linear NMSSE (2.13). The main goal is to establish the NMSSE as an alternative description for the unitary system-bath time evolution in terms of a “generalized environment”. Recall that the relative state  $\psi_t(\mathbf{z}^*) = \langle \mathbf{z}^* | \Psi_t \rangle$  can be expanded in a power-series

$$\begin{aligned} \psi_t(\mathbf{z}^*) &= \sum_{n_1, \dots, n_N} \psi_t(n_1, \dots, n_N) z_1^{*n_1} \dots z_N^{*n_N} \\ &= \sum_{K=0}^{\infty} \left( \sum_{\lambda_1, \dots, \lambda_K=1}^N \psi_t^{(K)}(\lambda_1, \dots, \lambda_K) z_{\lambda_1}^* \dots z_{\lambda_K}^* \right), \end{aligned} \quad (2.41)$$

where the second line amounts to a simple rearrangement of the summands to combine powers of  $\mathbf{z}^*$  with equal order  $K$ . The  $\lambda_i$  run over all modes  $\lambda_i = 1, \dots, N$  and the expansion-coefficients  $\psi_t^{(K)}(\lambda_1, \dots, \lambda_K)$  can be chosen completely symmetric under permutations of the  $\lambda_i$ . Except for a normalization constant,  $\psi_t(n_1, \dots, n_N)$  describes the bath state relative to an environmental number state  $|n_1, \dots, n_N\rangle$ .

Now, the key observation is that the Dyson series (2.22) provides a similar representation for  $\psi_t(Z^*)$  after rearranging all system operators and functional derivatives. Since  $\psi_0$  is independent from noise, that is  $\frac{\delta\psi_0}{\delta Z_s^*} = 0$ , only powers of  $Z_s^*$  with  $0 \leq s \leq t$  from  $H_{\text{tot}}(s)$  contribute. Using the usual symmetrization of the integral boundaries, the sought-after expansion reads

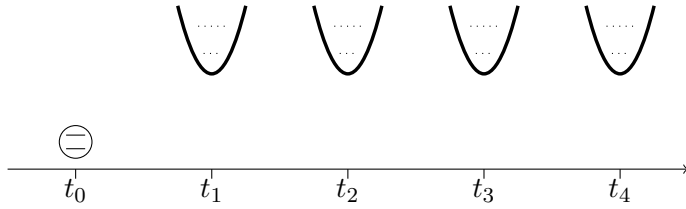
$$\psi_t(Z^*) = \sum_K \int_0^t dt_1 \dots \int_0^t dt_K \psi_t^{(K)}(t_1, \dots, t_K) Z_{t_1}^* \dots Z_{t_K}^*, \quad (2.42)$$

with  $\psi_t^{(K)}(t_1, \dots, t_K)$  totally symmetric under permutation of the  $t_i$ . Similar to the expansion (2.41) with respect to physical environmental oscillator modes  $\lambda$ , we propose to interpret Eq. (2.42) as an expansion with respect to fictitious modes indexed by  $t$ . Stretching the analogy even a little further, we refer to the latter as “*time-oscillators*”, although we have no expression for their “free” Hamiltonian let alone a harmonic oscillator form. From this point-of-view, the bath of time-oscillators takes the role of an environment for the system.

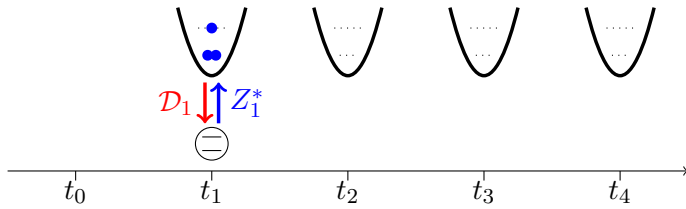
Remarkably, the environmental operators in the full Hamiltonian (2.23), namely multiplication by  $Z_t^*$  and  $\mathcal{D}_t$ , have a simple interpretation in this picture: The former simply acts as a creation operator for the time-oscillator-mode  $t$  exactly as multiplication by  $z_\lambda^*$  acts as a creation operator for the physical oscillator-mode  $\lambda$ . Of course, in the coherent state representation the corresponding annihilation operator is given by  $\partial_{z_\lambda^*}$ . The connection to the time-oscillator picture is most clearly explained using the expansion (2.41) yielding

$$\partial_{z_\lambda^*} \psi_t(\mathbf{z}^*) = \sum_{K=1}^{\infty} \left( \sum_{\lambda_1, \dots, \lambda_{K-1}=1}^N K \psi_t^{(K)}(\lambda_1, \dots, \lambda_{K-1}, \lambda) z_{\lambda_1}^* \dots z_{\lambda_{K-1}}^* \right),$$

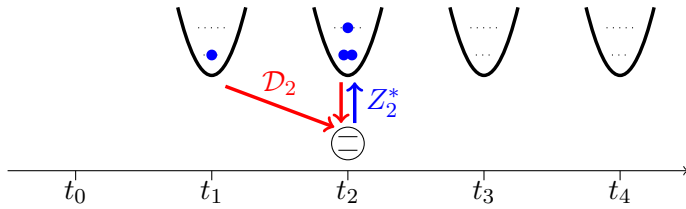
where we use the symmetry of  $\psi_t^{(K)}(\lambda_1, \dots, \lambda_K)$  under permutation of the arguments and the independence-condition  $\partial_{z_\lambda^*} z_\mu^* = \delta_{\lambda, \mu}$ . Similarly, annihilating an excitation of



- (A) At  $t = t_0$  all time-oscillators are in their ground-state due to the vacuum initial conditions.



- (B) At  $t = t_1$ , the system interacts with the first time-oscillator, which is left in an excited state due to dissipated energy from the system. Since the remaining environment is still in its ground-state, the interaction via  $\mathcal{D}_1$  is restricted to the first time-oscillator as well.



- (C) For the next step  $t = t_2$ , the excitation of the bath is time-local as well—in general, the creation operator  $Z_n^*$  only changes the state of the single time-oscillator  $t_n$ . However, memory effects arise due to the feedback of the environment:  $\mathcal{D}_2$  receives contributions from both preceding time steps, unless the weight-factor  $\alpha_1$  vanishes.

**Figure 2.2.:** Pictorial interpretation of the time evolution described by the NMSSE. The circle with two lines represents the system, while the harmonic potentials identify various time-oscillators.

the time-oscillator mode  $s$  for  $0 < s < t$  in Eq. (2.42) is achieved using the functional derivative

$$\frac{\delta \psi_t(Z^*)}{\delta Z_s^*} = \sum_K \int_0^t dt_1 \dots \int_0^t dt_{K-1} K \psi^{(K)}(t_1, \dots, t_{K-1}, s) Z_{t_1}^* \dots Z_{t_{K-1}}^*,$$

since it satisfies the continuum independence-condition  $\frac{\delta Z_s^*}{\delta Z_t^*} = \delta(t - s)$ .

However, there is an important difference to the true bosonic ladder-operators: As the microscopic definition (2.12) implies, the adjoint operator<sup>7</sup> of multiplication by  $Z_t^*$  is not the derivation  $\frac{\delta}{\delta Z_t^*}$ , but  $\mathcal{D}_t = \int ds \alpha(t - s) \frac{\delta}{\delta Z_s^*}$ . In other words, although we interpret  $Z_t^*$  as a creation operator of a time-oscillator mode  $t$ , the corresponding adjoint operator  $\mathcal{D}_t$  does not simply annihilate an excitation of the same mode, but of all modes  $s$  weighted by the correlation function  $\alpha(t - s)$ .

To explain the related interpretation of the NMSSE more clearly, we switch to a discrete time step  $\Delta t$  and set  $t_n = n\Delta t$ . We introduce the corresponding time-discrete “process”  $Z_n^* = \frac{1}{\Delta t} \int_{t_{n-1}}^{t_n} Z_t^* dt$  and the derivation operator  $\mathcal{D}_n = \sum_k \alpha_{n-k} \partial_{Z_k^*}$  in Appendix A. This allows us to approximate the time evolution for one step as

$$\psi_{t_n}(Z^*) = e^{\Delta t(LZ_n^* - L^\dagger \mathcal{D}_n)} e^{-i\Delta t H} \psi_{t_{n-1}},$$

with a free evolution of the system followed by an interaction with the time-oscillators—see Appendix A for the details. Already Fig. 2.2 displays the basic structure of the interaction

$$LZ_n^* - L^\dagger \mathcal{D}_n = LZ_n^* - L^\dagger \sum_k \alpha_{n-k} \frac{\partial}{\partial Z_k^*}.$$

Since the creation operator  $Z_n^*$  involves only a single time-oscillator, the latter receive an excitation only once during the time evolution. In contrast, the annihilation operators  $\partial_{Z_k^*}$  appear in each time step weighted by the bath-correlation function  $\alpha_{n-k}$ . Except for the Markov limit  $\alpha_{n-k} = \gamma \delta_{nk}$ , memory effects arise by coupling to previously excited time-oscillators. Of course, such a causal interpretation works only

---

<sup>7</sup>Since the scalar-product in the full system-bath Hilbert space is given by

$$\langle \Psi | \Phi \rangle = \int \frac{d^{2N}z}{\pi^N} e^{-|z|^2} \langle \psi(z^*) | \phi(z^*) \rangle = \mathbb{E} (\langle \psi(Z^*) | \phi(Z^*) \rangle),$$

this is exactly the statement of Novikov’s formula (2.27) with  $P_t$  replaced by  $\langle \psi(Z^*) | \phi(Z^*) \rangle$ .

for an initial vacuum state of the environment. If  $\partial_{Z_k^*} \psi_0 \neq 0$ , we get contributions to  $\mathcal{D}_n$  from all initially excited time-oscillators and therefore, the interpretation does not correspond to the common picture of an “environment with memory”.

## 2.5. Finite Temperature Theory

Until now, we were only concerned with the zero temperature theory, which is characterized by an initial product  $|\Psi_0\rangle = |\psi_0\rangle \otimes |\mathbf{0}\rangle$  with the environment in the vacuum state. It translates into our NMSSE-framework as the demand of vanishing functional derivatives  $\frac{\delta\psi_0}{\delta Z_s^*} = 0$  for arbitrary  $s$ . This property ensures the bounded integral domain of  $\mathcal{D}_t = \int ds \alpha(t-s) \frac{\delta}{\delta Z_s^*}$ , which on the other hand is crucial for a causal interpretation in terms of time-oscillators. Also, the  $O$ -operator substitution as well as the hierarchical equations of motion depend on the temperature-zero assumption. In order to treat a thermal environment at arbitrary temperature, we present a method that maps to the vacuum initial conditions.

Let us consider an initial product, where the bath is described by a Gibbs state  $\rho(\beta) = Z^{-1} e^{-\beta H_{\text{env}}}$ ; more precisely

$$\rho_0 = |\psi_0\rangle\langle\psi_0| \otimes \rho(\beta), \quad (2.43)$$

with the bath partition function  $Z = \text{Tr } e^{-\beta H_{\text{env}}}$  at inverse temperature  $\beta = T^{-1}$ . However, we cannot drop the requirement of separability for the initial state.

The thermo-field approach [SU83] is based on the simple trick that a thermal state  $\rho(\beta)$  can be expressed as vacuum in an enlarged environment, doubling the degrees of freedom. It is favored over other methods in the application to the NMSSE since it preserves its structure. Additionally, it constitutes a consistent way to include negative frequency oscillators in the environment, which on the other hand are required for the bath correlation function used to derive our hierarchy. The last point is further elaborated in Sect. 3.2. In the course of this section we follow the more detailed accounts of Yu and Strunz [Yu04, Str01].

The main idea is to introduce a second fictitious bath of oscillators  $\mathcal{B}$ , which is independent from the physical environment  $\mathcal{A}$  and does not interact with the sys-

tem. Expressing its degrees of freedom in ladder operators  $b_\lambda$  and  $b_\lambda^\dagger$  yields the new Hamiltonian in the Schrödinger picture

$$H_{\text{tot}} = H \otimes \mathbf{I} + \sum_{\lambda} (g_\lambda^* L \otimes a_\lambda^\dagger + g_\lambda L^\dagger \otimes a_\lambda) + \mathbf{I} \otimes \sum_{\lambda} \omega_\lambda (a_\lambda^\dagger a_\lambda - b_\lambda^\dagger b_\lambda). \quad (2.44)$$

Although the corresponding eigen-energies are not bounded from below due to negative frequencies of the fictitious oscillators, there are no stability problems since the latter do not interact with the physical degrees of freedom. For the same reason, the reduced time evolution obtained from Eq. (2.44) is identical to the original microscopic model (2.4). Both yield equal reduced density matrices provided we choose an initial state  $\tilde{\rho}$  for environments  $\mathcal{A}$  and  $\mathcal{B}$  that reproduces the environmental state in Eq. (2.43) after tracing over the unphysical degrees of freedom, that is

$$\text{Tr}_{\mathcal{B}} \tilde{\rho} = \rho(\beta). \quad (2.45)$$

Here,  $\text{Tr}_{\mathcal{B}}$  denotes the partial trace with respect to the fictitious degrees of freedom.

Remarkably, a solution  $\tilde{\rho}$  of Eq. (2.45) is given by a pure state projector on a vacuum state with respect to new annihilation operators  $A$ ,  $B$ . They are connected to the old ladder operators by a temperature dependent *Bogoliubov transformation*

$$\begin{aligned} A_\lambda &= \sqrt{\bar{n}_\lambda + 1} a_\lambda + \sqrt{\bar{n}_\lambda} b_\lambda^\dagger \\ B_\lambda &= \sqrt{\bar{n}_\lambda} a_\lambda^\dagger + \sqrt{\bar{n}_\lambda + 1} b_\lambda, \end{aligned}$$

with  $\bar{n}_\lambda = (\exp(\beta\omega_\lambda) - 1)^{-1}$  denoting the mean thermal occupation number of the (physical) oscillator mode  $\lambda$ . An extensive but elementary calculation reveals that  $\tilde{\rho} = |0_{AB}\rangle\langle 0_{AB}|$  with  $|0_{AB}\rangle = |0_A\rangle \otimes |0_B\rangle$  satisfies Eq. (2.45) [SU83]. The doubling in degrees of freedom ensures that the reduced density matrix obtained from an initial pure state  $|\tilde{\Psi}_0\rangle = |\psi_0\rangle \otimes |0_{AB}\rangle$  in the enlarged Hilbert space coincides with the

original state at finite temperature (2.43). Expressed in these new coordinates the total Hamiltonian (2.44) reads

$$\begin{aligned} H_{\text{tot}} = & H \otimes I + \sum_{\lambda} \sqrt{\bar{n}_{\lambda} + 1} \left( g_{\lambda}^* L \otimes A_{\lambda}^{\dagger} + g_{\lambda} L^{\dagger} \otimes A_{\lambda} \right) \\ & + \sum_{\lambda} \sqrt{\bar{n}_{\lambda}} \left( g_{\lambda} L^{\dagger} \otimes B_{\lambda}^{\dagger} + g_{\lambda}^* L \otimes B_{\lambda} \right) \\ & + I \otimes \sum_{\lambda} \omega_{\lambda} \left( A_{\lambda}^{\dagger} A_{\lambda} - B_{\lambda}^{\dagger} B_{\lambda} \right). \end{aligned} \quad (2.46)$$

This is identical to the zero temperature model, except now the system is coupled to two separate harmonic baths instead of one. Therefore, we need two independent processes  $Z_t^*$  and  $W_t^*$  for a stochastic version of Eq. (2.46) in general:

$$\begin{aligned} \partial_t \psi_t = & -iH\psi_t + LZ_t^*\psi_t - L^{\dagger} \int_0^t \alpha_1(t-s) \frac{\delta\psi_t}{\delta Z_s^*} ds \\ & + L^{\dagger} W_t^* \psi_t - L \int_0^t \alpha_2(t-s) \frac{\delta\psi_t}{\delta W_s^*} ds. \end{aligned} \quad (2.47)$$

All effects of the original thermal initial state are now encoded in the correlation functions

$$\alpha_1(t) = \sum_{\lambda} (\bar{n}_{\lambda} + 1) |g_{\lambda}|^2 e^{-i\omega_{\lambda} t} \quad \text{and} \quad \alpha_2(t) = \sum_{\lambda} \bar{n}_{\lambda} |g_{\lambda}|^2 e^{i\omega_{\lambda} t} \quad (2.48)$$

for  $Z_t^*$  and  $W_t^*$  respectively. Both are Gaussian, thus independence of  $Z^*$  and  $W^*$  is equivalent to vanishing mutual covariance  $\mathbb{E}(Z_t^* W_s) = \mathbb{E}(Z_t W_s) = 0$ .

As we doubled the bath degrees of freedom merely to cope with a thermal initial state, it is quite natural that the zero-temperature result (2.13) with a single noise process is recovered in the limit  $T \rightarrow 0$ : With vanishing occupation numbers  $n_{\lambda} \rightarrow 0$  both,  $\alpha_2$  and  $W_t^*$ , go to zero, while  $\alpha_1$  reproduces the original bath correlation function (2.7).

The thermo-field approach is especially simple for a self-adjoint coupling operator  $L = L^{\dagger}$ . Indeed, we can combine both processes in Eq. (2.47) into a single one, which

we denote by  $\tilde{Z}_t^* Z_t^* + W_t^*$ . Since  $Z^*$  and  $W^*$  are mutual independent by assumption and  $2\bar{n}_\lambda + 1 = \coth \frac{\beta\omega_\lambda}{2}$ , we find for the crucial correlation function

$$\mathbb{E}(\tilde{Z}_t \tilde{Z}_s^*) = \sum_{\lambda} \left( |g_{\lambda}|^2 \coth \frac{\beta\omega_{\lambda}}{2} \cos \omega_{\lambda}(t-s) - i \sin \omega_{\lambda}(t-s) \right). \quad (2.49)$$

Consequently, the finite temperature NMSSE with self-adjoint coupling operators is identical to the  $T = 0$  version except for a modified correlation function. It is not surprising that the combined correlation function (2.49) agrees with the result of Feynman and Vernon already encountered in Eq. (2.6), which is usually derived by means of path integration [FV63]. But the approach presented here is much more general since it can tackle any kind of open quantum system with linear coupling.

## 2.6. Jaynes-Cummings Model

The Jaynes-Cummings model was originally introduced to study the decay of an atom coupled to a single quantized mode of the electro-magnetic field in a cavity [JC63]. It describes a single electronic excitation of the atom with energy  $\omega$  above ground state in terms of an effective two level system with  $H = \frac{\omega}{2}\sigma_z$ . Other electronic levels can be neglected safely, if their excitation energy is much larger than  $\omega$  or far off-resonant compared to the cavity mode. In dipole and rotating-wave approximation the system's coupling operator to the bath is  $L = g\sigma_-$ , therefore, the corresponding NMSSE reads

$$\partial_t \psi_t(Z^*) = -i\frac{\omega}{2}\sigma_z \psi_t(Z^*) + g\sigma_- Z_t^* \psi_t(Z^*) - g\sigma_+ \int_0^t \alpha(t-s) \frac{\delta \psi_t(Z^*)}{\delta Z_s^*} ds. \quad (2.50)$$

supplied with initial conditions  $\psi_0(Z^*) = \psi_0$ . This approximation holds as long as the coupling strength  $g$  is very small compared to the cavity transition frequency. Only recently, experiments in circuit quantum electrodynamics detected effects from so called counter-rotating interaction terms [NDH<sup>+</sup>10]. Here, we also cover the more general case of a possibly structured environment.

The Jaynes-Cummings model is a rare example, where an analytic solution for the  $O$ -operator is known [DGS98], which we outline first. Afterwards, we present a

new solution-strategy, which is more in the spirit of this work, and discuss a possible problem of the  $O$ -operator substitution in numerical calculations.

### 2.6.1. O-Operator Method

As elaborated in Sect. 2.2.1 we can simplify the NMSSE (2.50) by replacing the functional derivative with an operator  $O(t, s, Z^*)$ . We try to solve the consistency condition (2.18) by a noise-independent ansatz [DGS98]

$$O(t, s) = gf(t, s)\sigma_- \quad (2.51)$$

Hence, all non-Markovian feedback from the environment is now encoded in the function  $f(t, s)$  to be determined. Plugging this ansatz into the evolution equation for  $O(t, s)$  yields

$$\partial_t f(t, s)\sigma_- = \left[ -i\frac{\omega}{2}\sigma_z - g^2 F(t)\sigma_+\sigma_-, f(t, s)\sigma_- \right] \quad (2.52)$$

with the shorthand notation  $F(t) := \int_0^t \alpha(t-s)f(t, s) ds$ . From its definition (2.17), we see that  $F(t)$  is also the coefficient of the integrated operator  $\bar{O}(t) = gF(t)\sigma_-$ . Since the operator algebra in Eq. (2.52) closes, our ansatz solves the equation of motion for  $O(t, s)$  provided  $f(t, s)$  evolves according to

$$\partial_t f(t, s) = (i\omega + g^2 F(t)) f(t, s), \quad 0 \leq s \leq t.$$

Appropriate initial conditions follow trivially from Eq. (2.19), namely  $f(s, s) = 1$ . In the special case of an exponential bath correlation function  $\alpha(t) = e^{-\gamma|t|-i\Omega t}$  we can also derive a differential equation that is closed in  $F$ , namely

$$\partial_t F(t) = 1 + (i(\omega - \Omega) - \gamma)F(t) + g^2 F(t)^2. \quad (2.53)$$

Such exponential correlation functions  $\alpha(t) = e^{-\gamma|t|-i\Omega t}$  play a major role in the subsequent work. Once  $F$  is known, we can determine solutions of the convolutionless NMSSE (2.16) for given noise realizations or—since  $O$  is independent of  $Z^*$ —directly calculate the reduced density operator using the master equation (2.28).

### 2.6.2. Noise-Expansion Method

In this section we propose a different approach to Eq. (2.50). It is based on the expansion discussed in Sect. 2.4, which allows us to express the quantum trajectories  $\psi_t(Z^*)$  in a functional Taylor series with respect to the noise process

$$\psi_t(Z^*) = \begin{pmatrix} \psi^+(t) \\ \psi^-(t) \end{pmatrix} + \int_0^t \begin{pmatrix} \psi_s^+(t) \\ \psi_s^-(t) \end{pmatrix} Z_s^* ds.$$

Due to the particular coupling structure of the model we make an ansatz at most linear in  $Z_t^*$ . As further elaborated in Sect. B.1 our NMSSE (2.50) reduces to a  $\mathbb{C}$ -valued integro-differential equation

$$\dot{\psi}^+(t) = -i\frac{\omega}{2}\psi^+(t) - g^2 \int_0^t \alpha(t-s)e^{i\frac{\omega}{2}(t-s)}\psi^+(s) ds \quad (2.54)$$

with initial conditions  $\psi^+(0) = \psi_0^+$ , which is nevertheless quite involved—even from a numerical point of view. Again, the situation simplifies dramatically for an exponential correlation function; the details are provided in Sect. B.2.

Nevertheless, we may still discover some illuminating consequences concerning the  $O$ -operator without an explicit solution for  $\psi^+(t)$ . With  $\psi^-(t) = \psi_0^- \exp(i\omega t/2)$  the full quantum trajectory reads

$$\psi_t(Z^*) = \begin{pmatrix} \psi^+(t) \\ \psi^-(t) \end{pmatrix} + g \int_0^t \begin{pmatrix} 0 \\ e^{i\frac{\omega}{2}(t-s)}\psi^+(s) \end{pmatrix} Z_s^* ds. \quad (2.55)$$

This allows us to calculate the functional derivative with respect to the noise process explicitly; for  $0 < s < t$  we find

$$\frac{\delta \psi_t(Z^*)}{\delta Z_s^*} = g \begin{pmatrix} 0 \\ e^{i\frac{\omega}{2}(t-s)}\psi^+(s) \end{pmatrix},$$

which agrees with our ansatz (2.51) if we choose

$$f(t, s) = \frac{\psi^+(s)}{\psi^+(t)} e^{i\frac{\omega}{2}(t-s)}. \quad (2.56)$$

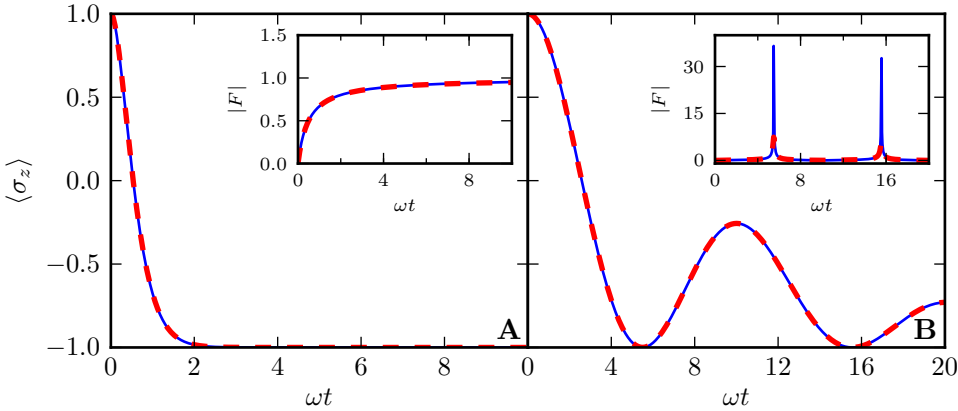


**Figure 2.3.:** Expectation value  $\langle \sigma_z \rangle$  for the Jaynes-Cummings model with an exponentially decaying bath correlation function  $\alpha(t) = \frac{\gamma}{2}e^{-\gamma|t|-i\Omega t}$  in resonance ( $\Omega = \omega$ ) and coupling strength  $g = \sqrt{2}$  calculated using Eq. (B.11). Insets show  $|F|$  representing magnitude of  $\bar{O}$ . **(A)** Strongly damped  $\gamma = 4\omega$ , **(B)** Weakly damped  $\gamma = 0.1\omega$ ; the dashed line represent the same parameter set, but slightly moved off-resonance ( $\Omega = 1.01\omega$ ).

A similar structure for the  $O$ -operator has been obtained before using a Heisenberg-operator technique [Str01].

Recall that the convolutionless NMSSE of the last section reduces to a nonlinear differential equation (2.53) for

$$F(t) = \int_0^t \alpha(t-s)e^{i\frac{\omega}{2}(t-s)} \frac{\psi^+(s)}{\psi^+(t)} ds, \quad (2.57)$$

where  $f(t, s)$  has already been replaced by the expression (2.56). We will now argue that it is exactly the denominator  $\psi^+(t)$  that may cause problems in a numerical integration of (2.53). Indeed, calculating the reduced density matrix from Eq. (2.55) and using the condition  $\text{Tr } \rho_t = 1$ , we find the connection  $\langle \sigma_z \rangle_{\rho_t} = 2|\psi^+(t)|^2 - 1$ .

Since for  $\gamma \neq 0$  the atom described by the two-level system is expected to relax to its ground state, the denominator in (2.57) eventually goes to zero. Even worse are local extremal points  $t_i$ , where  $\langle \sigma_z \rangle_{\rho_t} \approx -1$ , as we see in Fig. 2.3: The excitation in A decays almost exponentially due to the small memory time  $\tau = \gamma^{-1}$  of the environment. Therefore,  $\frac{\psi^+(s)}{\psi^+(t)} \approx 1$  in the relevant time scale  $s \in [t-\tau, t]$  of Eq. (2.57),

so  $|F|$  approaches a constant value uniformly. In contrast, the highly non-Markovian system B shows singular peaks in  $|F|$  for  $\omega t \approx 5, 15$ , where the expectation value of  $\sigma_z$  is approximately  $-1$ . These result from large fractions  $\frac{\psi^+(s)}{\psi^+(t)}$ , as the correlation function  $\alpha(t - s)$  does not decay rapidly enough to suppress contributions in the integral with  $\psi^+(s) \gg \psi^+(t)$ .

These two different types of behavior for  $|F|$  are quite similar to the resonantly driven harmonic oscillator with strong or weak damping. Also, notice how shifting the bath-frequency  $\Omega$  only slightly off-resonance results in a much smoother  $F$ —as the dashed line in Fig. 2.3 B shows—while  $\langle \sigma_z \rangle$  remains virtually unchanged. Actually, these large peaks do not contribute excessively to the end result, as they are canceled with the very small value of  $\psi^+(t)$  in  $\bar{O}(t)\psi_t(Z^*)$  (or in the corresponding master equation). Still, the numerical solution of Eq. (2.53) requires a more careful treatment for the resonant case in order to correctly reproduce these peaks and not diverge to infinity.

Of course, all statements made in this section only hold for the simple Jaynes-Cummings model, and it is not clear, whether the  $\bar{O}$ -operator behaves similarly for more realistic systems. Notwithstanding, an even more problematic behavior of  $\max_{m,n} |\bar{O}_{mn}(t)|$ , where  $\bar{O}_{mn}(t)$  are the matrix elements of  $\bar{O}(t)$  in the system-basis used, has been found in ZOFE-calculations for certain parameter regimes of more realistic systems<sup>8</sup>. As for a larger number of bath modes resonances are more likely to occur, the situation is much more delicate in that case. Likely, these numerical sophisticated problems are also responsible for divergences of higher order hierarchies in the  $O$ -operator making a systematic improvement of ZOFE quite involved. We come to the conclusion that it can be advantageous to devise a numerical scheme in terms of the more regular  $\bar{O}(t, Z^*)\psi_t(Z^*)$  instead, as sharp contributions during the propagation might be smoothed away—this is exactly the approach used for our stochastic hierarchical equations of motion presented in the next chapter.

---

<sup>8</sup>Gerhard Ritschel, private communications. ZOFE stands for zero-order functional expansion and was introduced in Sect. 2.2.1.

### 3. Hierarchy of Stochastic Pure States

The Jaynes-Cummings model from the last chapter is one of the rare cases where an analytical ansatz for  $\bar{O}$  is known. Numerical solution-methods of the convolutionless non-Markovian stochastic Schrödinger equation usually attack the consistency condition (2.18) directly using an expansion of  $\bar{O}$  with respect to the noise [YDGS99, RRSE11]. Although this provides an efficient algorithm for large parameter regimes, the problems presented in the last chapter impede systematic improvements.

With recent advances in super-computing, realistic biological and chemical systems came within the reach of the far more costly, but better-behaved and formally exact hierarchical-equations-of-motion (HEOM) approach [Tan06]. Although formally equivalent to the Feynman-Vernon influence functional, the HEOM-formalism is much better suited for numerical investigations, since it provides a systematic way to check convergence and does not require evaluation of highly-oscillatory path integrals. Summarized shortly, it amounts to dealing with memory effects in the influence-functional by introducing additional auxiliary density matrices (ADMs). Therefore, the single equation of motion for  $\rho_t$  is transferred into a much simpler hierarchy of memory-less differential equations, which allows for a straightforward numerical integration. However, the number of ADMs grows rapidly for highly non-Markovian systems. Combined with the  $N^2$ -scaling of the memory requirement<sup>1</sup> with the system's dimension  $N$ , this places enormous demands on the computational infrastructure.

In this chapter, we present the main result of this work: a hierarchy of stochastic, pure state trajectories in the spirit of the established HEOM-formalism. At the beginning, we derive the pure-state hierarchy based on the NMSSE in its linear, as well as nonlinear version. Since the derivation of the hierarchy crucially relies on an exponential bath-correlation function (or sums thereof), Sect. 3.2 is devoted to

---

<sup>1</sup>Sparse.matrix algorithms are able to reduce the  $N^4$ -scaling of the propagation matrices, but still, these are even more problematic than the ADMs.

an expansion of more general spectral densities at finite temperature providing the necessary form. Finally, we apply the hierarchy of stochastic pure states to the Spin-Boson model, investigating its accuracy in dependence on the sample size and number of auxiliary states.

### 3.1. Derivation of the Hierarchy

In this section, we present the main results of this work, namely an approach to solve the non-Markovian stochastic Schrödinger equation

$$\partial_t \psi_t(Z^*) = -i\hbar \psi_t(Z^*) + LZ_t^* \psi_t(Z^*) - L^\dagger \int_0^t \alpha(t-s) \frac{\delta \psi_t(Z^*)}{\delta Z_s^*} ds \quad (3.1)$$

numerically without resorting to the  $O$ -operator substitution. Therefore, we need to conceive a different way to deal with the non-locality of the functional derivative with respect to time and process realization, as it prevents the application of efficient Monte-Carlo methods, which are used to deal with stochastic Schrödinger equations in the Markovian regime [Car93, Per98]. It turns out that for certain correlation functions the linear NMSSE (3.1) is formally equivalent to an infinite hierarchy of completely local stochastic differential equations.

#### 3.1.1. Linear Hierarchy

The basic idea is to absorb the action of the functional derivative on  $\psi_t(Z^*)$  into an auxiliary pure state

$$\psi_t^{(1)}(Z^*) := \int_0^t \alpha(t-s) \frac{\delta \psi_t(Z^*)}{\delta Z_s^*} ds. \quad (3.2)$$

Hereinafter, we use the term ‘‘state’’ quite loosely for any vector in the system’s Hilbert space regardless of its norm. Recall that the integral boundaries arise only after we apply the derivative on states  $\psi_t(Z^*)$  that satisfy the additional condition  $\delta \psi_t(Z^*)/\delta Z_s^* = 0$  for  $s < 0$  and  $s > t$ . Therefore, we may write Eq. (3.2) more concisely as

$$\psi_t^{(1)}(Z^*) = \left( \int \alpha(t-s) \frac{\delta}{\delta Z_s^*} ds \right) \psi_t(Z^*) =: \mathcal{D}_t \psi_t(Z^*)$$

with the integrated functional derivation operator  $\mathcal{D}_t$ . For a finite environment,  $\mathcal{D}_t$  is simply the representation of the force operator (2.5) in the time-independent coherent state basis.

The equation of motion for  $\psi_t^{(1)}(Z^*)$  takes a form similar to the original NMSSE (3.1), provided  $\dot{\mathcal{D}}_t = \int \dot{\alpha}(t-s) \delta/\delta Z_s^* ds$  can be expressed in terms of known quantities. Of course, the simplest choice is an exponential bath correlation function

$$\alpha(t) = g e^{-\gamma|t| - i\Omega t} \quad (3.3)$$

with  $g$ ,  $\gamma$  and  $\Omega$  real. The absolute value of  $t$  in the exponent is necessary to ensure hermiticity  $\alpha(-t) = \alpha(t)^*$ . In Sect. C.1 we elaborate that such a correlation function simply gives

$$\dot{\mathcal{D}}_t \psi_t(Z^*) = -(\gamma + i\Omega) \mathcal{D}_t \psi_t(Z^*) \quad (3.4)$$

for solutions  $\psi_t(Z^*)$  of the NMSSE with vacuum initial conditions. We abbreviate the coefficient  $w = \gamma + i\Omega$  in order to simplify notation.

Now, let us return to the NMSSE. With the auxiliary stochastic state (3.2) it can be expressed as an inhomogeneous stochastic equation, namely

$$\partial_t \psi_t(Z^*) = -iH \psi_t(Z^*) + LZ_t^* \psi_t(Z^*) - L^\dagger \psi_t^{(1)}(Z^*).$$

By the construction in the previous paragraph, the last term satisfies the closely related equation

$$\begin{aligned} \partial_t (\mathcal{D}_t \psi_t) &= -w \mathcal{D}_t \psi_t + \mathcal{D}_t (-iH + LZ_t^* - L^\dagger \mathcal{D}_t) \psi_t \\ &= (-iH - w + LZ_t^*) \psi_t^{(1)} + [\mathcal{D}_t, Z_t^*] L \psi_t - L^\dagger \mathcal{D}_t \psi_t^{(1)}. \end{aligned} \quad (3.5)$$

Naturally,  $\mathcal{D}_t$  commutes with all system operators and itself. Not surprising, the functional derivative reappears in the equation for  $\psi_t^{(1)}$ , therefore, we need to introduce another auxiliary state  $\psi_t^{(2)}(Z^*)$ . This scheme leads to an infinite hierarchy of stochastic vectors in the system's Hilbert space

$$\psi_t^{(k)}(Z^*) := \mathcal{D}_t \psi_t^{(k-1)}(Z^*) = \mathcal{D}_t^k \psi_t(Z^*). \quad (3.6)$$

### 3. Hierarchy of Stochastic Pure States

---

Expressed in the new auxiliary states and with  $[\mathcal{D}_t, Z_s^*] = \alpha(t - s)$ , Eq. (3.5) reads

$$\partial_t \psi_t^{(1)}(Z^*) = (-iH - w + LZ_t^*) \psi_t^{(1)}(Z^*) + \alpha(0)L\psi_t^{(0)}(Z^*) - L^\dagger \psi_t^{(2)}(Z^*).$$

Along these lines it is straightforward to derive the full hierarchy of equations of motions for all  $\psi_t^{(k)}$ . Since the commutator  $[\mathcal{D}_t, Z_s^*]$  is a  $\mathbb{C}$ -number, each auxiliary state only couples to the order directly above and below

$$\partial_t \psi_t^{(k)}(Z^*) = (-iH - kw + LZ_t^*) \psi_t^{(k)}(Z^*) + k\alpha(0)\psi_t^{(k-1)}(Z^*) - L^\dagger \psi_t^{(k+1)}(Z^*). \quad (3.7)$$

The vacuum initial condition for the true quantum trajectory  $\delta\psi_0/\delta Z_s^* = 0$  requires all auxiliary states to vanish at  $t = 0$ .

Of course the infinite hierarchy is even more intricate to solve than the original NMSSE. To transform Eq. (3.7) into a practical scheme, we truncate the hierarchy at finite order. It is quite remarkable that this can be done in a self-consistent manner, which even incorporates the neglected orders approximately. This is derived most clearly using the equivalent integral equation for  $\psi_t^{(k)}$  (with  $w = \gamma + i\Omega$  reinserted)

$$\begin{aligned} \psi_t^{(k)}(Z^*) &= \int_0^t e^{-k\gamma(t-s)-ik\Omega(t-s)} \times \\ &\quad \times T_+ e^{\int_s^t -iH+LZ_u^* du} \left( k\alpha(0)L\psi_s^{(k-1)}(Z^*) - L^\dagger \psi_s^{(k+1)}(Z^*) \right) ds, \end{aligned} \quad (3.8)$$

as it satisfies Eq. (3.7) and the correct initial conditions. Here,  $T_+$  denotes positive time-ordering. Under the condition  $k\gamma \gg \omega_{\text{sys}}$ , where  $\omega_{\text{sys}}$  is a typical frequency for the system's free time evolution, the first exponential drops to zero before the remaining integrand changes noticeably. Therefore, the latter can be safely extracted from the integral setting  $s \approx t$

$$\psi_t^{(k)}(Z^*) = \left( k\alpha(0)L\psi_t^{(k-1)}(Z^*) - L^\dagger \psi_t^{(k+1)}(Z^*) \right) \int_0^t e^{-kw(t-s)} ds,$$

Evaluating the rest of the integral simply gives  $\frac{1-\exp(-kwt)}{kw}$ . As the second summand is relevant only for very small times  $t$ , it is dropped in the following work—including

it in a numerical implementation does not pose any additional difficulties. Thus, we have an approximate expression for the  $k^{\text{th}}$ -order auxiliary state

$$\psi_t^{(k)}(Z^*) = \frac{\alpha(0)}{w} L\psi_t^{(k-1)}(Z^*) - \frac{1}{kw} L^\dagger \psi_t^{(k+1)}(Z^*). \quad (3.9)$$

If we further assume that the second term, coupling to the order above, is suppressed by the prefactor  $\frac{1}{kw}$ , the infinite hierarchy terminates at finite order. However, since there is no simple assessment for the order of magnitude of individual auxiliary states  $\psi_t^{(k)}(Z^*)$ , this assumption needs to be checked for each calculation separately by increasing the truncation order. The remainder of Eq. (3.9), namely

$$\psi_t^{(k)}(Z^*) = \frac{\alpha(0)}{w} L\psi_t^{(k-1)}(Z^*), \quad (3.10)$$

is called “*terminator*” of the hierarchy. This procedure can be interpreted as a Markov approximation for the  $(k-1)^{\text{th}}$  auxiliary state similar to Eq. (2.24), since the memory-integral is replaced by a time-local expression.

Remarkably, the above argument does not solely rest on the exponential suppression by  $e^{-k\gamma(t-s)}$  in Eq. (3.8). As the results from Sect. 4.3 show, the hierarchy even terminates for  $\gamma = 0$  due to the highly oscillatory  $e^{-ik\Omega(t-s)}$ . Therefore, we propose a truncation criterion related to the one used within the HEOM-formalism [Tan06]

$$k(\gamma + |\Omega|) \gg \omega_{\text{sys}}, \quad (3.11)$$

which we will test in Sect. 3.3.2. It turns out that Eq. (3.11) is not a good criterion, since it neglects the crucial influence of the coupling strength  $g$ . So once again, in practical applications it is much more conclusive to check convergence of the results with the truncation order for each set of parameters individually.

### 3.1.2. Nonlinear Hierarchy

We mentioned in Sect. 2.3 how the efficiency of the Monte-Carlo scheme improves greatly, if we use comoving environmental basis states (2.37) and the corresponding nonlinear NMSSE. Up to a certain extend this idea can also be applied to our hierarchical equations of motion.

Seen as a function of coherent state labels  $\mathbf{z}^*$  instead of the process  $Z^*$ , the Girsanov-transformed auxiliary states are defined by

$$\tilde{\psi}_t^{(k)}(\mathbf{z}^*) := (\psi_t^{(k)} \circ \phi_t)(\mathbf{z}^*) = \psi_t^{(k)}(\phi_t(\mathbf{z}^*))$$

with the “phase-space” flow (2.37). Then, along the lines of the derivation leading to Eq. (3.7) we obtain its nonlinear form

$$\begin{aligned} \partial_t \tilde{\psi}_t^{(k)}(\mathbf{z}^*) &= \left( -iH - kw + LZ_t^* + L \int_0^t \alpha(t-s)^* \langle L^\dagger \rangle_s ds \right) \tilde{\psi}_t^{(k)}(\mathbf{z}^*) \\ &\quad + k\alpha(0)L\tilde{\psi}_t^{(k-1)} - (L^\dagger - \langle L^\dagger \rangle_t)\tilde{\psi}_t^{(k+1)}(\mathbf{z}^*), \end{aligned} \quad (3.12)$$

with the normalized expectation value taken with respect to the true quantum trajectory—or, put differently, with respect to the zeroth order auxiliary state

$$\langle L^\dagger \rangle_t = \frac{\langle \tilde{\psi}_t^{(0)}(Z^*) | L^\dagger | \tilde{\psi}_t^{(0)}(Z^*) \rangle}{\langle \tilde{\psi}_t^{(0)}(Z^*) | \tilde{\psi}_t^{(0)}(Z^*) \rangle}. \quad (3.13)$$

Deriving a terminator for the nonlinear version is completely analog to Eq. (3.10) and gives the same result.

Notice that the exponential correlation function necessary for the hierarchy also simplifies the treatment of the memory-term in Eq. (3.12). Indeed  $f(t) := \int_0^t \alpha(t-s)^* \langle L^\dagger \rangle_s ds$  satisfies

$$\dot{f}(t) = \alpha(0)\langle L^\dagger \rangle_t - w^* f(t). \quad (3.14)$$

Therefore, we only need to store the hierarchy and auxiliary function  $f$  for one time step in a numerical implementation—making this approach very memory-efficient.

But one caveat remains: For the convolutionless formulation we can go one step further and derive an equation for normalized pure state trajectories (2.40). However, such a hierarchy with all auxiliary states having unit norm seems to be unobtainable. Nonetheless, we expect that there is another version of the nonlinear hierarchy, which achieves a normalized zero-order state—this would tremendously improve the numerical accuracy of the expectation values (3.13) for large  $\langle \tilde{\psi}_t^{(0)}(Z^*) | \tilde{\psi}_t^{(0)}(Z^*) \rangle^2$ .

---

<sup>2</sup>I would like to thank Richard Hartmann for pointing this out.

### 3.1.3. Multiple Bath-Modes

Of course, most interesting systems cannot be modeled using a single exponential decaying correlation function (3.3). To accommodate a more complex environmental structure, we modify the hierarchy to handle a finite number of exponential modes coupling to the system with arbitrary operators. As the crucial points do not depend on the choice of linear or nonlinear version, we are only concerned with the former in this section to simplify notation.

The linear NMSSE for a finite number  $N$  of independent environments is derived similarly to the lines of Sect. 2.2 and reads

$$\partial_t \psi_t = -iH\psi_t + \sum_{j=1}^N L_j Z_{j,t}^* \psi_t - \sum_{j=1}^N L_j^\dagger \int_0^t \alpha_j(t-s) \frac{\delta \psi_t}{\delta Z_{j,t}^*} ds \quad (3.15)$$

with mutually independent noise processes satisfying

$$\mathbb{E} Z_{i,t} = 0, \quad \mathbb{E} Z_{i,t} Z_{j,s} = 0, \quad \text{and} \quad \mathbb{E} Z_{i,t} Z_{j,s}^* = \delta_{ij} \alpha_i(t-s).$$

Just as in the single-mode case, Eq. (3.15) is equivalent to an infinite hierarchy of auxiliary states if all correlation functions take the exponential form (3.3). Since all derivation operators  $\mathcal{D}_{j,t}$  corresponding to the processes  $Z_{j,t}^*$  mutually commute, the most general form of an auxiliary state is given by

$$\psi_t^{(k_1, \dots, k_N)} := \mathcal{D}_{1,t}^{k_1} \dots \mathcal{D}_{N,t}^{k_N} \psi_t. \quad (3.16)$$

Hereinafter, we use boldface symbols to abbreviate  $N$ -tuples such as  $\mathbf{k} = (k_1, \dots, k_n)$ . Summarily, the infinite hierarchy appertaining to Eq. (3.15) reads

$$\partial_t \psi_t^{(\mathbf{k})} = \left( -iH - \mathbf{k} \cdot \mathbf{w} + \sum_j L_j Z_{j,t}^* \right) \psi_t^{(\mathbf{k})} + \sum_j k_j \alpha_j(0) \psi_t^{(\mathbf{k}-e_j)} - \sum_j L_j^\dagger \psi_t^{(\mathbf{k}+e_j)}, \quad (3.17)$$

where  $e_j$  denotes the  $j$ -th unit vector in  $\mathbb{R}^N$  and  $\mathbf{k} \cdot \mathbf{w} = \sum_j k_j w_j$  is the euclidean scalar product<sup>3</sup>.

---

<sup>3</sup>Although  $\mathbf{w}$  is complex in general, the scalar product  $\mathbf{k} \cdot \mathbf{w}$  does not involve complex conjugation.

### 3. Hierarchy of Stochastic Pure States

---

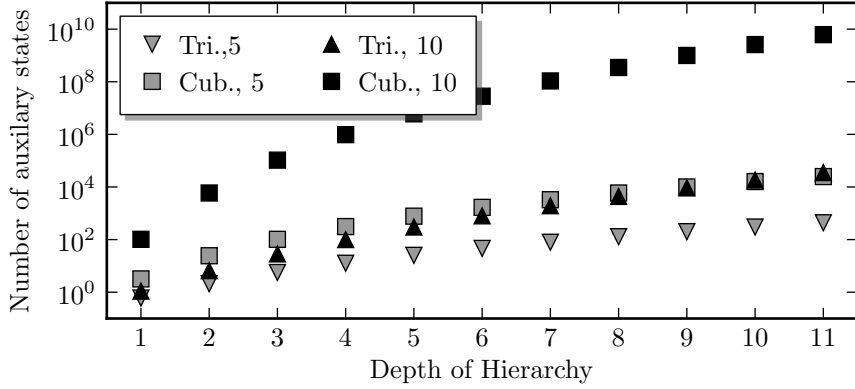


**Figure 3.1.:** Scaling of the number of auxiliary states with the truncation order  $D$  and number of modes  $N$ . Even for relatively small  $N$ , the triangular scheme (3.18) is far superior compared to the cubic truncation scheme with an exponential scaling law  $(D + 1)^N$ .

When it comes to truncating the hierarchy (3.17) the most obvious strategy is simply to cut off each mode separately at given order  $D$ . In other words the truncation condition reads  $0 \leq k_j \leq D$  for all  $j = 1, \dots, N$ ; any auxiliary state not satisfying it is either set to zero or replaced by the terminator

$$\psi^{(\mathbf{k}+\mathbf{e}_j)} = \sum_i \frac{(\mathbf{k} + \mathbf{e}_j)_i \alpha_i(0)}{(\mathbf{k} + \mathbf{e}_j) \cdot \mathbf{w}} L_i \psi_t^{(\mathbf{k} + \mathbf{e}_j - \mathbf{e}_i)}.$$

We refer to this as the “cubic truncation scheme” since the hierarchy’s shape resembles an  $N$ -cube. Clearly, the number of auxiliary states scales exponentially like  $(D + 1)^N$ , which makes the treatment of large systems with a highly structured spectral density virtually impossible.

Examining Eq. (3.17) closer, we notice that the term responsible for suppression of the  $\mathbf{k}^{\text{th}}$  auxiliary state is  $\exp(-\mathbf{k} \cdot \mathbf{w})$ . Instead of treating each mode individually, we use a condition better suited for the product  $\mathbf{k} \cdot \mathbf{w}$ , namely  $0 \leq |\mathbf{k}| \leq D$  with  $|\mathbf{k}| = \sum_j k_j$ . For  $N = 2$  the corresponding states form a triangular shape—hence the name “triangular truncation scheme”. The appropriate generalization to an arbitrary number of modes is an  $N$ -simplex with the number of elements given by

$$\sum_{d=0}^D \binom{d+N-1}{N-1} = \frac{(D+N)!}{D!N!}, \quad (3.18)$$

showing a much softer scaling with  $N$  compared to the cubic scheme. In Fig. 3.1 we display the number of auxiliary states required for a given number of modes and truncation order  $D$ . Clearly, the triangular truncation is far superior although for small  $N$  both methods are applicable. The difference is more pronounced for larger  $N$ .

Depending on the specific problem, additional truncation conditions may reduce the computational expenses without sacrificing accuracy. Especially environments that mix modes with large memory times and almost-Markovian modes provide many options for optimization. However, we do not elaborate this point any further and rely on the triangular truncation throughout this work.

## 3.2. Bath Correlation Function Expansion

The applicability of our hierarchical equations of motion to certain models depends predominantly on the ability to express the relevant bath correlation function

$$\alpha(t-s) = \int_0^\infty J(\omega) \left( \coth\left(\frac{\beta\omega}{2}\right) \cos\omega(t-s) - i \sin\omega(t-s) \right) d\omega \quad (3.19)$$

as a sum of exponentials like (3.3). Such exponentials arise as Fourier transforms of a Lorentzian spectral density

$$J(\omega) = \frac{1}{\pi} \frac{\gamma}{(\omega - \Omega)^2 + \gamma^2}. \quad (3.20)$$

Hence they can be obtained from Eq. (3.19) in the zero-temperature limit provided we extend the integral domain to include arbitrary negative frequencies as well. This unphysical assumption seems to be a good approximation to the exact case without negative frequencies for certain parameters as Fig. 3.2 shows: For  $\gamma \ll \Omega$  the Lorentzian density  $J$  is concentrated on the positive semi-axis and the negative frequency contributions vanish primarily. However, Eq. (3.20) is a prime example of a heavy-tailed distribution, having no finite moments except  $\int J(\omega) d\omega = 1$ , so this approximation needs to be handled with care.

A more systematic way to obtain the desired bath correlation function in the case  $T > 0$  involves anti-symmetrized spectral densities  $\tilde{J}(\omega) := J(\omega) - J(-\omega)$ . This way,

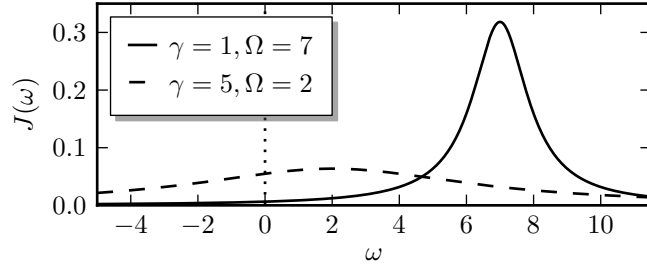


**Figure 3.2.:** Schematic comparison of Lorentzian spectral densities used to obtain exponential bath correlation functions (see Eq. (3.20) for notation). For  $\gamma \ll \Omega$  (blue line) the weight is concentrated on the positive semi-axis.

negative frequencies are included without any approximation. Indeed, since  $\tilde{J}$ ,  $\coth$ , and  $\sin$  are anti-symmetric and  $\cos$  is symmetric with respect to reflection at the origin we have

$$\int_0^\infty \tilde{J}(\omega)(\dots) d\omega = \frac{1}{2} \int_{-\infty}^\infty \tilde{J}(\omega)(\dots) d\omega. \quad (3.21)$$

Commonly used examples are Drude spectral densities in the HEOM-formalism or sums of anti-symmetrized Lorentzians, which are well suited to approximate highly-structured environments [MT99]. Although the discussion below works for a much larger class of spectral densities [RE], we assume  $\tilde{J}$  to have a finite number of mutually distinct poles lying off the real and imaginary axis.

To calculate the correlation function, we evaluate the integral (3.21) analytically using the residue theorem. While the poles of the anti-symmetric spectral density  $\tilde{J}$  are assumed to be known, there are different expansion schemes for the hyperbolic cotangent: Since many established HEOM-results are based on the Matsubara-spectrum decomposition, it is presented in detail. Nevertheless, it has been brought forward only recently that the Padé-expansion provides superior approximation scheme, especially for low temperature [HXY10, HLJ<sup>+</sup>11]. We achieve a much more convenient form by treating the real and imaginary part of  $\alpha(t) = a(t) + ib(t)$  separately, where the former

$$a(t) = \frac{1}{2} \int_{-\infty}^\infty \tilde{J}(\omega) \coth\left(\frac{\beta\omega}{2}\right) \cos\omega t d\omega = \frac{1}{2} \int_{-\infty}^\infty \tilde{J}(\omega) \coth\left(\frac{\beta\omega}{2}\right) e^{i\omega t} d\omega, \quad (3.22)$$

includes all thermal effects, while the imaginary part

$$b(t) = -\frac{1}{2} \int_{-\infty}^{\infty} \tilde{J}(\omega) \sin \omega t \, d\omega = \frac{1}{2i} \int_{-\infty}^{\infty} \tilde{J}(\omega) e^{i\omega t} \, d\omega$$

is identical for all temperatures.

In order to evaluate Eq. (3.22) for  $t > 0$ , we close the integration contour in the upper complex half-plane. The poles  $\omega = i\gamma_n = 2\pi n i / \beta$  of the hyperbolic cotangent are easily read off

$$\coth\left(\frac{\beta\omega}{2}\right) = \frac{1 + e^{-\beta\omega}}{1 - e^{-\beta\omega}}. \quad (3.23)$$

Indeed, the nominator as well as the denominator are analytical functions of  $\omega$ , but the latter vanishes for  $\omega = i\gamma_n$ . These are often referred to as Matsubara frequencies. By the usual formula for simple poles, we find for the residuum at the origin

$$\text{Res}_0\left(\coth\frac{\beta\omega}{2}\right) = \lim_{\omega \rightarrow 0} \omega \coth\frac{\beta\omega}{2} = \frac{2}{\beta}.$$

Of course, the remaining pole's residua are identical due to the periodicity of the hyperbolic cotangent.

Since we assumed that the poles of the spectral density lie off the imaginary axis—or at least are distinct from the poles of the hyperbolic cotangent—Eq. (3.22) reduces to a sum over individual poles in the upper complex half-plane for  $t > 0$

$$a(t) = \pi i \sum_{\omega'} \text{Res}_{\omega'}(\tilde{J}) \coth\left(\frac{\beta\omega'}{2}\right) e^{i\omega' t} + \frac{2\pi i}{\beta} \sum_{\gamma_n > 0} \tilde{J}(i\gamma_n) e^{-\gamma_n t}. \quad (3.24)$$

Here, the first sum involves all poles  $\omega'$  of  $\tilde{J}$  with  $\Im\omega' > 0$  and no special care is needed for the coth-pole at  $\omega = 0$  since  $\tilde{J}(0)$  vanishes anyway. Clearly,  $a(t)$  has the desired exponential form; the same hold true for  $b(t)$ . As  $e^{-\gamma_n t}$  suppresses contributions from large Matsubara frequencies unless  $t$  is very small, the infinite sum in Eq. (3.24) is truncated at finite order for numerical purposes.

In conclusion, we obtain an expansion of the bath correlation function of the form

$$\alpha(t) = \sum_n \alpha_n(t) = \sum_n g_n e^{-w_n t} \quad (t > 0), \quad (3.25)$$

with complex prefactors  $g_n$  in general. Therefore, the continuation to  $t < 0$  by  $\alpha_n(-t) = \alpha_n(t)^*$  produces a discontinuous jump at  $t = 0$ , since the right- and left-hand limits  $g_n = \alpha_n(0+)$  and  $g_n^* = \alpha_n(0-)$  differ. This is problematic for our NMSSE-hierarchy for two reasons: First, we need to generate realizations of the noise processes with  $\mathbb{E}(Z_{n,t}Z_{m,s}^*) = \delta_{mn}\alpha_n(t-s)$ , which is necessarily real and positive for  $t = s$  and  $m = n$ . For most practical applications, the imaginary parts of the individual modes in (3.25) approximately cancel and we can generate realizations for the corresponding sum-process, namely  $Z_t^* = \sum_n Z_{n,t}^*$  with  $\mathbb{E}(Z_tZ_s^*) = \alpha(t-s)$ . However, this does not apply to the Drude spectral density used in Sect. 4.2—we propose a different way to deal with the issue there. The second and more problematic consequence of complex prefactors  $g_n$  in Eq. (3.25) is that the singular contributions to  $\dot{\alpha}_n$  do not cancel in general. But since the discontinuous jump of the bath correlation function  $\alpha(t-s)$  at  $t = s$  cannot be reproduced within the stochastic average  $\mathbb{E}(Z_tZ_s^*)$  anyway, we ignore the additional term in  $\dot{\mathcal{D}}_t$  it causes.

### 3.3. Spin-Boson Model

The Spin-Boson model is a paradigmatic model used in the theoretical description of dissipative quantum dynamics [LCD<sup>+</sup>87, Wei99]. Despite being simple and numerically tractable, it displays properties also found in more complex systems—take for example the transition between a localized, essentially classical phase and a delocalized phase allowing quantum mechanical tunneling [FVN10]. Therefore, it is well suited to investigate properties of dissipative systems and the influence of an environment in general. Furthermore, it is often employed as an approximate description of systems with a continuous degree of freedom confined by a double well potential. Examples for the latter are the motion of defects in some crystalline solids or the magnetic flux trapped in a superconducting qubit [CL83]. We use it to demonstrate the superiority of the nonlinear compared to the linear hierarchy as well as the convergence of our hierarchy with increasing depth.

The Spin-Boson model consists of a two-level system with the free time evolution described by the Hamiltonian

$$H = -\frac{1}{2}\Delta\sigma_x + \frac{1}{2}\epsilon\sigma_z,$$

coupled linearly to a bath of harmonic oscillators with  $L = \sigma_z$ . For simplicity, all calculations in this section involve only a single exponential bath mode with correlation function  $\alpha(t) = g e^{-\gamma|t| - i\Omega t}$  and real parameters  $g, \gamma, \Omega$ .

### 3.3.1. Sample Size

Since our hierarchy is based upon a stochastic differential equation, it is crucial to assess its reliability in dependence on the sample size. In this section we study the convergence of our Monte-Carlo average with respect to the number of realizations. Particularly, we point out the superiority of the nonlinear version (3.12) over the linear hierarchy (3.7). In order to really emphasize the strengths and weaknesses of both approaches, we choose two quite distinct sets of parameters. Although it is not the only difference between both sets, we refer to them as the weakly and strongly coupled parameters—see Fig. 3.3 for the details. The former can even be treated using an improved perturbation scheme [GHZ10, HZ08].

In Fig. 3.3 we plot the expectation value of the spin-operator in  $z$ -direction for an initial eigenstate “spin up”. The case of weak coupling at the top shows almost no difference between the linear version on the left and the nonlinear version on the right. Nevertheless, the nonlinear version with 100 realizations reproduces the damping for large times better than the linear version as the peaks on the left hand side at  $t \cdot \Delta \approx 120, 160$  show. Even for 10 realizations the nonlinear hierarchy agrees better with the more exact results, overall. The only exception is the second peak at  $t \cdot \Delta \approx 5$ , where the linear version shows perfect agreement for all three sample sizes.

When it comes to the strongly coupled parameter set (bottom), the picture changes drastically: First, notice that the sample size has been increased by an order of magnitude to obtain a reliable result. Notwithstanding, the linear version does not display any visible changes for the different sample sizes shown. Hence, we cannot expect convergence for even larger numbers of realizations. It is only for very small time scales that both, left and right picture, agree up to a certain extent. In contrast, the nonlinear version improves steadily with growing sample size and already provides a very good approximation with only minor fluctuations at 1000 trajectories. Remarkably, even 100 realizations produce the correct qualitative features as the vanishing of  $\langle \sigma_z \rangle$  for large  $t$ , while the linear hierarchy is not capable of producing equally good

### 3. Hierarchy of Stochastic Pure States

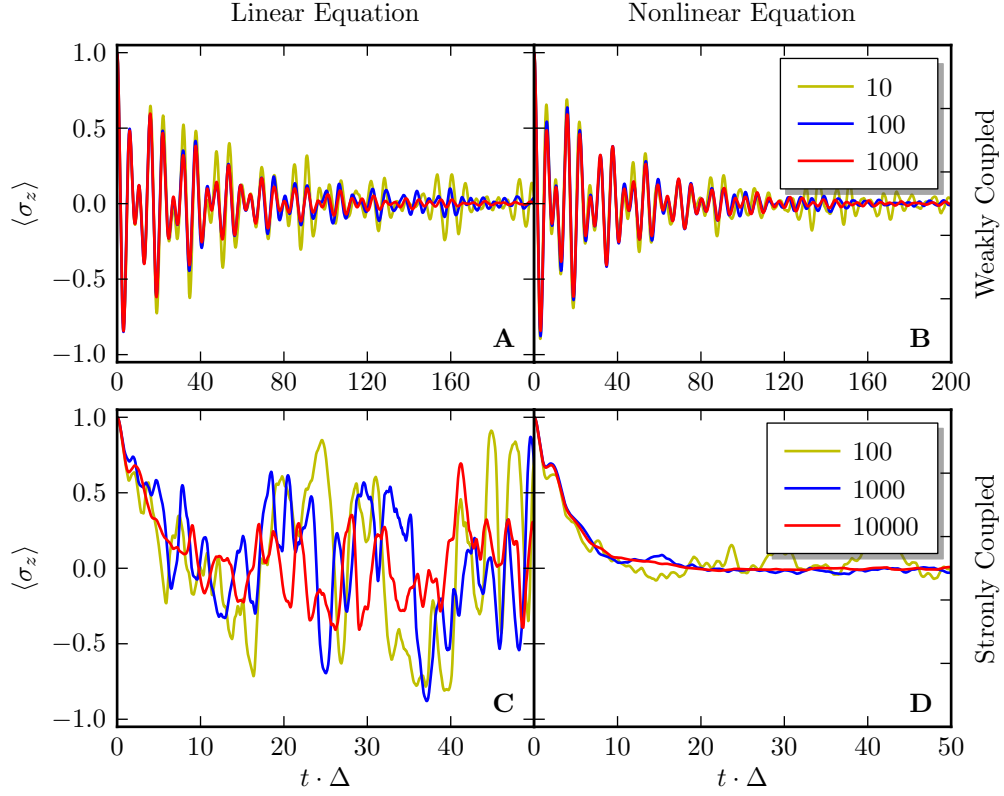


**Figure 3.3.:**  $\langle \sigma_z \rangle$  of the symmetric Spin-Boson model ( $\epsilon = 0$ ) using the linear (left) and nonlinear (right) NMSSE-hierarchy.  
**(A)** and **(C)** weakly coupled system with  $g = 0.18\Delta$ ,  $\gamma = 0.05\Delta$  and  $\Omega = \Delta$ . **(B)** and **(D)** strongly coupled system with  $g = 2\Delta$ ,  $\gamma = 0.5\Delta$  and  $\Omega = 2\Delta$ .

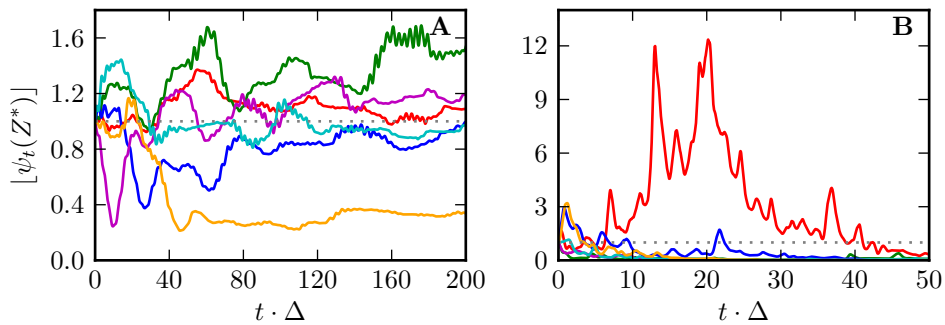


**Figure 3.4.:** Contributions (3.27) of single trajectories to the reduced density operator for the linear equations. **(A)** Weakly coupled parameters from Fig. 3.3 A. **(B)** Strongly coupled parameters from Fig. 3.3 C. The dotted line with constant value 1 indicates the contribution of each trajectory for the nonlinear equation.

results using a sample size more than 100 times larger.

To understand this behavior, recall that we have introduced the nonlinear equations in order to achieve an average over single realizations contributing equal amounts. As already mentioned in Sect. 2.3, individual trajectories of the linear version violate this requirement more or less severely. In order to get a better assessment of different contributions over time we have to rescale the norm as follows: First, we calculate the reduced density operator  $\rho_t$  by the usual Monte-Carlo average

$$\rho_t = \frac{1}{N} \sum_{n=1}^N |\psi_t(Z_n^*)\rangle\langle\psi_t(Z_n^*)| \quad (3.26)$$

over a large number of noise process realizations  $Z_n^*$ . Afterwards, we obtain a genuine, normalized density matrix by rescaling with  $(\text{Tr } \rho_t)^{-1}$ . Therefore, we can assess the contribution of a single trajectory  $\psi_t(Z_n^*)$  to Eq. (3.26) by  $|\psi_t(Z_n^*)|/N$  with

$$|\psi_t(Z_n^*)| = \sqrt{\frac{\langle\psi_t(Z_n^*)|\psi_t(Z_n^*)\rangle}{\text{Tr } \rho_t}}. \quad (3.27)$$

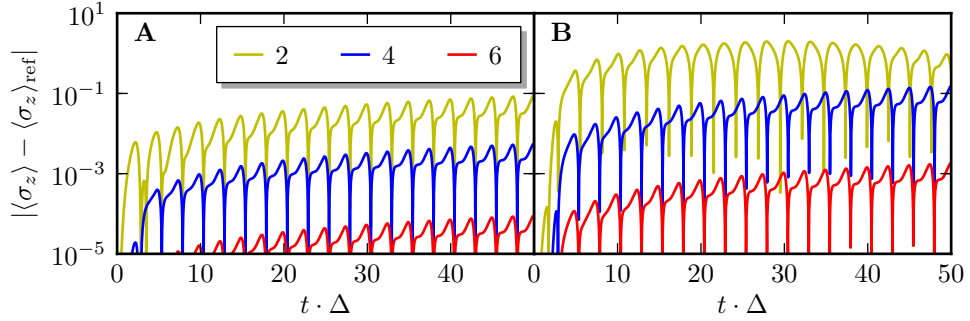
Since for the nonlinear equation the average in Eq. (3.26) is taken over normalized states  $\tilde{\psi}(Z_n^*) = \psi(Z_n^*)/|\psi(Z_n^*)|$ , the corresponding contribution  $|\tilde{\psi}_t(Z_n^*)|$  is one.

Figure 3.4 shows the contribution of a few single realizations used on the left hand side of Fig. 3.3. Clearly, the contribution of individual trajectories is quite different. But for the weakly coupled system on the left all trajectories remain roughly in the same order of magnitude. In contrast, the contributions on the right hand side, belonging to the strongly coupled system, all vanish for large  $t$ , but also show pronounced peaks for a few trajectories.

We conclude, that the nonlinear hierarchy is a drastic improvement in terms of numerical efficiency for the strongly coupled system, since the additional complexity is more than compensated by the reduced sample size. Therefore, all subsequent calculations shown in this work are based on the nonlinear hierarchy unless stated otherwise.

### 3. Hierarchy of Stochastic Pure States

---



**Figure 3.5.:** Deviation of  $\langle \sigma_t \rangle = \langle \psi_t(Z^* = 0) | \psi_t(Z^* = 0) \rangle$  for truncation order  $D = 2, 4, 6$  from the result for  $D = 8$ . Parameters for the bath correlation function are  $g = 0.5\Delta$ ,  $\gamma = \Delta$  and  $\Omega = 0$ .

(A) Results obtained from nonlinear NMSSE-hierarchy with terminator (3.10).

(B) Same as (A), but simply neglecting auxiliary states beyond order  $D$ .

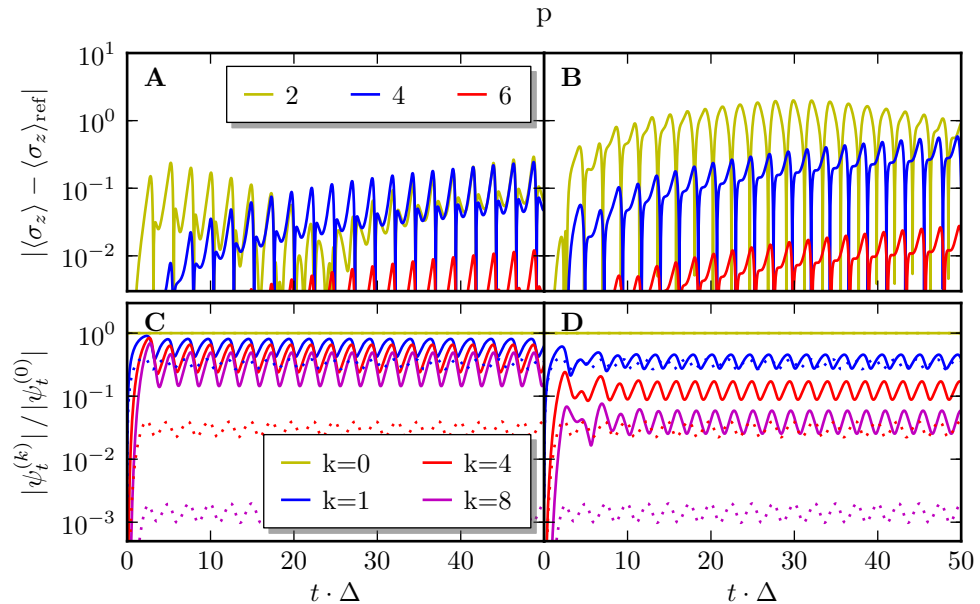


**Figure 3.6.:** (A) Same as Fig. 3.5 A, but with  $g = \Delta$ .

(B) Same as Fig. 3.5 A, but with  $\gamma = 0.5\Delta$ .

(C) Norm of individual auxiliary states for the nonlinear hierarchy truncated at  $D = 8$ ; parameters from (A). The dotted line indicates the result obtained with the original parameters used in Fig. 3.5.

(D) Same as (C), but with parameters from (B).

### 3.3.2. Truncation Order and Terminator

Apart from the sample size there is an even more significant factor limiting the applicability of our hierarchical equations of motion: As seen from Fig. 3.1 the number of auxiliary states required—and with it the computational expense—grows faster than linear with the truncation depth. We use the Spin-Boson model to study effects of the hierarchy-truncation since, contrary to the Jaynes-Cummings model presented in Sect. 2.6, the corresponding expansion of  $\psi_t(Z^*)$  does not terminate at any finite order. To eliminate deviations due to stochastic averaging, we investigate only the single trajectory  $\psi_t(Z^* = 0)$  of the nonlinear NMSSE.

In Fig. 3.5, we demonstrate the effectiveness of the terminator (3.10). For that matter, we calculate the deviation of  $\langle \psi_t(Z^* = 0) | \sigma_z | \psi_t(Z^* = 0) \rangle$  using truncation orders  $D = 2, 4, 6$  from the result with  $D = 8$ . Clearly, the application of the terminator improves the accuracy by about one order of magnitude in all three cases shown. Put differently, for the parameters under consideration, the terminator saves about one order in the hierarchy to obtain a given precision. Especially low-order calculations benefit from the additional corrections. Therefore, we employ the terminator (3.10) for the rest of this work.

Of course, even more relevant for the accuracy obtained with a given truncation order are the parameters of the bath correlation function. As discussed in Sect. 3.1.1, the treatment of highly non-Markovian systems requires more orders. The truncation condition (3.11) was introduced to obtain a first assessment of the size required. However, it does not account for the crucial assumption that allows us to neglect the term coupling to the order above in Eq. (3.9), namely its suppression by  $k^{-1}$ . In order to demonstrate that the latter is often supported by a decreasing magnitude of higher order terms, we display the norm of certain auxiliary states calculated with the same parameters as Fig. 3.5, except for a coupling constant twice as large and the value of  $\gamma$  halved in Fig. 3.6 C and D, respectively. Results corresponding to the original parameter set are indicated by dotted lines. Clearly, both an increase in the coupling strength and a decrease in the inverse memory time  $\gamma$  result in a stronger contribution of higher-order auxiliary states. This can also be seen in Fig. 3.6 A and B, where the deviation of  $\langle \sigma_z \rangle$  for different truncation orders is shown. Compared to Fig. 3.5, where  $D = 4$  was sufficient to achieve a precision of about  $10^{-3}$ , the same

### *3. Hierarchy of Stochastic Pure States*

---

level of confidence is not reached in Fig. 3.6 with the modified parameters, even for  $D = 6$ .

We come to the conclusion, that the truncation condition (3.11) is not sufficient to ensure a good approximation by the truncated hierarchy, since it does not pose any restriction on the coupling strength  $g$ . Also, we will demonstrate in Sect. 4.2 that often a much smaller value for  $D$  suffices than required by (3.11). Therefore, it is crucial to check the accuracy of a result varying the truncation order by  $\pm 1$ .

## 4. Molecular Aggregates and the NMSSE

An interesting field of application for the methods derived in the last chapter can be found in the investigation of molecular aggregates. Although the latter may consist of hundreds or thousands of electrons and nuclei, some of its properties can be explained in terms of an open quantum system with only a few relevant degrees of freedom [MK11]. In general, a molecular aggregate is an assembly of smaller constituents (for example molecules or quantum dots), where each still acts as an individual. By virtue of the mutual interaction between those constituents, or monomers, new collective phenomena arise.

At the beginning of this chapter, we introduce an effective description of molecular aggregates, which leads to the standard open model from Sect. 2.1. Subsequently, the NMSSE-hierarchy is employed to calculate energy transfer in light harvesting systems and compared to established results to demonstrate its usefulness. Finally, we show that the same approach is particularly well suited to calculate absorption spectra of molecular aggregates. As the main goal of this chapter is to demonstrate the applicability of the NMSSE, we focus only on certain aspects of the models under investigation.

### 4.1. The Aggregate Hamiltonian

Let us consider a molecule composed of electrons and point-like nuclei described quantum mechanically by canonical-conjugated pairs of operators  $(p_j, q_j)$  and  $(P_j, Q_j)$  respectively. Its Hamiltonian is given by

$$H_{\text{mol}} = T_{\text{el}} + T_{\text{nuc}} + U_{\text{el-el}} + U_{\text{nuc-nuc}} + U_{\text{el-nuc}} \quad (4.1)$$

#### 4. Molecular Aggregates and the NMSSE

---

with the kinetic energies  $T$  and appropriate Coulomb interactions  $U$ . We drop possible contributions from internal spin degrees of freedom, since they induce only negligible corrections for the systems under consideration. Of course, a universal and exact solution of the corresponding Schrödinger equation is virtually impossible, however, we can approximate (4.1) by the standard open-system model for the conditions under consideration [MK11]. As a first major approximation we assume a Born-Oppenheimer separation between the electronic and nuclear coordinates. This enables us to include the motion of nuclei mediated by the Coulomb potential  $U_{\text{el-nuc}}$  adiabatically when calculating the electron-dynamics from Eq. (4.1). Therefore, we can reorganize the summands in the Hamiltonian (4.1) more appropriately to

$$H_{\text{mol}} = H_{\text{el}}(\mathbf{Q}) + T_{\text{nuc}} + U_{\text{nuc-nuc}}, \quad (4.2)$$

where the notation  $H_{\text{el}}(\mathbf{Q}) = T_{\text{el}} + U_{\text{el-el}} + U_{\text{el-nuc}}(\mathbf{Q})$  indicates that we regard the electronic Hamiltonian to depend only parametrically on the nuclear coordinates  $\mathbf{Q}$ . For the energy scales under consideration, we only have to treat the valence electrons explicitly; electrons on lower energy levels are included into the “environmental” nuclear part.

Besides contributions of the form (4.1) for each individual molecule, the aggregate-Hamiltonian contains intermolecular interactions between electrons and nuclei in all possible combinations. Since we aim to treat the electronic degrees of freedom separately, it is most appropriately rewritten similarly to Eq. (4.2)

$$H_{\text{agg}} = H_{\text{el}}(\mathbf{Q}) + T_{\text{vib}} + U_{\text{vib-vib}}. \quad (4.3)$$

Here we use the more general notion of vibrational degrees of freedom, which not only comprises the intra- and intermolecular nuclear coordinates, but also possible environmental degrees of freedom not belonging to the aggregate. For example, the latter can be found in molecular compounds immersed in a liquid solvent.

The Born-Oppenheimer approximation on the molecular level allows us to analyse the electronic part separately from the vibrational part of Eq. (4.3) for a fixed set

#### 4.1. The Aggregate Hamiltonian

---

of vibrational coordinates  $\mathbf{Q}$ . Splitting up the former into contributions from each individual electron and interaction terms gives

$$H_{\text{el}}(\mathbf{Q}) = \sum_m H_m^{(\text{el})}(\mathbf{Q}) + \frac{1}{2} \sum_{m,n} U_{mn}^{(\text{el-el})}(\mathbf{Q}), \quad (4.4)$$

where  $H_m^{(\text{el})}(\mathbf{Q})$  contains the  $m^{\text{th}}$  electron's kinetic energy as well as its coupling to the vibrational degrees of freedom and  $U_{mn}$  is simply the Coulomb interaction between the  $m^{\text{th}}$  and  $n^{\text{th}}$  electron. For each given environmental configuration  $\mathbf{Q}$ , the “free” Hamiltonians  $H_m^{(\text{el})}(\mathbf{Q})$  define adiabatic electronic eigenstates states by

$$H_m^{(\text{el})}(\mathbf{Q})\varphi_{ma}(q, \mathbf{Q}) = \epsilon_{ma}(\mathbf{Q})\varphi_{ma}(q, \mathbf{Q}).$$

Here, the index  $m$  runs over all electrons under consideration and  $a$  is a quantum number used to label the individual states, which we assume to be ordered by the corresponding energies. Similarly to the Hartree-Fock method, we build up an expansion basis for the total electronic state by a product ansatz

$$\phi_{\mathbf{a}}(\mathbf{q}, \mathbf{Q}) = \prod_m \varphi_{m,a_m}(q_m, \mathbf{Q}). \quad (4.5)$$

In general, the product needs to be anti-symmetrized to fulfill the Pauli exclusion principle.

If there is at most one relevant valence electron per molecule, which is furthermore tightly bound, then the situation simplifies dramatically: In this case, the spreading of the single-electron states  $|\varphi_{ma}\rangle = |m, a\rangle$  is small compared to the distance between two molecules and we can neglect the overlap  $\langle m, a | n, b \rangle$  for different molecules  $m \neq n$ . Consequently Eq. (4.5) yields a complete basis for the electronic degrees of freedom. Expressed in this product of eigenstates, the purely electronic Hamiltonian (4.4) reads

$$\begin{aligned} H_{\text{el}}(\mathbf{Q}) &= \sum_{m,a} \epsilon_{m,a}(\mathbf{Q}) |m, a\rangle \langle m, a| \\ &+ \frac{1}{2} \sum_{\substack{m,n \\ a,b,a',b'}} U_{mn}(aa', bb')(\mathbf{Q}) |m, a; n, b\rangle \langle m, a'; n, b'|, \end{aligned} \quad (4.6)$$

#### 4. Molecular Aggregates and the NMSSE

---

with the matrix elements of the Coulomb interaction<sup>1</sup>

$$U_{mn}(aa', bb') = \langle m, a; n, b | U_{mn} | m, a'; n, b' \rangle.$$

Note that all terms in Eq. (4.6) still depend on vibrational coordinates. For example the matrix element  $U_{mn}(aa'; bb')$  is influenced by the distance between the  $m^{\text{th}}$  and  $n^{\text{th}}$  molecule, while the electronic eigenenergies  $\epsilon_{m,a}$  primarily depend on the positions of other electrons belonging to the same molecule.

Of course, the complete electronic system described by Eq. (4.6) is still too large for a numerical propagation, therefore, we impose additional simplifications. If, initially, there is only a single valence electron in its lowest excited state  $S_1$  above its ground state<sup>2</sup>  $S_0$  and if the energy gap between the states  $S_1$  and  $S_2$  is large compared to the corresponding electronic coupling strength, then it is sufficient to take into account only the  $S_0$  states  $|m, 0\rangle$ , as well as the first excited states  $|m, 1\rangle$ . Under these restrictions, the matrix elements  $U_{mn}(aa', bb')$  can be classified with respect to a few physical processes such as electrostatic interactions or charge-induced transitions [MK11]. The dominant contribution  $U_{mn}(01; 10)$  (and its reverse process  $U_{mn}(10; 01)$ ) describes an excitation of the  $n^{\text{th}}$  electron induced by a  $S_1 \rightarrow S_0$  transition of the  $m^{\text{th}}$  electron. In the following, we neglect all but the last classes of processes, which is frequently called Heitler-London approximation.

Restricting the allowed electronic states to the two lowest energy levels has a remarkable interpretation in terms of quasi-particles. First, we define the ground state for the electronic system

$$|0_{\text{el}}\rangle = \prod_n |n, 0\rangle. \quad (4.7)$$

The product

$$|m\rangle = |m, 1\rangle \prod_{n \neq m} |n, 0\rangle \quad (4.8)$$

describes an excited electron localized on the  $m^{\text{th}}$  molecule, which we refer to as an exciton of the electronic system. By virtue of the Heitler-London approximation,

---

<sup>1</sup>This does not include the exchange interaction, since we assume vanishing mutual overlap for the electronic states.

<sup>2</sup>Here  $S_0$  describes the lowest energy state of the valence electron with all other electrons of the molecule fixed, not to be confused with the atomic ground states.

the Hamiltonian (4.6) conserves the number of excitons. Therefore, initial states  $|m\rangle$  (or linear combinations thereof) remain in the one-exciton Hilbert space  $\mathcal{H}^{(1)}$ . The interaction matrix elements

$$V_{mn} = V_{nm} = \langle m, 0; n, 1 | U_{mn} | m, 1; n, 0 \rangle$$

allow us to express the restriction of  $H_{\text{el}}$  to  $\mathcal{H}^{(1)}$  as

$$H_{\text{el}}^{(1)}(\mathbf{Q}) = \sum_m \epsilon_m(\mathbf{Q}) |m\rangle \langle m| + \sum_{m,n} V_{mn}(\mathbf{Q}) |n\rangle \langle m|.$$

Similar,  $H_{\text{el}}^{(0)}(\mathbf{Q}) = \epsilon_0(\mathbf{Q}) |0_{\text{el}}\rangle \langle 0_{\text{el}}|$  is the electronic Hamiltonian in the zero-exciton subspace. For the rest of this section, we assume the  $V_{mn}$  to be independent of vibrational degrees of freedom; the general case is treated along the same line.

Up to this point, we have neglected the dynamical evolution of the vibrational environment, which is essential in a complete description of a molecular aggregate. Here, we use a harmonic approximation for all vibrational degrees of freedom, which formally amounts to expanding the site energies  $\epsilon_m(\mathbf{Q})$  in a Taylor series. While the constant term yields purely electronic site energies, the linear term provides the coupling to the bath. Expressing the vibrational modes in terms of ladder operators  $A_{m,\lambda}$  and  $A_{m,\lambda}^\dagger$  yields the full aggregate Hamiltonian for a single exciton

$$\begin{aligned} H_{\text{agg}}^{(1)} = & \sum_m \epsilon_m |m\rangle \langle m| + \sum_{m,n} V_{mn} |m\rangle \langle n| + \sum_{m,\lambda} \omega_{m,\lambda} A_{m,\lambda}^\dagger A_{m,\lambda} \\ & + \sum_{m,\lambda} g_{m,\lambda} |m\rangle \langle m| \otimes (A_{m,\lambda}^\dagger + A_{m,\lambda}), \end{aligned} \quad (4.9)$$

This matches the microscopic model presented in Sect. 2.1: a bath of harmonic oscillators linearly coupled to the electronic system. To alleviate notation further, we have assumed that each vibrational mode only couples to one specific localized exciton. Investigations based on a mixed quantum and classical description of the electronic and vibrational degrees of freedom, respectively, have shown that the harmonic model constitutes a good approximation [VEAG12]—at least for the FMO-complex considered in the next section.

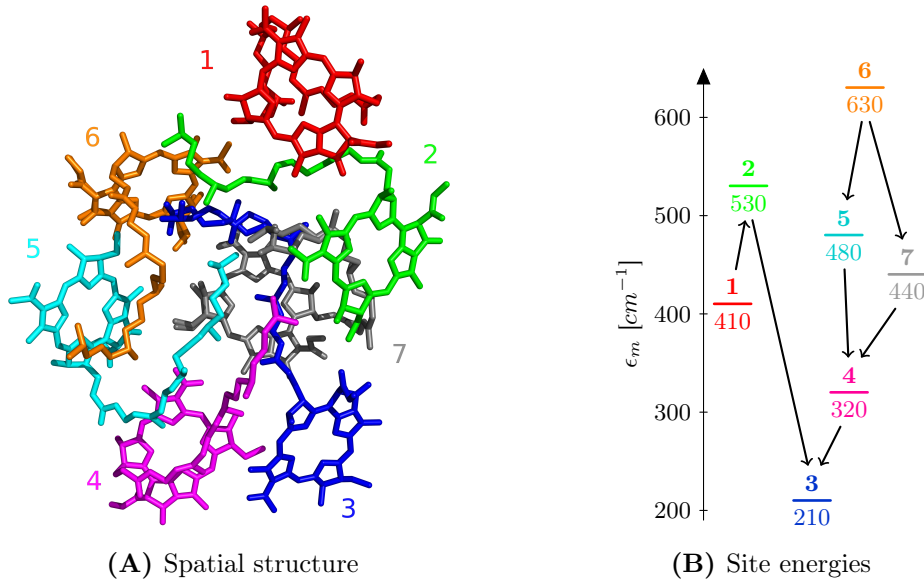


**Figure 4.1.:** Spatial structure and site energies of the simplified FMO-monomer with seven BChls.

(A) Spatial structure with coloring and numbering used throughout this section. This figure was created using PYMOL based on the PDB entry 3ENI [Sch10, TCABA09].

(B) Site energies of *Chlorobaculum tepidum* [AR06], an irrelevant global offset of 12 000 cm<sup>-1</sup> is subtracted. Solid black lines indicate dominant couplings leading to the two distinct transport channels.

## 4.2. Energy Transfer in Light-Harvesting Complexes

As a first exemplary application of our hierarchical equations of motion, we study energy transfer in the Fenna-Matthews-Olson (FMO) complex found in low-light adapted green sulfur bacteria. This protein complex plays a crucial role in connecting the light harvesting antenna (chlorosome) to the photosynthetic reaction center, where the absorbed solar energy is converted to a charge gradient. The FMO complex is fascinating not only by virtue of its relatively small size—making it an ideal model for numerical investigation—but particularly due to the strong influence of quantum mechanical effects on the energy transfer, even at physiological temperature [SBS97, ECR<sup>+</sup>07].

The FMO protein complex is subdivided into three identical monomers, each comprising eight bacteriochlorophyll pigments (BChls). In contrast to the first seven BChls, the eighth was only discovered in recent years due to its rather weak coupling to the remaining BChls and instability during the isolation procedure in experiments [TCABA09]. As the main goal here is to show the applicability and reliability of our hierarchical equations of motion, we ignore BChl number eight in what follows—this simplified model has been investigated thoroughly with a vast array of methods, for example in the HEOM and ZOFE-formalism [IF09, RRSE11]. For the same reason, we also restrict our attention to an individual monomer. As shown by Ritschel et al. [RRS<sup>+</sup>11], such a limitation is reasonable for the short time scales under consideration as the inter-monomeric interaction strength is rather weak.

In Fig. 4.1A we display the spatial structure and numbering of the BChls in a single monomer. The BChls 1 and 6 are situated in the vicinity of the light harvesting antenna and receive captured excitation energy, while BChl 3 acts as an energy sink to the reaction center. As both site energies  $\epsilon_n$  and electronic coupling strengths  $V_{mn}$  depend on the protein environment, different values for different species can be found in the literature. Here, we use the data obtained from optical spectroscopy in *Chlorobaculum tepidum* [AR06], see Fig. 4.1B and Table C.2. Although the spectral density may be important for the details of the excitation transfer, no comprehensive information on this matter is available at present. Especially well-suited for the HEOM formalism and used in the reference [IF09] are Drude spectral densities

$$J(\omega) = \frac{2\lambda}{\pi} \frac{\gamma\omega}{\omega^2 + \gamma^2}, \quad (4.10)$$

because, except for low-temperature corrections, they yield a single exponential mode in the bath correlation function. For the reorganization energy and relaxation time, we employ the values  $\lambda = 35 \text{ cm}^{-1}$  and  $\gamma^{-1} = 50 \text{ fs}$ , respectively, which were obtained from 2D electronic spectroscopy experiments [RSCE<sup>+</sup>08]. The spectral density and its corresponding bath correlation functions for  $T = 77 \text{ K}$  and  $T = 300 \text{ K}$  are shown in Fig. 4.4. We postpone the detailed calculations for the latter’s exponential decomposition to Sect. C.2.

Figure 4.2 shows the results of our calculations at cryogenic temperature  $T = 77 \text{ K}$  using pure state hierarchy as well as the established HEOM-results of Ishizaki and

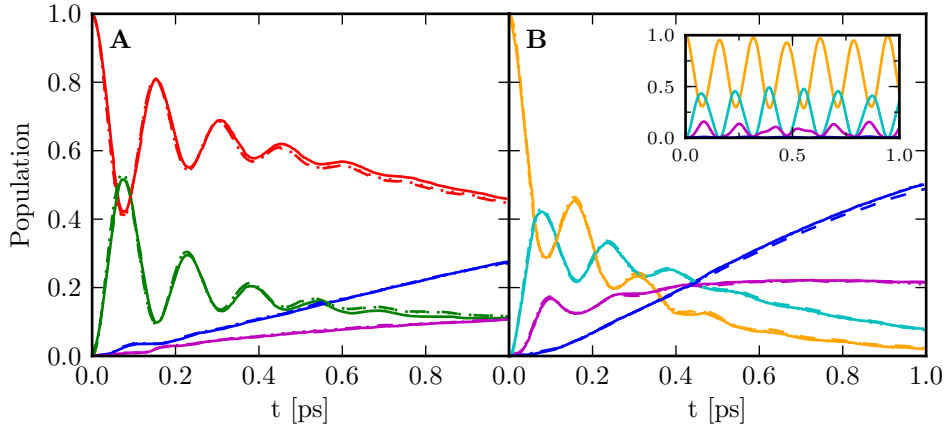


**Figure 4.2.:** Exciton transfer of the simplified FMO-monomer with seven BChls at 77 K using the NMSSE-hierarchy up to first (dotted) and second order (dashed) averaged over 10000 trajectories. For comparison, the solid line shows the reference results of Ishizaki and Fleming [IF09], which were obtained in the HEOM approach. We show the population for BChls 1–4 (**A**) and BChls 3–6 (**B**) with initial excitation on site 1 and 6 respectively (see Fig. 4.1A for the color code). The inset displays a purely electronic system without coupling to the vibrational degrees of freedom. Details on parameters can be found in Sect. C.3.

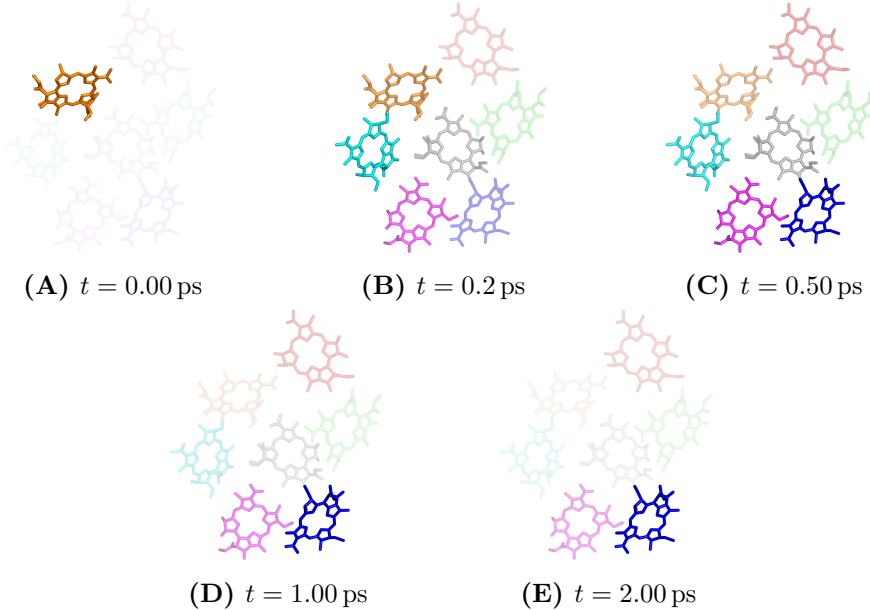


**Figure 4.3.:** Same as Fig. 4.2 B. The intensity of each molecule represents the population of the associated exciton state. For the sake of clarity we do not show the full molecular structure.

Fleming [IF09]. Both initial excitations move remarkably fast and directed—and up to  $t = 700$  fs in a quantum-coherent, wavelike fashion—toward the energy sink at BChl 3. However, the final population of the latter is only about half as large on the left hand side due to the relatively high site energy of BChl 2. This prolongs the lifetime of an exciton-state on BChl 1 significantly, or, put differently, the electronic excitation remains on the first site for a long time.

It was conjectured that this barrier is partly responsible for the high yield of the FMO-complex [IF09]. Indeed, the relatively small energy gap  $\Delta\epsilon = 200 \text{ cm}^{-1}$  between the first and third BChl is overcome quite easily by virtue of thermal excitation leading to a loss of population on the third site through this channel. The larger gap of  $\Delta\epsilon = 300 \text{ cm}^{-1}$  between the second and the third molecule suppresses depopulation much more efficiently. This is exactly where quantum effects influence the operation significantly: The subsidiary energetic minima at BChl 1, which would practically trap a classical-hopping excitation, is overcome much quicker due to quantum-mechanical delocalization.

No such initial “energy barrier” exists for the transport starting at BChl 6, therefore, the yield at BChls 3 and 4 is almost three-quarters of the total population at  $t = 1$  ps. For even longer times, all other sites show almost complete depopulation as shown in Fig. 4.3.

In the inset to Fig. 4.2 we also show the dynamics for a purely electronic system: As expected, the population shows a purely oscillatory behavior with no effective excitation transport, thus emphasizing the importance of vibrational degrees of freedom in the exciton energy transfer.

Remarkably, the results of first and second order in the NMSSE-hierarchy are almost indistinguishable from each other and agree very well with the reference. Calculations including one more order (not shown) verify that the second order is already enough to obtain convergence in these parameter regimes. As we show in Sect. C.3, the inverse correlation time<sup>3</sup> of the dominant mode is given by  $\gamma = 106 \text{ cm}^{-1}$ . Therefore, the proposed truncation condition (3.11), namely  $\omega_{\text{sys}} \ll D\gamma$ , with the typical system frequency  $\omega_{\text{sys}} \approx 500 \text{ cm}^{-1}$  is too restricting, yet. This strengthens the state-

---

<sup>3</sup>Recall our notation  $\alpha(t) = g e^{-\gamma t}$  for  $t > 0$ .

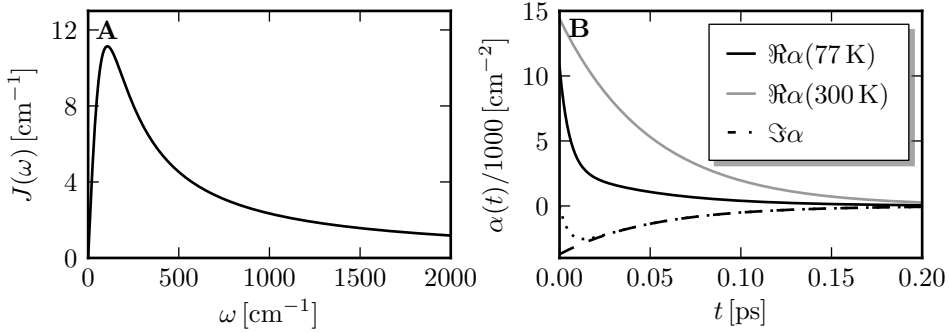


**Figure 4.4.:** Environmental parameters used for the FMO-complex. **(A)** Drude spectral density with reorganization energy  $\lambda = 35 \text{ cm}^{-1}$ , and relaxation time  $\gamma^{-1} = 50 \text{ fs}$ . **(B)** Bath correlation function at 77 K and 300 K. The imaginary part with (dotted) and without (dashed) almost-Markovian correction is identical for both (for details see Table C.1).

ment that convergence with respect to truncation order should be checked individually for each set of parameters.

Nevertheless, we do not obtain complete agreement with the reference in Fig. 4.2 A for the reason discussed at the end of Sect. 3.2. As shown in the appendix, the bath correlation function of a Drude spectral density always has a discontinuous jump in its imaginary part at the origin. This manifests in the complex prefactor  $g$  of the exponential mode, which cannot be adjusted by the low-temperature correction term as the dashed line in Fig. 4.4 B indicates. But since  $\alpha(t)$  is related to our driving processes  $Z_t^*$  by  $\alpha(t-s) = \mathbb{E}(Z_t Z_s^*)$ , we cannot reproduce such a correlation function in the driving noise. However, we approximate the discontinuous jump by including an additional, almost-Markovian mode with purely imaginary  $g$ , such that  $\Im\alpha(t)$  goes smoothly to zero as  $t \rightarrow 0$  while changing  $\alpha$  as little as possible—the result is indicated by a dotted line in Fig. 4.4 B. Since the low-temperature correction mode is already approximated with an almost-Markovian mode, this does not increase the computational expense.

The exciton dynamics at physiological temperature in Fig. 4.5 shows a similar qualitative behavior. However, the transfer is less efficient and directed, as decoherence leads to a much stronger smearing of the excitation over all BChls, even the ones

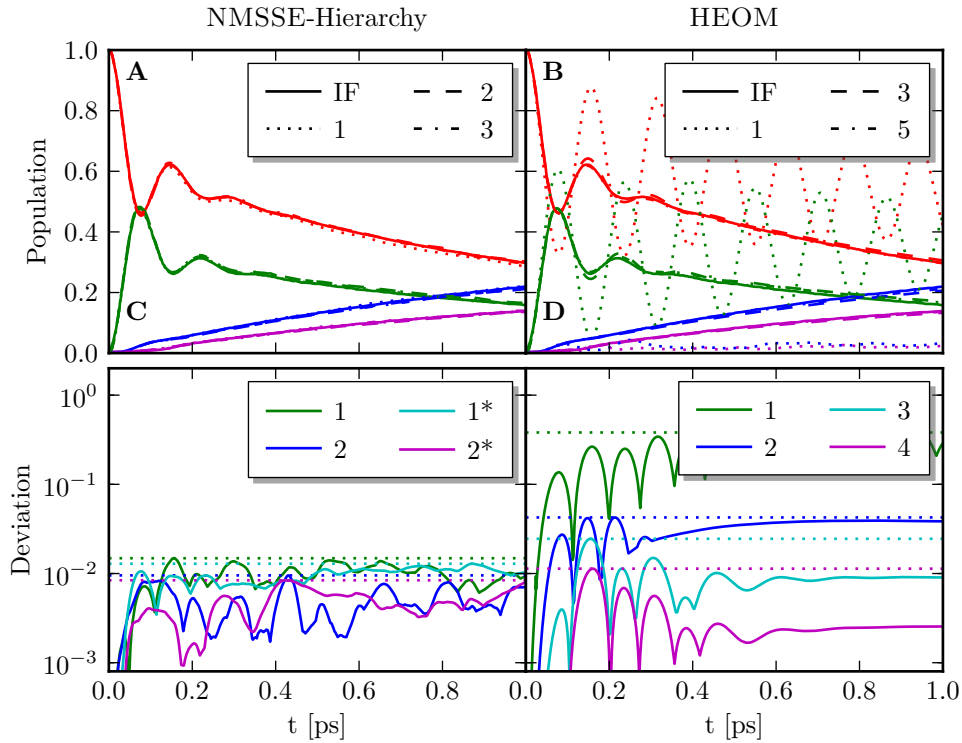


**Figure 4.5.:** Exciton transfer of the simplified FMO-monomer at 300 K for BCHls 1–4 with initial excitation on site 1 and internal convergence check of the hierarchies. Solid lines display the reference results [IF09].

(A) NMSSE-hierarchy with 10000 realizations and truncation orders 1–3.

(B) Same sets of parameters, but calculated in the HEOM formalism with truncation at orders 1, 3 and 5 using PHI [SS12].

(C) The deviation of the stochastic hierarchy with respect to its third order result. Dotted lines indicate the maximum value over time. The starred curves correspond to a larger sample size of 50000 realizations.

(D) Same as (C), but for the HEOM calculation. Here, the reference is the fifth order result.

not shown in this picture. For the same reason, the wave-like motion only lasts up to  $t \approx 400$  fs. Notwithstanding, at  $t = 1$  ps the population of the relevant, third BChl is 0.2—still about two-thirds of the result at cryogenic temperature—and increases further.

This time, the NMSSE-hierarchical equations of motion reproduce the results of Ishizaki-Fleming almost exactly and once again, differences between first, second and third order are negligible. We see in Fig. 4.4 that the imaginary part of  $\alpha(0)$  is now very small compared to its real part, therefore, the deviations it caused at 77 K are not relevant at higher temperatures. Nevertheless, the differences between first and second order are more pronounced than in the low temperature calculations. Of course, this is due to the larger real-part of the coupling constant  $\Re\alpha(0) = \Re g = 14279 \text{ cm}^{-1}$  compared to  $\Re g = 2916 \text{ cm}^{-1}$  for  $T = 77 \text{ K}$ , as discussed in Sect. 3.3.2. The second, almost-Markovian mode is irrelevant for the truncation due to its large inverse correlation-time  $\gamma = 1000 \text{ cm}^{-1}$ .

On the right hand side of Fig. 4.5 B, we carry out the same calculations in the HEOM-formalism [SS12]. Clearly, for a good approximation we need a much larger truncation order. The first order calculation displays highly undamped oscillations and further auxiliary states are necessary to get the qualitative picture right. We have found that a truncation at fifth order is necessary to correctly reproduce the coherent oscillations between 0 fs and 300 fs.

To check internal convergence of each method systematically, we proceed as follows: First we define a measure for deviation of a given reduced density matrix  $\rho(t) = \rho_D(t)$ , obtained from a numerical calculation up to order  $D$ , with respect to some reference  $\rho^{\text{ref}}(t)$  as

$$A[\rho(t), \rho^{\text{ref}}(t)] = \max_n |\rho_{nn}(t) - \rho_{nn}^{\text{ref}}(t)|. \quad (4.11)$$

Since we confine our discussion to the population of the exciton states  $n$  given by  $\rho_{nn}$ ,  $A$  reflects the deviations seen in the pictures. Also, we are only interested in the convergence of the density matrix or pure state hierarchy itself, therefore, the reference state  $\rho^{\text{ref}} = \rho_D$  is calculated with the same method and selected by increasing the truncation order  $D$  until  $A[\rho_{D-1}(t), \rho_D(t)] \approx 10^{-2}$ . This amounts to  $D = 3$  for the NMSSE-hierarchy and  $D = 5$  for the HEOM-formalism. The accuracy of lower-order calculations with respect to the chosen reference is shown in Fig. 4.5 C and D for the NMSSE and the density matrix hierarchy, respectively.

We already mentioned in the general discussion above that within the pure state hierarchy, the first order's deviation from the third order of about 2% is barely visible in Fig. 4.5 A. In contrast, the same accuracy is obtained in the HEOM-formalism not until we truncate the hierarchy at third order (neglecting even stronger deviations for  $t < 300$  fs). But there is a major difference between the two approaches: The HEOM-calculations show the largest discrepancy at the initial wave-like motion and then the accuracy improves by about an order of magnitude, whereas the deviations of the NMSSE-hierarchy remain more or less constant after  $t = 0.2$  ps for the first order or oscillate irregularly for the second order calculations. These observations indicate that at this level of accuracy the errors of the Monte-Carlo sampling play a significant role. We check this statement by repeating the same calculations using a larger sample size—a star marks the corresponding results in Fig. 4.5. The slightly better accuracy supports this statement, but a clear confirmation would require a tremendous number of realizations.

In conclusion, the discussion above shows that the hierarchical equations based on the nonlinear NMSSE provide a highly efficient method to calculate exciton energy transfer dynamics in the FMO-complex. We obtain almost perfect agreement for both, 77 K and 300 K, with the established results of Ishizaki and Fleming in first order calculations. The discrepancy of these to higher order calculations is less than a few percent, demonstrating very rapid convergence with respect to the truncation order. Of course, the achieved accuracy is completely unnecessary for most investigations on biological systems, because the theoretical model itself is usually much less reliable due to approximations and experimental errors for the parameters involved. Also, the improved numerical efficiency, due to a reduced number of auxiliary states<sup>4</sup> and propagating Hilbert space vectors instead of density matrices, is more than compensated by the large sample size required. However, the stochastic hierarchies' advantages really come to fruition when dealing with more complex systems. For example, data from fluorescence line-narrowing measurements on *Prosthecochloris aesturaii* indicate [AR06] that more realistic spectral densities are far

---

<sup>4</sup>In the case of a single bath mode, we have eight auxiliary states for  $D = 1$  compared to 330 for  $D = 4$ .

more structured, requiring about 25 exponential modes<sup>5</sup>. This amounts to 176 auxiliary states for  $D = 1$  compared to a tremendous number of 41 million states required by a fourth-order calculation. Although it is not clear, if such a low-order truncation still produces accurate results for more structured environments, the improved convergence compared to the HEOM-formalism might be crucial for the treatment of more realistic systems.

### 4.3. Absorption Spectra of Molecular Aggregates

The second exemplary application of our pure-state hierarchy is the calculation of absorption spectra in molecular aggregates. In general, the NMSSE provides a highly efficient framework to attack this problem, since all the relevant information is encoded in a single realization  $\psi_t(Z^* = 0)$  and no stochastic average is necessary. In a previous work based on the convolutionless formulation (2.16) in ZOFE approximation, good agreement with the exact pseudo-mode approach<sup>6</sup> was achieved in large parts of the parameter space [RSE11]. However, for intermediate values of the electronic coupling  $V_{mn}$  noticeable deviations occurred. Here, we show that the linear hierarchy (3.7) is equally well suited for this task, but with the additional benefit that a systematic improvement is achieved by increasing the truncation order.

#### 4.3.1. NMSSE for Spectra

In this section, we demonstrate the simple connection between solutions of the linear NMSSE with  $Z_t^* = 0$  and absorption spectra of molecular aggregate at zero temperature [REWS09, RSE11]. Using the thermo-field construction from Sect. 2.5, we can treat an arbitrary thermal environment along the same lines [RSE]. Clearly, for  $T = 0\text{ K}$  the initial state of the aggregate is given by  $|0_{\text{el}}\rangle \otimes |0\rangle$  with the electronic ground state  $|0_{\text{el}}\rangle$  defined in Eq. (4.7) and the vibrational ground state  $|0\rangle$ . In dipole-

---

<sup>5</sup>The spectral density of Fig. 2 in the cited reference can be approximately described with 12 anti-symmetrized Lorentzians, each amounting to two exponential modes. Additional correction terms are necessary depending on the temperature.

<sup>6</sup>The pseudo-mode approach amounts to replacing exponential modes of the bath correlation function by a harmonic oscillator coupled to a Markovian environment [Ima94]. Although formally exact, this approach is quite limited in application due to large computational demands.

approximation, the absorption coefficient of light with frequency  $\nu$  and polarization  $\vec{E}$  is given by [MK11]

$$A(\nu) = \Re \left( \int_0^\infty e^{i\nu t} M(t) dt \right), \quad (4.12)$$

where the dipole-correlation function reads

$$M(t) = \langle 0_{\text{el}} | \langle 0 | \vec{\mu} \cdot \vec{E} e^{-iH_{\text{agg}}t} \vec{\mu} \cdot \vec{E}^* | 0_{\text{el}} \rangle | 0 \rangle. \quad (4.13)$$

Here,  $\vec{\mu} = \sum_m \vec{\mu}_m$  denotes the total dipole operator of the aggregate and  $H_{\text{agg}} = H_{\text{el}}^{(0)} + H_{\text{el}}^{(1)} + H_{\text{env}}$  is the total aggregate Hamiltonian restricted to the electronic subspace with at most one exciton. Provided the dipole-operators are independent of the vibrational degrees of freedom, inserting complete sets of electronic basis vectors  $\sum_m |m\rangle \langle m|$  in Eq. (4.13) yields

$$M(t) = \sum_{m,n} d_m^* d_n \langle m | \langle 0 | e^{-iH_{\text{agg}}t} | n \rangle | 0 \rangle \quad (4.14)$$

with the transition dipole-elements projected in the direction of polarization

$$d_m = \langle m | \vec{\mu} \cdot \vec{E}^* | 0_{\text{el}} \rangle.$$

Since the expectation value of the time evolution operator in Eq. (4.14) includes only contributions from the one-exciton subspace, it is equivalent to

$$M(t) = \left( \sum_m d_m^* \langle m | \langle 0 | \right) e^{-iH_{\text{agg}}^{(1)}t} \left( \sum_n d_n | n \rangle | 0 \rangle \right) = |\mathbf{d}|^2 \langle \Psi_0 | \Psi_t \rangle.$$

with  $H_{\text{agg}}^{(1)} = H_{\text{el}}^{(1)} + H_{\text{env}}$  given by Eq. (4.9). Here,  $|\Psi_t\rangle$  denotes the solution to

$$\partial_t |\Psi_t\rangle = -iH_{\text{agg}}^{(1)} |\Psi_t\rangle, \quad |\Psi_0\rangle = |\psi_0\rangle \otimes |0\rangle \quad (4.15)$$

with the initial electronic state  $|\psi_0\rangle = |\mathbf{d}|^{-1} \sum_m d_m |m\rangle$ . The sum of the dipole-elements  $|\mathbf{d}|^2 = \sum_n |d_n|^2$  is introduced to ensure normalization of  $|\psi_0\rangle$ .

Equation (4.15) is already very close to the microscopic version of our NMSSE. The only difference to Eq. (2.11) is that the latter is formulated in the interaction

picture. However, transforming the time evolution picture leaves the scalar product  $\langle \Psi_0 | \Psi_t \rangle$  and the initial state  $|\Psi_0\rangle = |\psi_0\rangle \otimes |0\rangle$  unchanged. Therefore, we can insert the resolution of unity for coherent states (2.9) and obtain

$$M(t) = |\mathbf{d}|^2 \int \frac{d^{2N}z}{\pi^N} \langle \psi_0 | \psi_t(z^*) \rangle \langle 0 | z \rangle,$$

where  $\psi_t(z^*)$  is the solution to Eq. (2.11). As  $\langle 0 | z \rangle = 1$  and  $\langle \psi_0 | \psi_t(z^*) \rangle$  is analytical in  $z^*$ , the only term of the corresponding Taylor series that is not canceled by the integral is independent of  $z^*$ . In other words, the dipole correlation function expressed in terms of solutions  $\psi_t(Z^*)$  of the linear NMSSE reads

$$M(t) = |\mathbf{d}|^2 \langle \psi_0 | \psi_t(z^* = 0) \rangle = |\mathbf{d}|^2 \langle \psi_0 | \psi_t(Z^* = 0) \rangle. \quad (4.16)$$

Of course, this does not imply that we can simply neglect the functional derivative in the NMSSE. Nevertheless, the corresponding hierarchy (3.7) is completely local in  $Z_t^*$ , so we can set  $Z_t^* = 0$  in each order. In conclusion, assuming a single exponential bath mode  $\alpha(t) = g e^{-(\gamma+i\Omega)t}$  ( $t > 0$ ), the relevant trajectory  $\psi_t(Z^* = 0) =: \psi_t^{(0)}$  satisfies the following set of equations

$$\partial_t \psi_t^{(k)} = (-iH - k(\gamma + i\Omega)\psi_t^{(k)} + k\alpha(0)\psi_t^{(k-1)} - L^\dagger \psi_t^{(k+1)}), \quad (4.17)$$

with initial conditions  $\psi_0^{(0)} = \psi_0$  and  $\psi_0^{(k)} = 0$  ( $k \geq 1$ ).

### 4.3.2. Results

As a demonstration, we investigate absorption spectra of linear aggregates with identical monomers and parallel dipole-moments in this section. For the electronic interaction we assume nearest-neighbor coupling with equal strength, that is  $V_{mn} = (V\delta_{m,n+1} + V\delta_{m,n-1})$ . The vibrational degrees of freedom are described by a single exponential mode  $\alpha(t) = e^{-\gamma|t|-i\Omega t}$ . We use the results of Roden, Strunz and Eisfeld [RSE11] obtained in the exact pseudo-mode approach as a reference, but also compare a few aspects to the ZOFE-results from the same work.

Figure 4.6 displays the spectra of a dimer for two widths of the spectral density, namely  $\gamma = 0.25\Omega$  and  $\gamma = 0.1\Omega$ , and different coupling strengths  $V$ . Using the truncation order  $D = 5$  (dashed line), we obtain perfect agreement with the reference

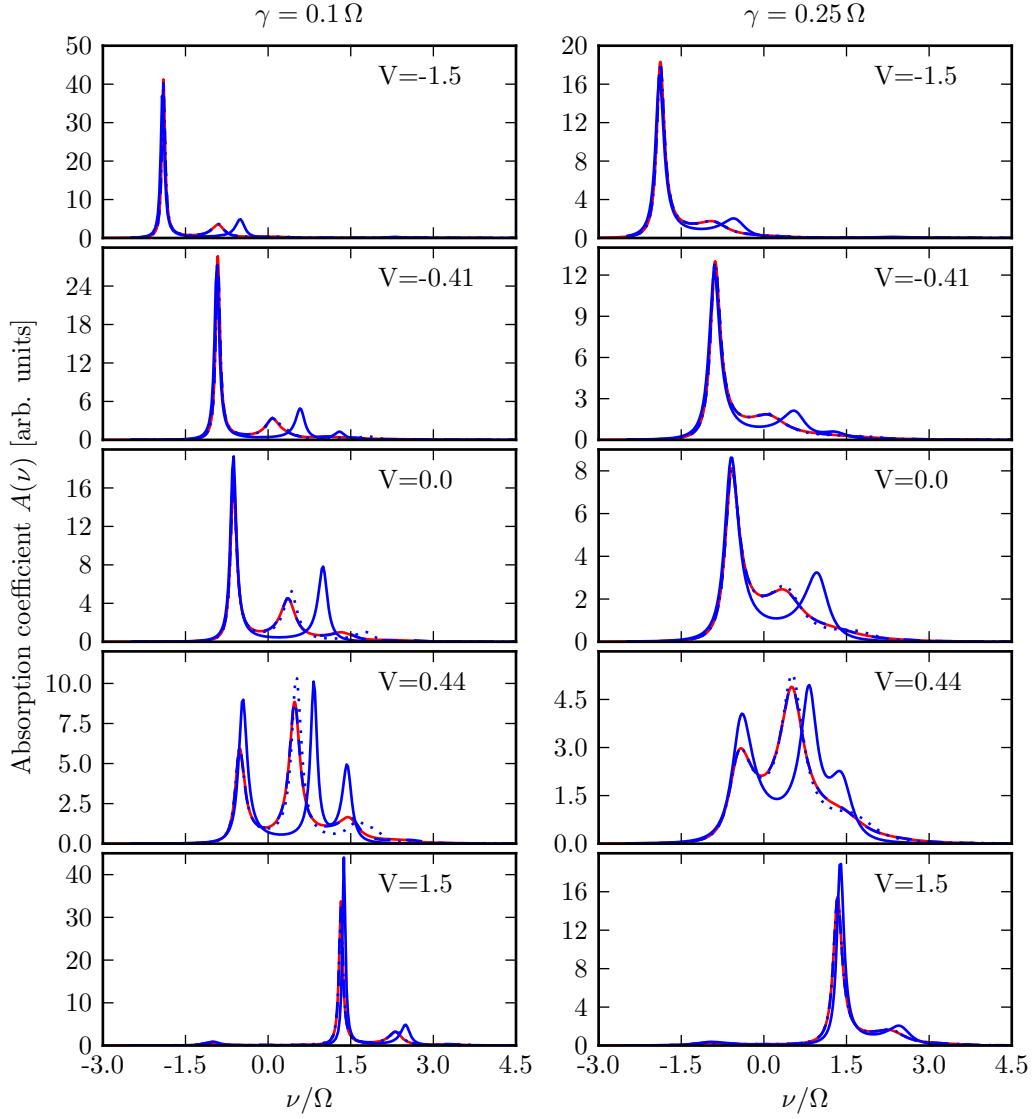


**Figure 4.6.:** Absorption spectra of a dimer and a single-mode bath correlation function with  $g = 0.64 \Omega$ ,  $\gamma = 0.1 \Omega$  (left) and  $\gamma = 0.25 \Omega$  (right). The NMSSE-hierarchy results (blue) with truncation at first (solid), third (dotted) and fifth (dashed) order are compared to the pseudo-mode spectra (red).

#### 4. Molecular Aggregates and the NMSSE

---

for all values of  $V$ . To investigate the behavior for smaller truncation orders, we also show the results for  $D = 1$  (solid) and  $D = 3$  (dotted). Not surprising, these approximate the exact result better in the case of larger  $\gamma = 0.25$  compared to  $\gamma = 0.1$ . Similar to the ZOFE-approach, best agreement is achieved for large values of  $|V|$ , because the impact of the environment is reduced by a strong electronic Hamiltonian. For smaller  $|V|$ , the influence of the environment grows and more auxiliary states are needed in order to reproduce the reference's results. However, while ZOFE is exact for  $V = 0$  [RSE11], the first order NMSSE-hierarchy shows about the same amount of deviation as in the  $V = -0.41$  plot.

Remarkably, the NMSSE-hierarchy improves systematically with increasing truncation order. Already the first order calculations reproduce the position of the lowest energy peak—and for  $V < 0$  the magnitude as well—with very high precision. This behavior continues for the next peaks, too, as the spectra for  $V = 0.44$  show: Although the higher-frequency spectrum  $\nu > 0$  is obtained correctly only for the maximum truncation order  $D = 5$ , the position of the second peak is well-approximated at the intermediate value  $D = 3$ .

To strengthen this statement, we study a more complex system, namely a PTCDA dimer with a bath correlation function consisting of six exponential modes. The latter was already used as an approximation to a realistic environment in pseudo-mode calculations [RED<sup>+</sup>11]. In contrast to the rest of this work, all modes under consideration are purely oscillatory, that is  $\gamma = 0$ . Nevertheless, Fig. 4.7 clearly shows a behavior similar to the previous spectra 4.6 with increasing truncation order  $D$ : Even the first order  $D = 1$  yields the correct position of the lowest major peak at wavenumber  $k \approx -800 \text{ cm}^{-1}$  with good precision, but fails at higher energies. The next order shown ( $D = 3$ ) roughly reproduces the correct magnitude and position for the three characteristic peaks on the left and approximately indicates the smaller structure between the two major peaks at  $k \approx -800 \text{ cm}^{-1}$  and  $k \approx 700 \text{ cm}^{-1}$ . The latter marks the upper boundary for the region where the two highest order calculations with  $D = 5$  and  $D = 7$  practically coincide. For even higher wavenumber, deviations are pronouncedly visible but not random. Roughly, the highest order calculation only improves the position and magnitude of the peaks that are already present for  $D = 5$ .

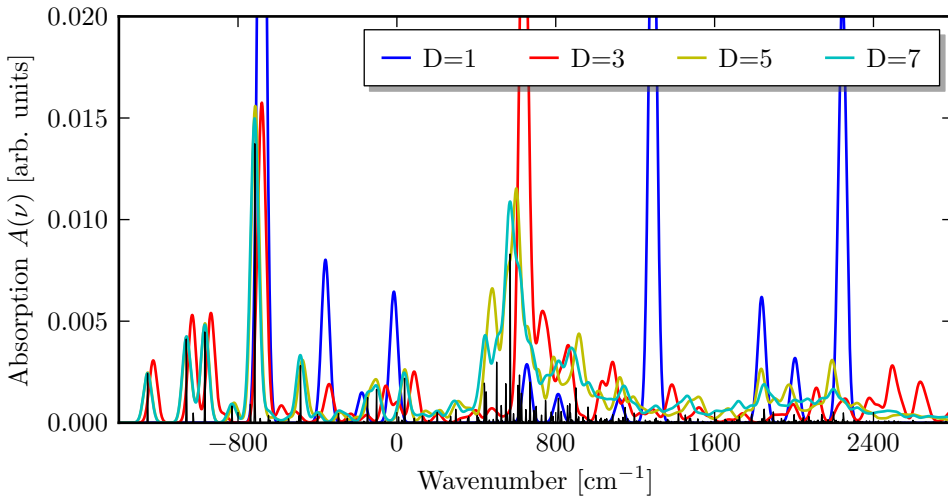


**Figure 4.7.:** Absorption spectrum for the PTCDA-dimer convoluted with a Gaussian of width  $\sigma = 20 \text{ cm}^{-1}$  with electronic coupling  $V = 600 \text{ cm}^{-1}$  and different truncation orders  $D$  of the hierarchy. The black lines display the sharp peaks of the spectrum for  $D = 7$  with a much narrower enveloping Gaussian ( $\sigma = 1 \text{ cm}^{-1}$ ). We use a bath correlation function with six purely-oscillatory exponentials, see Table C.3 for the parameters [RED<sup>+</sup>11, Tab. 1 D].

Summarizing the above, we have demonstrated that the hierarchy of pure states provides an efficient tool to study absorption spectra of quantum aggregates. In contrast to the study of the time evolution of a reduced density matrix, the calculation of spectra in the NMSSE-formalism requires no Monte-Carlo average over several realizations. Therefore, one major advantage of the NMSSE compared to density-matrix formalisms, namely the propagation of state vectors, really comes into its own. This combined with the very predictable behavior for a growing number of hierarchy orders allows studying large-dimensional systems coupled to a highly structured environment, especially the low-energy part of the spectra. Besides, we have also demonstrated that truncation of the NMSSE-hierarchy is possible for  $\gamma \rightarrow 0$ , exemplifying applicability of this approach even in the highly non-Markovian limit.



## 5. Conclusions and Outlook

Starting with the goal to investigate large open quantum systems coupled to structured environments, we devised a hierarchy of quantum trajectories in this work. Since it extends the benefits of Monte-Carlo methods from the Markovian regime to the more general case of a non-Markovian environment, the newly-devised approach is highly suited to attack problems of current research.

With the NMSSE constituting the foundation of this work, we recalled its derivation based on a microscopic model for the system and its environment in Chapter 2. Subsequently, the most challenging characteristic of the NMSSE, namely the appearance of a functional derivative with respect to the noise involving the complete history of the system, was discussed based on the Jaynes-Cummings model. Beside the established  $O$ -operator substitution, we introduced a new direct approach that makes use of a functional Taylor series of the quantum trajectory with respect to the noise. With the help of the latter, we were able to explain the resonant peaks showing up in the magnitude of the  $O$ -operator for certain sets of parameters which are likely responsible for divergences in a numerical propagation. The observation that these large contributions disappear in the NMSSE due to cancellation with small components of the quantum trajectory has convinced us to attack the problem of the functional derivative directly.

For that matter, we derived a hierarchy of linear stochastic Schrödinger equations in Chapter 3 by absorbing the memory integral with the derivatives into auxiliary pure states. The corresponding nonlinear hierarchy constitutes an important result of this work, since it dramatically reduces the sample size required for the Monte-Carlo average. We demonstrated this statement with the help of the Spin-Boson model, which was also used to demonstrate the influence of the truncation order on the accuracy of the results.

## *5. Conclusions and Outlook*

---

The main part of this work is the investigation of exciton energy transfer in light-harvesting complexes in Chapter 4. With quantum effects responsible for its remarkable efficiency, the FMO-protein complex constitutes a great example of how quantum mechanics influences the operation of living cells. Our calculations from Sect. 4.2 confirm the results from prior work that even at physiological temperature the coherent, wave-like motion of excitons is crucial for the operation of the FMO-complex. As we demonstrated, the NMSSE-hierarchy is capable of reproducing the established results obtained in the HEOM-formalism. Even more, our newly-devised approach achieves the same precision as the established density matrix hierarchy consuming only a fraction of the computational resources. Although the Monte-Carlo evaluation requires the propagation of many trajectories, the NMSSE-hierarchy benefits from the reduced number of auxiliary states due to the smaller truncation order necessary. Besides, the calculation of independent realizations is easily distributed to many computers.

The second application of the pure state hierarchy presented in this work is the study of optical absorption spectra of molecular aggregates. Since the latter is reduced to the calculation of a single pure state trajectory, no Monte-Carlo average is necessary. Also, we have demonstrated that the low-energy part of the absorption spectrum can be obtained with less computational expense than the full spectrum. This makes the NMSSE highly interesting for the study of systems that are currently out of reach from established methods as the lowest energy peaks are often sufficient to assess the structure of the complex roughly.

With the reliability and efficiency of the NMSSE-hierarchy demonstrated in this work, future investigation will have to attack new problems. For example, we have restricted the investigation in Sect. 4.2 to very simple spectral densities. The treatment of a more realistic environment will clearly benefit from the improved convergence of the NMSSE-hierarchy with respect to the truncation order. Therefore, the question, how details of the spectral density affect the energy transfer, constitutes a suitable subject of future work. This problem has already been treated in the ZOFE-approach [RRSE11], however, it is not sure if the latter is still valid for the parameters under consideration. Since we can check the accuracy of a calculation simply by com-

---

paring with higher-order results, the NMSSE-hierarchy may shed some light into this question.

A further point, which has not been treated in this work at all, is that quantum trajectories contain more information than the reduced density operator. Indeed, since the NMSSE is equivalent to the microscopic Schrödinger equation introduced in Sect. 2.1, the set of all quantum trajectories contains—at least in principle—all information on the environment and the system-bath entanglement. It is a fascinating question, if it is possible to gain knowledge about the full state from the finite set of trajectories calculated in a Monte-Carlo simulation.

Finally, future work should investigate how a large class of initial conditions can be treated in the NMSSE-formalism. Throughout this thesis, we have only considered a product state with the environment at thermal equilibrium. Especially the treatment of initially entangled states with the NMSSE remains an open problem.



## A. Discrete Time Evolution of Time-Oscillators

In this chapter we rewrite the full time evolution operator for the NMSSE

$$U(t, 0) = T_+ \exp \left( \int_0^t -iH + LZ_s^* - L^\dagger \mathcal{D}_s \, ds \right) \quad (\text{A.1})$$

for discrete time steps  $t_k = k\Delta t$  ( $k \in \mathbb{Z}$ ) and small  $\Delta t$ . We show that under these conditions it can be approximated by an alternating product of the free evolution operator  $\exp(-i\Delta t H)$  of the system and

$$U_n = \exp(\Delta t LZ_n^* - \Delta t L^\dagger \mathcal{D}_n) \quad (\text{A.2})$$

accounting for the bath-interaction. Here, the discrete “noise-process” is given by

$$Z_n^* := \frac{1}{\Delta t} \int_{t_{n-1}}^{t_n} Z_t^* \, dt \quad (\text{A.3})$$

with the corresponding derivative-operator

$$\mathcal{D}_n := \frac{1}{\Delta t} \int_{t_{n-1}}^{t_n} \mathcal{D}_t \, dt = \frac{1}{\Delta t} \int_{t_{n-1}}^{t_n} \int \alpha(t-s) \frac{\delta}{\delta Z_s^*} \, ds \, dt.$$

For the latter, we find the familiar representation  $\mathcal{D}_n = \sum_k \alpha_{n-k} \frac{\partial}{\partial Z_k^*}$ , since

$$\begin{aligned} \mathcal{D}_n Z_k^* &= \frac{1}{(\Delta t)^2} \int_{t_{n-1}}^{t_n} dt \int_{t_{k-1}}^{t_k} dt' \int ds \alpha(t-s) \frac{\delta Z_{t'}^*}{\delta Z_s^*} \\ &= \frac{1}{(\Delta t)^2} \int_{t_{n-1}}^{t_n} dt \int_{t_{k-1}}^{t_k} dt' \alpha(t-t') \\ &=: \alpha_{n-k} \end{aligned}$$

### A. Discrete Time Evolution of Time-Oscillators

---

and  $\sum_{k'} \alpha_{n-k'} \frac{\partial Z_k^*}{\partial Z_{k'}^*} = \alpha_{n-k}$  coincide.

Starting from the Schrödinger time evolution for the microscopic model introduced in Sect. 2.1, we use Trotter's product formula to separate the system's free evolution

$$|\Psi_t\rangle = e^{-it(H+H_{\text{env}}+H_{\text{int}})}|\Psi_0\rangle = \lim_{n \rightarrow \infty} \left( e^{-it(H_{\text{env}}+H_{\text{int}})/n} e^{-itH/n} \right)^n |\Psi_0\rangle. \quad (\text{A.4})$$

Since in the following we are only interested in the qualitative picture, we drop the limit and assume a sufficiently small time step  $\Delta t = t/n$ . Similar to the derivation of the NMSSE, we switch to the interaction picture with respect to  $H_{\text{env}}$  and denote the corresponding state by  $|\tilde{\Psi}_t\rangle$ . The propagator of the interaction part reads

$$\tilde{U}_{\text{int}}(t, s) = e^{+itH_{\text{env}}} e^{-i(t-s)H_{\text{int}}} e^{-isH_{\text{env}}} = T_+ e^{-i \int_s^t \tilde{H}_{\text{int}}(\tau) d\tau},$$

where  $\tilde{H}_{\text{int}}(t)$  is the time-dependent interaction from the microscopic model, namely

$$\tilde{H}_{\text{int}}(t) = L \sum_{\lambda} g_{\lambda}^* e^{-i\omega_{\lambda} t} z_{\lambda}^* + L^\dagger \sum_{\lambda} g_{\lambda} e^{i\omega_{\lambda} t} \partial_{z_{\lambda}^*}. \quad (\text{A.5})$$

Here, we choose the coherent state-representation used throughout this work. Also, the initial state  $|\Psi_0\rangle = |\psi_0\rangle \otimes |0\rangle$  remains unchanged under the time evolution picture transformation. Therefore, we can rewrite Eq. (A.4) using  $t_k = k\Delta t$

$$\begin{aligned} \tilde{\psi}_{t_n}(Z^*) &= e^{it_n H_{\text{env}}} \left( e^{-i\Delta t(H_{\text{env}}+H_{\text{int}})} e^{-i\Delta tH} \right)^n \psi_0 \\ &= \tilde{U}_{\text{int}}(t_n, t_{n-1}) e^{-i\Delta tH} e^{it_{n-1} H_{\text{env}}} \left( e^{-i\Delta t(H_{\text{env}}+H_{\text{int}})} e^{-i\Delta tH} \right)^{n-1} \psi_0 \\ &= \tilde{U}_{\text{int}}(t_n, t_{n-1}) e^{-i\Delta tH} \tilde{U}_{\text{int}}(t_{n-1}, t_{n-2}) \dots \tilde{U}_{\text{int}}(t_1, t_0) e^{-i\Delta tH} \psi_0. \end{aligned}$$

This is almost the sought-after form, since  $\tilde{U}_{\text{int}}(t_n, t_{n-1})$  and  $U_n$  defined in Eq. (A.2) coincide except for the time-ordering operator. However, the latter only yields corrections proportional to  $\Delta t$ , which we already neglected using the Trotter product formula. In conclusion, we can rewrite the full time evolution operator (A.1) (dropping the tilde for the interaction-picture) as

$$\psi_{t_n}(Z^*) = U_n e^{-i\Delta tH} U_{n-1} \dots U_1 e^{-i\Delta tH} \psi_0. \quad (\text{A.6})$$

## B. Analytic Solution of the Jaynes-Cummings Model

### B.1. General Approach

Here, we present in full detail the analytic solution of the Jaynes-Cummings model introduced in Sect. 2.6. For zero temperature the relevant NMSSE can always be expressed in terms of a single process

$$\partial_t \psi_t(Z^*) = -i\frac{\omega}{2}\sigma_z \psi_t(Z^*) + g\sigma_- Z_t^* \psi_t(Z^*) - g\sigma_+ \int \alpha(t-s) \frac{\delta \psi_t(Z^*)}{\delta Z_s^*} ds. \quad (\text{B.1})$$

with initial conditions  $\psi_0(Z^*) = \psi_0$ . We make an ansatz for the quantum trajectory at most linear in  $Z_s^*$

$$\psi_t(Z^*) = \psi(t) + \int_0^t \psi_s(t) Z_s^* ds \quad (\text{B.2})$$

and incorporate the  $Z_s^*$ -independence of  $\psi_t(Z^*)$  for  $s < 0$  and  $s > t$  using a bounded integral domain. The “+”-component of our NMSSE with the ansatz (B.2) reads

$$\begin{aligned} \dot{\psi}_t^+(t) + \psi_t^+(t) Z_t^* + \int_0^t \dot{\psi}_s^+(t) Z_s^* ds \\ = -i\frac{\omega}{2} \left( \psi^+(t) + \int_0^t \psi_s^+(t) Z_s^* ds \right) - g \int_0^t \alpha(t-s) \psi_s^-(t) ds, \end{aligned} \quad (\text{B.3})$$

where the dot indicates derivation with respect to  $t$ . In order to separate contributions of different order in  $Z_s^*$ , we apply the functional derivative  $\delta/\delta Z_s^*$  to the last equation

$$\psi_t^+(t) \delta(t-s) + \int_0^t \dot{\psi}_{s'}^+(t) \delta(s-s') ds' = -i\frac{\omega}{2} \int_0^t \psi_{s'}^+(t) \delta(s-s') ds'. \quad (\text{B.4})$$

## B. Analytic Solution of the Jaynes-Cummings Model

---

Choosing  $s \in (0, t)$  leaves us with a simple ordinary differential equation with solution  $\psi_s^+(t) = C_s \exp(-i\omega t/2)$ . Since there is only one term in Eq. (B.4) proportional to  $\delta(t - s)$ ,  $\psi_t^+(t)$  and thus the constant  $C_t$  must vanish. Formally, this amounts to integrating (B.4) over a small interval  $(t - \varepsilon, t + \varepsilon)$  with respect to  $s$ . In the limit  $\varepsilon \rightarrow 0$  all terms except the first go to zero. On the other hand, we can isolate all terms independent of  $Z_s^*$  in Eq. (B.3) simply by taking the expectation value, yielding

$$\dot{\psi}^+(t) = -i\frac{\omega}{2}\psi^+(t) - g \int_0^t \alpha(t-s)\psi_s^-(t) ds. \quad (\text{B.5})$$

We postpone its solution to the end of this section.

The “-” component of Eq. (B.1) is quite similar to (B.3):

$$\begin{aligned} \dot{\psi}^-(t) + \psi_t^-(t)Z_t^* &+ \int_0^t \dot{\psi}_s^-(t)Z_s^* ds \\ &= i\frac{\omega}{2} \left( \psi^-(t) + \int_0^t \psi_s^-(t)Z_s^* ds \right) + g\psi^+(t)Z_t^*, \end{aligned} \quad (\text{B.6})$$

where we have already used that  $\psi_s^+(t) = 0$ . Comparing all terms independent of  $Z_s^*$  leads to  $\psi^-(t) = \psi_0^- e^{i\frac{\omega}{2}t}$ . In the same manner as we derived Eq. (B.4), we can treat all terms proportional to  $Z_s^*$ . There is an additional singular terms proportional to  $Z_t^*$  due to the driving process in Eq. (B.1). It gives rise to the boundary condition

$$\psi_t^-(t) = g\psi^+(t) \quad (\text{B.7})$$

The contributions proportional to  $Z_s^*$  under the integral  $\dot{\psi}_s^-(t) = i\frac{\omega}{2}\psi_s^-(t)$  for  $0 < s < t$  are solved by  $\psi_s^-(t) = C_s \exp(i\omega t/2)$ , where  $C_s$  is determined by (B.7). Therefore, we find

$$\psi_s^-(t) = g\psi^+(t) e^{i\frac{\omega}{2}(t-s)}.$$

Together with (B.5) we obtain a closed equation for  $\psi^+(t)$

$$\dot{\psi}^+(t) = -i\frac{\omega}{2}\psi^+(t) - g^2 \int_0^t \alpha(t-s)e^{i\frac{\omega}{2}(t-s)}\psi^+(s) ds. \quad (\text{B.8})$$

Hence, we may replace the original NMSSE (B.1) by a  $\mathbb{C}$ -valued integro-differential equation. The full solution to Eq. (B.1) in terms of  $\psi^+(t)$  is written out in Eq. (2.55).

## B.2. Exponential Bath Correlation Function

Equation (B.8) still contains a memory integral, which makes it tremendously hard to find an analytical solution. The situation is noticeably simpler for

$$\alpha(t-s) = \sum_{j=1}^N g_j e^{-\gamma_j |t-s| - i\Omega_j(t-s)}. \quad (\text{B.9})$$

Since  $\psi^+(t)$  only depends on values of  $\alpha(t-s)$  for  $s \geq t$ , we can assume  $\gamma = 0$  without loss of generality. Similar to our hierarchical equations of motion, we absorb the problematic terms into auxiliary functions

$$\phi_j(t) := \int_0^t \alpha_j(t-s) e^{i\frac{\omega}{2}(t-s)} \psi^+(s) ds. \quad (\text{B.10})$$

This allows us to rewrite Eq. (B.8) as a system of  $(N+1)$  ordinary differential equations

$$\begin{aligned} \dot{\psi}^+(t) &= -i\frac{\omega}{2}\psi^+(t) - g^2 \sum_{j=1}^N \phi_j(t) \\ \dot{\phi}_j(t) &= g_j \psi^+(t) + i\left(\frac{\omega}{2} - \Omega\right) \phi_j(t) \end{aligned}$$

with constant coefficients and initial conditions  $\psi^+(0) = \psi_0^+$  as well as  $\phi_j(0) = 0$ . In the special case  $N = 1$  the diagonalization of the coefficient matrix can be carried out analytically. With the shorthand notation  $\tilde{\Omega} = \sqrt{(\omega - \Omega)^2 + 4g^2}$  and  $g_1$  absorbed into the coupling strength  $g$ , the solution to Eq. (B.8) reads

$$\psi^+(t) = \frac{\psi_0^+}{2\tilde{\Omega}} \left( (\omega - \Omega + \tilde{\Omega}) e^{-i\frac{\Omega+\tilde{\Omega}}{2}t} - (\omega - \Omega - \tilde{\Omega}) e^{-i\frac{\Omega-\tilde{\Omega}}{2}t} \right). \quad (\text{B.11})$$



# C. NMSSE-Hierarchy and Application

## C.1. The Memory-Integral Term

In this section we discuss the crucial simplification, how an exponential bath correlation function  $\alpha(t) = g e^{-\gamma|t| - i\Omega t}$  with real parameters  $g, \gamma, \Omega$  leads to

$$\dot{\mathcal{D}}_t \psi_t(Z^*) = (-\gamma + i\Omega) \mathcal{D}_t \psi_t(Z^*) \quad (\text{C.1})$$

for the noise-derivation operator  $\mathcal{D}_t = \int \alpha(t-s) \delta/\delta Z_s^* ds$  applied to a solution of the NMSSE with vacuum initial conditions, that is  $\frac{\delta \psi_0}{\delta Z_s^*} = 0$ .

For what follows the bath correlation function is best written as

$$\alpha(t) = g e^{-\gamma t - i\Omega t} \Theta(t) + g e^{\gamma t - i\Omega t} \Theta(-t).$$

using the Heaviside function  $\Theta(t)$ . In order to determine  $\dot{\mathcal{D}}_t = \int \dot{\alpha}(t-s) \delta/\delta Z_s^* ds$ , we need to calculate

$$\dot{\alpha}(t) = g(-\gamma - i\Omega) e^{-\gamma t - i\Omega t} \Theta(t) + g(\gamma - i\Omega) e^{\gamma t - i\Omega t} \Theta(-t) + g\delta(t) - g\delta(t).$$

Notice that the singular time-derivatives  $\dot{\Theta}(t) = \delta(t)$  cancel. This shows clearly, that  $\dot{\mathcal{D}}_t = (-\gamma - i\Omega) \mathcal{D}_t$  does not hold on the level of operators. Even the vanishing of the functional derivative  $\delta \phi_t(Z^*)/\delta Z_s^*$  for  $s > t$  with some arbitrary stochastic state  $\phi_t(Z^*)$  does not imply  $\dot{\mathcal{D}}_t \phi_t(Z^*) \sim \mathcal{D}_t \phi_t(Z^*)$  as the following example shows: Take a noise expansion (2.42) of the form  $\phi_t(Z^*) = \varphi \cdot (Z_t^* + Z_{t'}^*)$ , where  $\varphi$  is some  $Z_t^*$  independent system state and  $0 < t' < t$ . It clearly satisfies the required boundary conditions, but using  $\Theta(0) = 1/2$  we find

$$\dot{\mathcal{D}}_t \phi_t(Z^*) = (\dot{\alpha}(0) + \dot{\alpha}(t-t')) \varphi = g \left( -i\Omega - (\gamma + i\Omega) e^{-(\gamma+i\Omega)(t-t')} \right) \varphi$$

which is not proportional to

$$\mathcal{D}_t \phi_t(Z^*) = (\alpha(0) + \alpha(t-t'))\varphi = g \left( 1 + e^{(-\gamma+i\Omega)(t-t')} \right) \varphi.$$

The problematic first summand arises due to singular behavior of  $\delta\phi_t(Z^*)/\delta Z_s^*$  at the upper integral bound  $s = t$ .

However, such problems do not occur once we restrict  $\dot{\mathcal{D}}_t$  to solutions of our NMSSE (3.1) with vacuum initial conditions. Indeed, since  $\delta\psi_t/\delta Z_t^* \sim L\psi_t$  as shown in Sect. 2.2.2, the functional derivative of  $\psi_t(Z^*)$  at the upper bound is regular and therefore has vanishing weight under the integral. This is how we obtain Eq. (C.1).

## C.2. Drude Spectral Densities

This section is dedicated to the calculation of the expansion of the bath correlation function

$$\alpha(t) = \sum_{n=0}^{\infty} g_n e^{-\gamma_n t} \quad (t > 0) \tag{C.2}$$

for a Drude spectral density

$$J(\omega) = \frac{2\lambda}{\pi} \frac{\gamma\omega}{\omega^2 + \gamma^2}$$

with poles  $\omega = \pm i\gamma$  and residues  $\text{Res}_{\pm i\gamma}(J) = \frac{\gamma\lambda}{\pi}$ . Let us write  $\alpha(t) = a(t) + ib(t)$  with the corresponding integrals

$$a(t) = \frac{1}{2} \int J(\omega) \coth\left(\frac{\beta\omega}{2}\right) e^{i\omega t} d\omega \quad \text{and} \quad b(t) = \frac{1}{2i} \int J(\omega) e^{i\omega t} d\omega.$$

As already mentioned in Sect. 3.2, these integrals are solved using the residue theorem: For  $t > 0$  we have to include only poles with positive imaginary part, so Eq. (3.24) gives

$$\begin{aligned} a(t) &= i\gamma\lambda \coth\left(\frac{i\beta\gamma}{2}\right) e^{-\gamma t} + \frac{2\pi i}{\beta} \sum_{\gamma_n} \frac{2\lambda}{\pi} \frac{i\gamma\gamma_n}{-\gamma_n^2 + \gamma^2} e^{-\gamma_n t} \\ &= \gamma\lambda \cot\left(\frac{\beta\gamma}{2}\right) e^{-\gamma t} + \frac{4\lambda\gamma}{\beta} \sum_{\gamma_n} \frac{\gamma_n}{\gamma_n^2 - \gamma^2} e^{-\gamma_n t}, \end{aligned}$$

where the last sum is taken over Matsubara frequencies  $\gamma_n = 2\pi n/\beta$ ,  $n \geq 1$ . For convenience we also set  $\gamma_0 = \gamma$ . Similarly, we have for the imaginary part

$$b(t) = \gamma\lambda e^{-\gamma t}.$$

In conclusion, we obtain for the parameters in the expansion (C.2)

$$g_0 = \gamma\lambda \left( \cot\left(\frac{\beta\gamma}{2}\right) - i \right) \quad \text{and} \quad g_{n \geq 1} = \frac{4\lambda\gamma}{\beta} \frac{\gamma_n}{\gamma_n^2 - \gamma^2}.$$

Since  $g_0$  has non-vanishing imaginary part and  $\alpha(-t) = \alpha(t)^*$ , a bath correlation function obtained from a Drude spectral density has a discontinuous jump at  $t = 0$ .

### C.3. Parameters for Calculations

We now turn to the concrete values used in Sect. 4.2 and in the calculations of Ishizaki-Fleming [IF09]. Compared to the inverse relaxation time  $\gamma_0 = 106 \text{ cm}^{-1}$ , the first Matsubara frequency  $\gamma_1 = 1310 \text{ cm}^{-1}$  at  $T = 300 \text{ K}$  is quite large. Additionally, the opposite holds for the corresponding coupling strengths  $g_0 = (14279 - 3716i) \text{ cm}^{-2}$  and  $g_1 = 2381 \text{ cm}^{-2}$ , respectively. Hence, we follow the reference and drop all low-temperature correction terms with  $n \geq 1$  in Eq. (C.2).

For cryogenic temperature  $T = 77 \text{ K}$ , a single mode with  $g_0 = (2916 - 3716i) \text{ cm}^{-2}$  is not sufficient, since the first low-temperature correction term is given by  $\gamma_1 = 336 \text{ cm}^{-2}$  and  $g_1 = 2628 \text{ cm}^{-2}$ . However, the latter was approximated by a purely Markovian mode  $\gamma_1 e^{-\gamma_1 t} \approx \delta(t)$  by Ishizaki-Fleming in order to keep the number of modes as small as possible for the HEOM-approach. The implementation of the NMSSE-hierarchies could not handle a true Markovian mode, so we resort to an exponential mode with  $\tilde{\gamma}_1 > 1000 \text{ cm}^{-1}$  in order to obtain good agreement.

Besides the modes used in the reference, we also added a third almost-Markovian mode  $g_2, \gamma_2$  in order to have a purely real  $\alpha(0) = \sum_n g_n$ . All results are summarized in Table C.1.

	Fig. 4.2	Fig. 4.5
$g_0 \text{ [cm}^{-2}\text{]}$	$2916 - 3716i$	$14279 - 3716i$
$\gamma_0 \text{ [cm}^{-1}\text{]}$	106	106
$g_1 \text{ [cm}^{-2}\text{]}$	7814*	—
$\gamma_1 \text{ [cm}^{-1}\text{]}$	1000*	—
$g_2 \text{ [cm}^{-2}\text{]}$	3716i	3716i
$\gamma_2 \text{ [cm}^{-1}\text{]}$	1000	1000

**Table C.1.:** Parameters for the bath correlation function  $\alpha(t) = \sum_n g_n e^{-\gamma_n t}$  used in Sect. 4.2. Values marked with a star are approximated Markov-modes from the reference. The third mode is merely used to remove the imaginary part of  $\alpha(0)$ .

$H_{mn} \text{ [cm}^{-1}\text{]}$	1	2	3	4	5	6	7
1	<b>410</b>	-87.7	5.5	-5.9	6.7	-13.7	-9.9
2		<b>530</b>	30.8	8.2	0.7	11.8	4.3
3			<b>210</b>	-53.5	-2.2	-9.6	6.0
4				<b>320</b>	-70.7	-17.0	-63.3
5					<b>480</b>	81.1	-1.3
6						<b>630</b>	39.7
7							<b>440</b>

**Table C.2.:** Matrix elements of the purely electronic Hamiltonian used in Sect. 4.2. Consists of site energies (bold) and electronic coupling elements for *Chlorobaculum tepidum* [AR06]. An irrelevant global offset of  $12\,000 \text{ cm}^{-1}$  has been subtracted from the site energies.

$g_i \text{ [cm}^{-2}\text{]}$	21068	12406	57868	414743	220556	626749
$\Omega_i \text{ [cm}^{-1}\text{]}$	229	421	567	1263	1416	1616

**Table C.3.:** Parameters used in Fig. 4.7 and the reference [RED<sup>+</sup>11, Tab. 1 D]. All exponential modes are purely oscillatory, that is  $\gamma_i = 0$ .

# Bibliography

- [AL87] R. Alicki and K. Lendi. *Quantum Dynamical Semigroups and Applications*. 1987.
- [AR06] J. Adolphs and T. Renger. How proteins trigger excitation energy transfer in the FMO complex of green sulfur bacteria. *Biophysical journal*, 91(8):2778–2797, 2006.
- [Bar61] V. Bargmann. On a hilbert space of analytic functions and an associated integral transform part i. *Communications on Pure and Applied Mathematics*, 14(3):187–214, 1961.
- [Ber03] Ø. Bernt. *Stochastic Differential Equations*. Springer, 2003.
- [BG09] A. Barchielli and M. Gregoratti. *Quantum Trajectories and Measurements in Continuous Time: The Diffusive Case*, volume 782. Springer, 2009.
- [BP02] H.-P. Breuer and F. Petruccione. *The Theory of Open Quantum Systems*. Oxford University Press on Demand, 2002.
- [BR03] O. Bratteli and D. W. Robinson. *Operator algebras and quantum statistical mechanics 1: C\*-and W\*-algebras. Symmetry groups. Decomposition of states*, volume 1. Springer, 2003.
- [Car93] H. Carmichael. *An Open Systems Approach to Quantum Optics: Lectures Presented at the Université Libre de Bruxelles, October 28 to November 4, 1991*. Lecture Notes in Computer Science. Springer Berlin Heidelberg, 1993.
- [CL83] A. O. Caldeira and A. J. Leggett. Quantum tunnelling in a dissipative system. *Annals of Physics*, 149(2):374 – 456, 1983.

## Bibliography

---

- [DGS98] L. Diósi, G. Gisin, and W. T. Strunz. Non-markovian quantum state diffusion. *Phys. Rev. A*, 58:1699–1712, Sep 1998.
- [Dió96] L. Diósi. Exact semiclassical wave equation for stochastic quantum optics. *Quantum and Semiclassical Optics: Journal of the European Optical Society Part B*, 8(1):309, 1996.
- [DS97] L. Diósi and W. T. Strunz. The non-markovian stochastic schrödinger equation for open systems. *Physics Letters A*, 235(6):569 – 573, 1997.
- [DS11] W. L. Dunn and J. K. Shultis. *Exploring Monte Carlo Methods*. Access Online via Elsevier, 2011.
- [ECR<sup>+</sup>07] G. S. Engel, T. R. Calhoun, E. L. Read, T.-K. Ahn, T. Mančal, Y.-C. Cheng, R. E. Blankenship, and G. R. Fleming. Evidence for wavelike energy transfer through quantum coherence in photosynthetic systems. *Nature*, 446(7137):782–786, 2007.
- [FHS10] R. P. Feynman, A. R. Hibbs, and D. F. Styer. *Quantum Mechanics and Path Integrals*. Dover books on physics. Dover Publications, Incorporated, 2010.
- [FV63] R. P. Feynman and F. L. Vernon. The theory of a general quantum system interacting with a linear dissipative system. *Annals of physics*, 24:118–173, 1963.
- [FVN10] S. Florens, D. Venturelli, and R. Narayanan. Quantum phase transition in the spin boson model. In *Quantum Quenching, Annealing and Computation*, pages 145–162. Springer, 2010.
- [Gar85] C. W. Gardiner. *Handbook of stochastic methods*, volume 3. Springer Berlin, 1985.
- [GHZ10] C. Gan, P. Huang, and H. Zheng. Non-markovian dynamics of a biased qubit coupled to a structured bath. *Journal of Physics: Condensed Matter*, 22(11):115301, 2010.

- [GW02] J. Gambetta and H. M. Wiseman. Non-markovian stochastic schrödinger equations: Generalization to real-valued noise using quantum-measurement theory. *Physical Review A*, 66(1):012108, 2002.
- [GZ04] C. W. Gardiner and P. Zoller. *Quantum Noise: A Handbook of Markovian and non-Markovian Quantum Stochastic Methods with Applications to Quantum Optics*, volume 56. Springer, 2004.
- [HLJ<sup>+</sup>11] J. Hu, M. Luo, F. Jiang, R.-X. Xu, and Y. Yan. Padé spectrum decompositions of quantum distribution functions and optimal hierarchical equations of motion construction for quantum open systems. *The Journal of Chemical Physics*, 134(24):244106, 2011.
- [HXY10] J. Hu, R.-X. Xu, and Y. Yan. Communication: Padé spectrum decomposition of fermi function and bose function. *The Journal of chemical physics*, 133:101106, 2010.
- [HZ08] P. Huang and H. Zheng. Quantum dynamics of a qubit coupled with a structured bath. *Journal of Physics: Condensed Matter*, 20(39):395233, 2008.
- [IF09] A. Ishizaki and G. R. Fleming. Theoretical examination of quantum coherence in a photosynthetic system at physiological temperature. *Proceedings of the National Academy of Sciences*, 106(41):17255–17260, 2009.
- [Ima94] A. Imamoglu. Stochastic wave-function approach to non-markovian systems. *Physical Review A*, 50(5):3650, 1994.
- [JC63] E. T. Jaynes and F. W. Cummings. Comparison of quantum and semi-classical radiation theories with application to the beam maser. *Proceedings of the IEEE*, 51(1):89–109, 1963.
- [JZYY12] J. Jing, X. Zhao, J. Q. You, and T. Yu. Time-local quantum-state-diffusion equation for multilevel quantum systems. *Phys. Rev. A*, 85:042106, Apr 2012.

## Bibliography

---

- [Kos72] A. Kossakowski. On quantum statistical mechanics of non-hamiltonian systems. *Reports on Mathematical Physics*, 3(4):247–274, 1972.
- [KS12] S. Krönke and W. T. Strunz. Non-markovian quantum trajectories, instruments and time-continuous measurements. *Journal of Physics A: Mathematical and Theoretical*, 45(5):055305, 2012.
- [LCD<sup>+</sup>87] A. J. Leggett, S. Chakravarty, A. T. Dorsey, Matthew P. A. Fisher, Anupam Garg, and W. Zwerger. Dynamics of the dissipative two-state system. *Rev. Mod. Phys.*, 59:1–85, Jan 1987.
- [Lin76] G. Lindblad. On the generators of quantum dynamical semigroups. *Communications in Mathematical Physics*, 48(2):119–130, 1976.
- [MK11] V. May and O. Kühn. *Charge and Energy Transfer Dynamics in Molecular Systems*. Wiley, 2011.
- [MT99] C. Meier and D. J. Tannor. Non-markovian evolution of the density operator in the presence of strong laser fields. *The Journal of chemical physics*, 111:3365, 1999.
- [NDH<sup>+</sup>10] T. Niemczyk, F. Deppe, H. Huebl, E. P. Menzel, F. Hocke, M. J. Schwarz, J. J. García-Ripoll, D. Zueco, T. Hümmer, E. Solano, et al. Circuit quantum electrodynamics in the ultrastrong-coupling regime. *Nature Physics*, 6(10):772–776, 2010.
- [Nov65] E. A. Novikov. Functionals and the random-force method in turbulence theory. *Sov. Phys. JETP*, 20(5):1290–1294, 1965.
- [Per98] I. C. Percival. *Quantum State Diffusion*. Cambridge University Press, 1998.
- [RE] G. Ritschel and A. Eisfeld. On analytic bath correlation functions obtained from broader class of spectral densities.
- [RED<sup>+</sup>11] J. Roden, A. Eisfeld, M. Dvořák, O. Bünermann, and F. Stienkemeier. Vibronic line shapes of ptcda oligomers in helium nanodroplets. *The Journal of chemical physics*, 134:054907, 2011.

- [REWS09] J. Roden, A. Eisfeld, W. Wolff, and W. Strunz. Influence of complex exciton-phonon coupling on optical absorption and energy transfer of quantum aggregates. *Physical Review Letters*, 103(5):058301, 2009.
- [RRS<sup>+</sup>11] G. Ritschel, J. Roden, W. T. Strunz, A. Aspuru-Guzik, and A. Eisfeld. Absence of quantum oscillations and dependence on site energies in electronic excitation transfer in the fenna–matthews–olson trimer. *The Journal of Physical Chemistry Letters*, 2(22):2912–2917, 2011.
- [RRSE11] G. Ritschel, J. Roden, W. T. Strunz, and A. Eisfeld. An efficient method to calculate excitation energy transfer in light-harvesting systems: Application to the fenna–matthews–olson complex. *New Journal of Physics*, 13(11):113034, 2011.
- [RSCE<sup>+</sup>08] Elizabeth L. Read, G. S. Schlau-Cohen, G. S. Engel, J. Wen, R. E. Blankenship, and G. R. Fleming. Visualization of excitonic structure in the fenna-matthews-olson photosynthetic complex by polarization-dependent two-dimensional electronic spectroscopy. *Biophysical journal*, 95(2):847–856, 2008.
- [RSE] G. Ritschel, W. T. Strunz, and A. Eisfeld. (in preparation).
- [RSE11] J. Roden, W. T. Strunz, and A. Eisfeld. Non-markovian quantum state diffusion for absorption spectra of molecular aggregates. *The Journal of Chemical Physics*, 134(3):034902, 2011.
- [SB01] P. Stelmachovic and V. Buzek. Dynamics of open quantum systems initially entangled with environment: Beyond the kraus representation. *Phys. Rev. A*, 64:062106, Nov 2001.
- [SBS97] S. Savikhin, D. R. Buck, and W. S. Struve. Oscillating anisotropies in a bacteriochlorophyll protein: Evidence for quantum beating between exciton levels. *Chemical physics*, 223(2):303–312, 1997.
- [Sch10] Schrödinger, LLC. The PyMOL molecular graphics system, version 1.3r1. August 2010.
- [Sch11] W. P. Schleich. *Quantum Optics in Phase Space*. Wiley. com, 2011.

## Bibliography

---

- [SDG99] W. T. Strunz, L. Diósi, and N. Gisin. Open system dynamics with non-markovian quantum trajectories. *Phys. Rev. Lett.*, 82:1801–1805, Mar 1999.
- [SS12] J. Strümpfer and K. Schulten. Open quantum dynamics calculations with the hierarchy equations of motion on parallel computers. *Journal of chemical theory and computation*, 8(8):2808–2816, 2012.
- [Str96] W. T. Strunz. Linear quantum state diffusion for non-markovian open quantum systems. *Physics Letters A*, 224(1–2):25 – 30, 1996.
- [Str01] W. T. Strunz. Stochastic schrödinger equation approach to the dynamics of non-Markovian open quantum systems. Habilitation thesis, June 2001.
- [SU83] G. W. Semenoff and H. Umezawa. Functional methods in thermofield dynamics: A real-time perturbation theory for quantum statistical mechanics. *Nuclear Physics B*, 220(2):196–212, 1983.
- [Tan06] Yoshitaka Tanimura. Stochastic liouville, langevin, fokker–planck, and master equation approaches to quantum dissipative systems. *Journal of the Physical Society of Japan*, 75(8):082001, 2006.
- [TCABA09] D. Tronrud, A. Camara-Artigas, R. Blankenship, and J.P. Allen. Crystal structure of the fenna-matthews-olson protein from chlorobaculum tepidum, May 2009.
- [VEAG12] S. Valleau, A. Eisfeld, and A. Aspuru-Guzik. On the alternatives for bath correlators and spectral densities from mixed quantum-classical simulations. *The Journal of chemical physics*, 137:224103, 2012.
- [Wei99] U. Weiss. *Quantum Dissipative Systems (Second Edition)*. Series in Modern Condensed Matter Physics. World Scientific Publishing Company Incorporated, 1999.
- [WM08] D. F. Walls and G. J. Milburn. *Quantum Optics*. Springer, 2008.
- [WM10] H. M. Wiseman and G. J. Milburn. *Quantum Measurement and Control*. Cambridge University Press, 2010.

- [YDGS99] T. Yu, L. Diósi, N. Gisin, and W. T. Strunz. Non-markovian quantum-state diffusion: Perturbation approach. *Phys. Rev. A*, 60:91–103, Jul 1999.
- [YDGS00] T. Yu, L. Diósi, Nicolas G., and W. T. Strunz. Post-markov master equation for the dynamics of open quantum systems. *Physics Letters A*, 265(5):331–336, 2000.
- [Yu04] T. Yu. Non-markovian quantum trajectories versus master equations: Finite-temperature heat bath. *Physical Review A*, 69(6):062107, 2004.

## **Danksagung**

An erster Stelle möchte ich mich natürlich ganz herzlich bei Herr Prof. Strunz für die Betreuung während der Diplomarbeit bedanken. Sie haben es mir durch die Freiheit bei der Aufgabenstellung ermöglicht, den Verlauf dieser Arbeit größtenteils selber zu bestimmen. Außerdem haben Sie mich in zahlreichen Diskussionen immer wieder auf den richtigen Weg zurückgebracht. Weiterhin möchte ich bei Herr Dr. Großmann dafür bedanken, dass er sich als Zweitgutachter zur Verfügung gestellt hat.

Alexander Eisfeld möchte ich für die vielen Gespräche, Korrekturen und Hinweise danken, die maßgeblich zum Entstehen dieser Arbeit beigetragen haben—auch wenn mein erster Entwurf allen deinen Veröffentlichungen widersprach. Gerhard Ritschel möchte ich für seine Hilfe bei vielen Details der Rechnungen und für seine Unterstützung bei allem was mit Temperatur zu tun hat bedanken.

Natürlich wäre diese Danksagung nicht vollständig ohne eine Erwähnung der ganzen TQO-Arbeitsgruppe. Insbesondere möchte ich mich bei Franziska Peter bedanken, auch wenn ich nicht sagen darf wofür. Lena Simon möchte ich für das Korrekturlesen in sprichwörtlich letzter Minute danken. Bei Richard Hartmann möchte ich mich für die Diskussionen und Erkenntnisse zum Thema dieser Arbeit bedanken, auch wenn ich glaube dass  $\gamma \neq 0$  gelten sollte.

Bei meinen Eltern möchte ich herzlichst für die tatkräftige Unterstützung während der Studienzeit bedanken.

## **Erklärung**

Hiermit versichere ich, dass ich die vorliegende Arbeit ohne unzulässige Hilfe Dritter und ohne Benutzung anderer als der angegebenen Hilfsmittel angefertigt habe. Die aus fremden Quellen direkt oder indirekt übernommenen Gedanken sind als solche kenntlich gemacht. Die Arbeit wurde bisher weder im Inland noch im Ausland in gleicher oder ähnlicher Form einer anderen Prüfungsbehörde vorgelegt.

Daniel Süß

Dresden, 7. Dezember 2013